

**Investigating white matter changes underlying
overactive bladder in multiple sclerosis with diffusion
MRI**

Xixi Yang

Thesis presented for the degree of

Doctor of Philosophy

of the

University College London

Department of Brain Repair and Rehabilitation
and Uro-neurology Department
Institute of Neurology
and National Hospital for Neurology and Neurosurgery
University College London

I, Xixi Yang, confirm that the work presented in this thesis is my own. Where information has been derived from other sources, I confirm that this has been indicated in the thesis.

Abstract

Lower urinary tract symptoms (LUTS) are presented in more than 80% of multiple sclerosis (MS) patients. Current understanding of LUT control is based on studies exploring activities in grey matter (GM) and investigating functional correlations with LUTS. The relationship between white matter (WM) changes and overactive bladder (OAB) symptoms are limited to findings in small vessel disease, and the nature of the association between WM changes and OAB symptoms is poorly understood.

Advanced diffusion-weighted magnetic resonance imaging (MRI) techniques provide non-invasive techniques to study WM abnormalities and correlates to clinical observations. The overarching objectives of this work are to explore WM abnormalities subtending OAB symptoms in MS, and to reconstruct the structural network underpinning the working model of lower urinary tract (LUT) control. Using Tract-Based Spatial Statistics (TBSS), OAB symptoms related WM abnormalities in MS can be identified, and a structural network subtending OAB symptoms in MS can be subsequently created.

The findings of this work illustrate the correlation between OAB symptoms severity and WM abnormalities in MS. These were observed in regions in frontal lobes and non-dominant hemisphere, including corpus callosum, anterior corona

radiata bilaterally, right anterior thalamic radiation, superior longitudinal fasciculus bilaterally, and right inferior longitudinal fasciculus. The structural network created for OAB symptoms in MS connected regions known to be involved in the working model of LUT control, and the network identified connectivity between insula and frontal lobe, which is the key circuit for perception of bladder fullness. Moreover, structural connectivity between insula-temporal lobe and insula-occipital lobe were observed, which may underpin changes seen in functional MRI (fMRI) studies.

The novel findings of this study present WM abnormalities and structural connectivity subtending LUTS in MS with diffusion-weighted imaging (DWI). The techniques used in this work can be applied to other patterns of LUTS and other neurological diseases.

Impact Statement

The brain white matter (WM) abnormalities were not sufficiently investigated in lower urinary tract symptoms (LUTS), especially an aspect of LUTS in a neurological condition. The current understanding of neural correlates of LUTS were focused on changes in grey matter (GM) activities with functional magnetic resonance imaging (fMRI) and positron emission computed tomography (PET), and white matter hyperintensity (WMH) studies with limited approaches, concluded from various cohorts of people, including health and disease. However, the nature of the correlation between WM abnormalities and OAB symptoms was poorly understood, especially in a specific neurological disease. This work is the first study investigating the commonest LUTS (OAB symptoms) in a neurological condition, multiple sclerosis (MS).

The methods applied in this work were all internally validated and explored to find out the WM correlates with OAB symptoms in MS. The results not only confirmed current finding of specific WM tracts from previous studies, but also identified the importance of non-dominant hemisphere for OAB symptoms in MS. This work also proposed the structural connectivity network subtending OAB symptoms in MS. Together with the current lower urinary tract (LUT) working model providing functional connectivity network for LUTS, this work successfully compensated the current understanding of neural correlates with LUTS. This work has been

presented in meetings and conferences, and selected to be a finalist at the Young Talent session at *The 7th International Neuro-Urology meeting, Zurich*. The work from chapter 5 has been submitted to *Annals of Clinical and Translational Neurology (ACTN)*, and the manuscript derived from Chapter 6-7 is in preparation for submission to *Journal of Neurology, Neurosurgery and Psychiatry (JNNP)*.

The network-based analysis offered a novel framework of studying structural connectivity, which may underpin the working model for LUT control system. The advanced diffusion-weighted magnetic resonance imaging (MRI) techniques combined with the analysis methods used in this work provided potential application in further clinical practice, and could be extended to other further investigations in other aspects of LUTS in other neurological conditions, improving our understanding of neuro-pathology and evaluating neural changes at different stages of disease. The findings regarding LUTS may further help with diagnosis and treatment regarding LUTS in neurological diseases.

To conclude, this work extends current knowledge on LUTS, highlights the importance of multidisciplinary study and the use of novel techniques in clinical research. The validated technique applications are transferable across neurological conditions. In the end, the work will result in first-author publications and could help to inform future clinical practice.

献给亲爱的妈妈

Acknowledgements

One of the challenges during my PhD is to find an appropriate way to express my acknowledgements to my supervisors, mentors, and all colleagues from clinical and research prospects. This multidisciplinary project would never be completed without their constant and unconditional support. Words are hard to express my appreciation, and I would demonstrate my warm and sincere gratitude to all of them.

I would like to express my deep gratitude to my supervisors, Dr. Jalesh Panicker, Prof. Claudia Wheeler-Kingshott and Dr. Martina Liechti, for their professional, warm-hearted and excellent supervision. It was my honour to be supervised by the best and work with them during my PhD. They made me feel lucky to meet with at this age and their characters would definitely give me positive impact in my future life.

Dr. Jalesh Panicker, an inspiring neurologist specialised in uro-neurology, set me an outstanding example for being a clinician, who should have both clinical and research thinking. I am influenced by his patient attitude and professional judgement as a clinician, his clear way of thinking and brilliant guidance as a supervisor, and his considerate caring as a mentor.

Prof. Claudia Wheeler-Kingshott, a world leader in MR physics, sharing brilliant ideas, persistent pursuit and optimistic attitude with all colleagues. Her clear instructions, efficient way of working and modest expression strongly joint colleagues from different backgrounds together, opened the door of MRI world for me, offered me promotional meetings with multidisciplinary suggestions, and provided me cheerful and vigorous working atmosphere.

Dr. Martina Liechti, a conscientious scientist with biology background, took me by the hand and taught me how strict attitude a scientist should have. I benefited from her diligent working, her advices from distance when working at Zurich, her way of dealing with scientific data, and her dialectical thinking.

I am grateful to Dr. Ahmed Toosy, a neurologist specialised in MS and a fantastic collaborator, for his invaluable recommendations at our weekly meetings and his generous help for clinical examinations and EDSS evaluations for participants.

There are some people without whom I would never complete this project. I would like to thank Dr. Marios Yiannakas and Ms. Gwen Gonzales for their time and unconditional support during MRI acquisition. I would also like to thank Dr. Jeremy Chataway, Prof. Olga Ciccarelli and their clinical team for their enthusiastic help for participants recruitment. I am grateful to Ms. Mahreen Pakzad for her brilliant advices regarding all urological and uro-neurological questions.

I am thankful to Dr. Ferran Prados and Dr. Baris Kanber for their help with image analysis and work on XNAT. I would like to thank Dr. Thalys Charalambous for his explanation and guidance on tractography pipelines and connectivity reconstruction. I am also thankful to Dr. Gloria Castellazzi for her patient

instructions and encouragement every time I struggled with analysis, and her unconditional help with connectivity analysis and machine learning approaches. I am grateful to Dr. Carole Sudre for her sincere help on bullseye analysis and plots. I am also grateful to Dr. Carmen Tur for her professional suggestions on statistics.

Thanks to everyone at Uro-Neurology department, National Hospital for Neurology and Neurosurgery, especially the nurse team, for their daily support, teaching and caring and offering me a warm-hearted working and living environment.

Thanks to all members at Queen Square Multiple Sclerosis Research Centre for providing me cheerful and organised working space during my PhD.

Thanks to all participants attending my project and all their efforts on research.

Thanks to the examiners of my MPhil/PhD transfer and final PhD viva for taking time and evaluating my work.

Thanks to my friend Jiaying Zhang for her detailed explanations, encouragement and company at the beginning of my work regarding MRI analysis.

I would conclude the acknowledgements thanking my family: my father Guang Yang, my mother Yingjie Song. In spite of the distance, they supported me during the ups and downs with endless love and never made me feel alone. 感谢你们常伴左右，任我飞翔！

30th July 2019

Xixi Yang

“为中华之崛起而读书”

--- 周恩来 ---

Table of contents

Abstract	3
Impact Statement	5
Acknowledgements	8
Table of contents	12
List of figures	15
List of tables	16
List of abbreviations	17
List of publications	20
Chapter 1	23
1. Introduction	23
1.1. Background	23
1.2. Objectives	24
1.3. Structure of the thesis	25
Chapter 2	27
2. Neurogenic bladder symptoms in multiple sclerosis	27
2.1. Lower urinary tract	27
2.2. Lower urinary tract dysfunction following neurological disease	29
2.3. Overview of multiple sclerosis	32
2.4. Lower urinary tract involvement in multiple sclerosis	37
2.5. Strategies to study lower urinary tract symptoms in multiple sclerosis ...	38
Chapter 3	41
3. Current understanding of the higher control of lower urinary tract functions	41
3.1. Current understanding of neurological correlates of the lower urinary tract functions.....	41

3.2. White matter structural changes leading to lower urinary tract dysfunction	49
3.3. Motivation of the design for this thesis	50
Chapter 4	54
4. Diffusion-weighted imaging and related analysis approaches	54
4.1. Basic principles of diffusion-weighted imaging in neuroscience research	54
4.2. Common artefacts during MRI acquisition	56
4.3. Brain network analysis	57
4.4. Application of diffusion-weighted imaging in multiple sclerosis	63
4.5. Research scheme of this thesis	66
Chapter 5	71
5. Exploring association between white matter changes and overactive bladder symptoms in multiple sclerosis with diffusion MRI	71
5.1. Introduction	72
5.2. Methods	74
5.3. Results	82
5.4. Discussions	96
5.5. Remaining question and further direction	100
Chapter 6	104
6. Whole brain structural connectome reconstruction	104
6.1. Introduction	105
6.2. Methods	106
6.3. Results	117
6.4. Discussion	124
6.5. Conclusion	125

6.6. Remaining question and further direction	127
Chapter 7.....	130
7. Brain structural network for overactive bladder in multiple sclerosis	130
Section A. Structural network subtending overactive bladder symptoms in multiple sclerosis	132
7.1. Introduction	132
7.2. Methods	135
7.3. Results	140
7.4. Discussion	149
7.5. Conclusion	152
7.6. Remaining question and further direction	153
Section B. Structural network based on the working model of LUT control	154
7.7. Introduction	154
7.8. Methods	156
7.9. Results	159
7.10. Discussion	163
7.11. Conclusion	165
Chapter 8.....	169
8. Limitations, conclusion and future directions	169
8.1. Limitations	169
8.2. Conclusion	171
8.3. Future directions	173
Appendices	176

List of figures

Figure 2.1. Innervation of the lower urinary tract.....	28
Figure 2.2. Patterns of lower urinary tract dysfunction following neurological disease.....	31
Figure 3.1. Working model of the lower urinary tract control system	45
Figure 4.1. A model graph of tractogram.....	59
Figure 4.2. An example of brain connectome matrix.....	60
Figure 4.3. Summary of the main measures estimated with graph analysis	62
Figure 5.1. WM skeleton and significant results from TBSS	93
Figure 5.2. Frequency plots of lesion volume in terms of median and IQR in (a) MS-no-LUTS and (b) MS-OAB	94
Figure 5.3. Bullseye plots showing significant results from TBSS.....	95
Figure 6.1. MRI processing procedure for whole brain connectivity reconstruction.....	109
Figure 6.2. Lesion masking on PD-weighted image and T1-weighted imaging with lesion filled	120
Figure 6.3. Brain parcellation.....	121
Figure 6.4. Brain segmentation.....	122
Figure 6.5. Whole brain connectome matrix.....	123
Figure 7.1. MS-network and MS-OAB-network.....	148
Figure 7.1. LUT working model network.....	162

List of tables

Table 2.1. Main results from previous studies in MS using TBSS.	34
Table 2.2. Main results from previous studies in MS using tractography.	36
Table 3.1. The LUT related GM regions and the coordinates abstracted from different studies	46
Table 5.1. Demographic characteristics of HC and MS patients	84
Table 5.2. FA values of mean skeleton in HC, MS and MS sub-groups ..	87
Table 5.3. Correlations between FA values and clinical scores	89
Table 5.4. Analysis results without relative significance	90
Table 6.1. List of 120 GM regions used in whole brain connectivity reconstruction	112
Table 6.2. Demographic and network characteristics of HC and MS participants	118
Table. 7.1. Demographic characteristics of HC, MS, MS-no-LUT and MS- OAB participants	141
Table 7.2. The GM regions selected for the OAB symptoms in MS	142
Table 7.3. List of GM regions having statistically significant streamlines in between, in group difference between HC and MS	144
Table 7.4. List of GM regions having statistically significant streamlines in between, in group difference between MS-no-LUT and MS-OAB	146
Table 7.5. List of the GM regions for LUT working model network.....	161

List of abbreviations

ACT	Anatomically constrained tractography
AD or Da	Axial diffusivity
BC	Betweenness centrality
BCT	Brain connectivity toolbox
BD	Bladder diary
BD-dayf	Day time frequency from bladder diary
BD-max	Maximum voided volume from bladder diary
BD-nightf	Night time frequency from bladder diary
BGIT	Basal ganglia thalami and infratentorial regions
Botox	Botulinum toxin A
BPH	Benign prostatic hyperplasia
CC	Clustering coefficient
CIS	Clinically isolated syndrome
CNS	Central nervous system
CSD	Constrained spherical deconvolution
CSF	Cerebrospinal fluid
DEG	Degree
DO	Detrusor overactivity
DSD	Detrusor sphincter dyssynergia
DWI	Diffusion weighted imaging
EDSS	Expanded Disability Status Scale
EPI	Echo planar imaging
FA	Fractional anisotropy
fMRI	Functional magnetic resonance imaging
FRONT	Frontal lobe
FSL	FMRIB Software Library
GE	Global efficiency
GIF	Geodesic Information Flow
GLM	General Linear Model
GM	Grey matter
HC	Healthy controls
ICIQ_FLUTS	International Consultation on Incontinence questionnaire for female lower urinary tract symptoms
ICIQ_FLUTS-f	ICIQ_FLUTS – frequency
ICIQ_FLUTS-i	ICIQ_FLUTS – incontinence
ICIQ_FLUTS-v	ICIQ_FLUTS – voiding
ICIQ-LUTSqol	International consultation on Incontinence Questionnaire – quality of life
ICIQ-OAB	International consultation on Incontinence Questionnaire – Overactive bladder

ICIQ-QoL	International consultation on Incontinence Questionnaire – quality of life
IMP	Inferior mesenteric plexus
IPSS	International Prostate Symptom Score questionnaire
IQR	Interquartile range
LE	Local efficiency
LUT	Lower urinary tract
LUTD	Lower urinary tract dysfunctions
LUTS	Lower urinary tract symptoms
MCC	Maximum cystometric capacity
MD	Mean diffusivity
MNI	Montreal Neurological Institute
MRI	Magnetic resonance imaging
MS	Multiple sclerosis
MSA	Multiple system atrophy
NAWM	Normal appearing white matter
NHPT	Nine-hole peg test
OAB	Overactive bladder
OCC	Occipital lobe
ON	Onuf's nucleus
PAG	Periaqueductal gray
PAR	Parietal lobe
PC	Participation coefficient
PD	Proton density
PET	Positron emission Computed tomography
PMC	Pontine micturition centre
PP	Pelvic plexus
PPMS	Primary progressive multiple sclerosis
PTNS	Percutaneous tibial nerve stimulation
PVR	Post-void residual
RD or Dr	Radial diffusivity
RRMS	Relapsing remitting multiple sclerosis
Sa	Sacral parasympathetic area
SCI	Spinal cord injury
SHP	Superior hypogastric plexus
SIFT2	Spherical-deconvolution informed filtering of tractograms
SMA	Supplementary motor area
SPECT	Single-photon computerized tomography
SPMS	Secondary progressive multiple sclerosis
SSEP	Somatosensory evoked potential
TBSS	Tract-based spatial statistics
TEMP	Temporal lobe

TFCE	Threshold-Free Cluster Enhancement
th	Thalamus
USP	Urinary Symptom Profile
USP-LS	USP - Low stream
USP-OAB	USP - overactive bladder
USP-SUI	USP - stress urinary incontinence
UTI	Urinary tract infection
WM	White matter
WMD	White matter disease
WMH	White matter hyperintensity

List of publications

Journal publications

Xixi Yang, Martina Liechti, Baria Kanber, Carole Sudre, Gloria Castellazzi, Jiaying Zhang, Marios C. Yiannakas, Gwen Gonzales, Ferran Prados Carrasco, Ahmed T. Toosy, Claudia A. M. Gandini Wheeler-Kingshott, Jalesh N. Panicker.

A cross-sectional exploratory study of white matter magnetic resonance diffusion measures in Multiple Sclerosis with overactive bladder. (Submitted to *Annals of Clinical and Translational Neurology*).

Xixi Yang, Gloria Castellazzi, Martina D. Liechti, Thalys Charalambous, Baris Kanber, Marios C. Yiannakas, Gwen Gonzales, Feeran Prados Carrasco, Ahmed T. Toosy, Jalesh N. Panicker, Claudia A. M. Gandini Wheeler-Kingshott.

Structural network indicating overactive bladder in multiple sclerosis. (In preparation for submission to *Journal of Neurology, Neurosurgery and psychiatry*).

Xixi Yang, Manlu Wang, Sara Simeoni, Prazad Malladi, Martina D. Liechti, Jalesh N. Panicker. Men reporting genital numbness- is there a neurological cause? (In preparation for submission to a *Journal of Sexual Medicine*).

Marios C. Yiannakas, Martina D. Liechti, Nutakarn Budtarad, Patrick Cullinane, **Xixi Yang**, Ahmed T. Toosy, Jalesh N. Panicker, Claudia A. M. Gandini Wheeler-

Kingshott. **Grey matter and white matter segmentation of the human conus medullaris: reliability, normative values, and natural variability in healthy volunteers.** (Accepted by *Journal of Neuroimaging*).

Conference abstracts

Xixi Yang, Martina D. Liechti, Ferran Prados Carrasco, Marios C. Yiannakas, Gwen Gonzales, Ahmed T. Toosy, Claudia A. M. Gandini Wheeler-Kingshott, Jalesh N. Panicker. **Investigating white matter changes underlying the overactive bladder in Multiple Sclerosis using diffusion MRI.** (7th International Neuro-Urology Meeting, Zurich, Switzerland, 2019; selected for Swiss Continence Foundation Young Talent Award competition).

Xixi Yang, Manlu Wang, Sara Simeoni, Prazad Malladi, Martina D. Liechti, Jalesh N. Panicker. Men reporting genital numbness- is there a neurological cause? (7th International Neuro-Urology Meeting, Zurich, Switzerland, 2019).

Xixi Yang, Martina D. Liechti, Ferran Prados Carrasco, Marios C. Yiannakas, Gwen Gonzales, Ahmed T. Toosy, Claudia A. M. Gandini Wheeler-Kingshott, Jalesh N. Panicker. **A cross-sectional exploratory magnetic resonance imaging study evaluating white matter diffusion measures for the**

overactive bladder in Multiple Sclerosis. (Queen Square Symposium, London, UK, 2018).

Martina D. Liechti, Nuttakarn Budtarad, D. R. Altmann, **Xixi Yang**, Ahmed T. Toosy, David H. Miller, Jalesh N. Panicker, Claudia A. M. Gandini Wheeler-Kingshott, Marios C. Yiannakas. **Feasibility of Grey Matter and White Matter Segmentation of the Conus Medullaris: A Pilot *In Vivo* Investigation in the Neurologically Intact Spinal Cord.** (International Society for Magnetic Resonance in Medicine, Honolulu, USA, 2017).

Marios. C. Yiannakas, Martina D. Liechti, P. Cullinane, **Xixi Yang**, Ahmed T. Toosy, Jalesh N. Panicker, Claudia A. M. Gandini Wheeler-Kingshott. **Normalised Grey Matter and White Matter Volumes in the Neurologically Intact Conus Medullaris.** (International Society for Magnetic Resonance in Medicine, Honolulu, USA, 2017).

Chapter 1

1. Introduction

1.1. Background

The lower urinary tract (LUT) is tightly regulated by a complex system of neural control in health, and this is commonly affected following neurological disease. In multiple sclerosis (MS), LUT symptoms (LUTS) are reported in more than 80% of patients, and have a significant negative impact on quality of life (QoL). The commonest reported LUTS in MS are urinary urgency, with or without urgency urinary incontinence and usually associated with daytime urinary frequency and nocturia, collectively called as urinary storage or overactive bladder (OAB) symptoms.

In recent years, magnetic resonance imaging (MRI), in particular functional MRI (fMRI) has provided considerable insight into the central neural control of LUT functions. There are a number of regions identified that consistently show changes of neural activities during bladder-specific tasks. These studies focus on the changes of grey matter (GM) activities, however MS is overwhelmingly a white matter (WM) disease and the nature of the association between WM

abnormalities and LUTS is unknown. Structural MRI studies in patients with small vessel disease affecting WM suggest that the anterior thalamic radiation and the superior longitudinal fasciculus are specifically important for LUT functions and are involved in continence control. WM hyperintensity (WMH) in the anterior corona radiata and the cingulate gyrus are reported to predict urinary incontinence and degree of bother. There is a lack of information on WM findings subtending LUTS in neurological conditions.

For MS, MRI has been established as a useful tool for the diagnosis and monitoring the disease progress. Different from the conventional MRI techniques, which are used to detect the number and volume of WM lesions and brain volume (atrophy), advanced MRI techniques have become available to explore widespread white matter abnormalities in MS, such as diffusion-weighted imaging (DWI). DWI is a developed MRI quantitative method, which is sensitive to the microscopic random thermal motion of water. There are several DWI scalar indices can capture some properties of the WM tracts, and DWI is extensively used to perform WM tractography to assess the circuitry basis of neural changes in neurological diseases.

1.2. Objectives

To better understand the WM abnormalities subtending the commonest LUTS (OAB symptoms) in MS, the specific aims of this thesis are, using advanced DWI MRI techniques, to explore:

1. microstructural WM changes in MS patients subtending OAB symptoms;
2. associations between different microstructural WM indices and clinical scores of OAB symptoms;
3. differences in the structural connectivity network between MS patients with OAB symptoms and those without LUTS;
4. WM connectivity underpinning the functional network controlling LUT functions.

1.3. Structure of the thesis

This thesis is structured as follows:

Chapter 2 reviews the neural control of LUT functions in health, and how these are affected in MS.

Chapter 3 reviews the current understanding of the higher control of LUT functions based on findings derived from brain imaging studies, and the current working model of LUT control.

Chapter 4 reviews basic knowledge of MRI, the techniques used to study the WM, particularly DWI techniques, and analysis approaches used in this thesis. In this chapter, studies that have used advanced DWI techniques to explore the WM abnormalities in MS are also reviewed.

In chapter 5, the WM changes in MS are investigated, and the association between the WM changes and the severity of OAB symptoms are explored, using advanced DWI techniques with Tract-Based Spatial Statistic (TBSS).

In chapter 6, the whole brain probabilistic tractogram is generated and the whole brain structural connectivity network is reconstructed (to apply for analysis in chapter 7), with advanced network reconstruction approaches, improving the biologically meaningful information of the network. A structural network subtending MS is created by comparing the difference between the network measures between healthy controls (HC) and MS.

In chapter 7, the structural network subtending OAB symptoms in MS is created based on the whole brain connectivity network reconstructed in chapter 6, by comparing the differences of network measures between MS with OAB symptoms and MS without LUTS. Another structural network is created based on the working model of LUT control derived from previous brain imaging studies. Similarities and comparison between the two structural networks are explored and used to explain the current understanding of neural control of the LUT functions.

Chapter 8 illustrates the limitations, concludes the work and presents the future directions.

Chapter 2

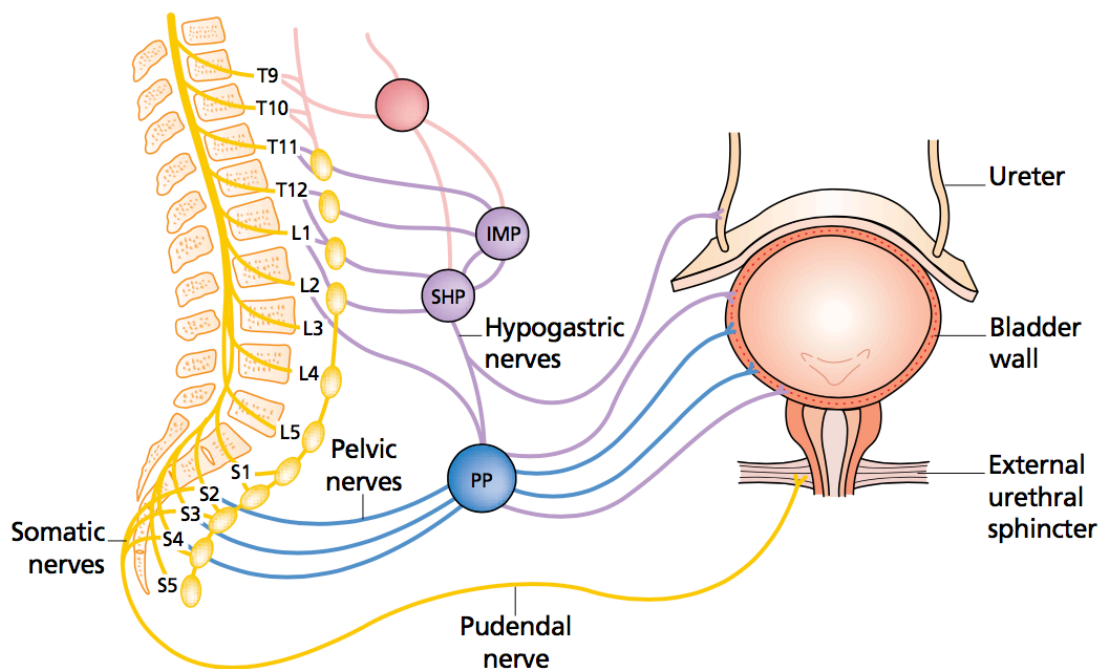
2. Neurogenic bladder symptoms in multiple sclerosis

2.1. Lower urinary tract

The LUT is made up of the bladder and the urethra, and plays two important roles: storage of urine and periodic emptying (Panicker, Fowler and Kessler, 2015). A complex neural system is acting an important role between storage and voiding function, like a switching circuit (Fowler, Griffiths and De Groat, 2008). Micturition is a well-coordinated task involving synergistic activity between the smooth muscle of the bladder (detrusor) and striated and smooth muscles of the urethra (external and internal sphincters, respectively) and is regulated by intact innervation in the peripheral and central nervous system (CNS; Figure 2.1; Panicker, 2016). In health, the LUT remains in the storage phase for 99.8% of the time, and this is, mediated by the parasympathetic innervation that inhibits detrusor contractions resulting in a low compliant passive filling with urine (Fowler, Griffiths and De Groat, 2008). Tonic contraction of the urethral sphincters mediated by pudendal and sympathetic innervation helps to maintain continence (Panicker, de Sèze and Fowler, 2010). As a result, intravesical pressures are maintained below 10 cm H₂O (Fowler, Griffiths and De Groat, 2008). When switching to the voiding phase, the pelvic floor muscles and external and internal

urethral sphincters become relaxed, along with detrusor contractions mediated by the parasympathetic innervation, and in the end, result in voiding and bladder emptying (Panicker, de Sèze and Fowler, 2010).

Figure 2.1. Innervation of the lower urinary tract.



IMP, inferior mesenteric plexus; SHP, superior hypogastric plexus; PP, pelvic plexus. (Panicker, 2016.) Innervations in purple are sympathetic nerves, and the ones in blue are parasympathetic nerves.

Maintenance of normal LUT functions rely on an intact neural pathway from peripheral nerve derived from the lower spinal cord to suprapontine level, through the regulation centre in the brainstem (Fowler, Griffiths and De Groat, 2008). The sympathetic innervation originates from the thoracolumbar level (T11-L2), and the parasympathetic and pudendal nerves are from the sacral spinal cord (Fowler, Griffiths and De Groat, 2008). These lower cord micturition centres are regulated by centres in the brainstem through tracts in the spinal cord. During storage phase, the pontine micturition centre (PMC) is inhibited by signals arising from the periaqueductal grey (PAG), and when it is thought appropriate to void, the PMC is released from tonic inhibition from the PAG. Several cortical and subcortical regions present importance in regulation of micturition due to their roles for cognitive behaviours and awareness of visceral sensations, including prefrontal cortex, insula and anterior cingulate gyrus (Panicker, Fowler and Kessler, 2015).

2.2. Lower urinary tract dysfunction following neurological disease

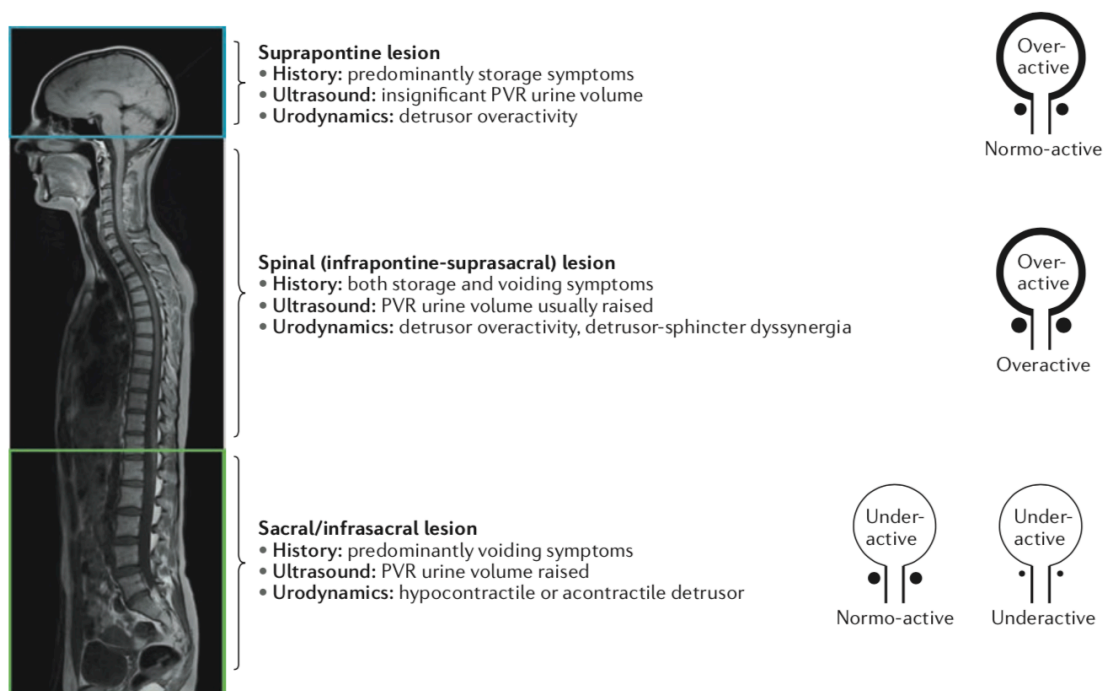
Considering the intricate innervations of the LUT across the central and peripheral nervous system, it is therefore not surprising that LUT dysfunction (LUTD) is common after neurological diseases, leading to LUTS with urinary storage and/or voiding symptoms. LUTS are commonly reported following neurological disease and has a pronounced impact on patients' quality of life (Panicker, Fowler and Kessler, 2015). There are different patterns of LUTS that can manifest after neurological disease and this is influenced by the site of neurological lesion and the disease process (Panicker, Fowler and Kessler,

2015). Patients complain of varying degrees of urinary urgency, with or without urgency urinary incontinence, and usually associated with frequency and nocturia (collectively called OAB symptoms), and/or hesitancy, poor stream and retaining urine (named as voiding symptoms; Wein and Rovner, 2002; Abrams *et al.*, 2003). Depending on different part and level of the impairment along the neural pathway, the OAB and voiding symptoms can appear independently or together in various of neurological disorders (Araki *et al.*, 2003; Fowler, Griffiths and De Groat, 2008). Based on previous reports, in general, the OAB symptoms affect nearly 17% of individuals in the United States and 12-17% in Europe, with a financial burden on the health care system exceeding \$24.9bn (£15.75bn; €19.01bn; Stewart *et al.*, 2003; Onukwugha *et al.*, 2009).

LUTD is commonly following different types of neurological diseases, such as MS, multiple system atrophy (MSA), dementia, cerebrovascular disease, Parkinson's disease and spinal cord injury, etc (Panicker, 2016). Characteristic patterns of LUTD can occur according to the site or level of the lesions (Figure 2.2; (Panicker, Fowler and Kessler, 2015). Detrusor overactivity (DO) and reduced bladder capacity is considered to be affected by relevant suprapontine or spinal cord lesions. Lesions localized at suprapontine level result in spontaneous involuntary detrusor contraction as a result of loss of tonic inhibition from the PMC (Fowler, Griffiths and De Groat, 2008). Lesions affecting the spinal cord (localization at infrapontine to suprasacral level), lead to involuntary detrusor contraction resulting from the emergence of a C-fibre mediated segmental reflex (Fowler, Griffiths and De Groat, 2008). Detrusor-sphincter dyssynergia (DSD), is characterised by simultaneous contraction of the detrusor and urethral sphincter,

and is typically found following infrapontine-suprasacral spinal cord lesions (Panicker, Fowler and Kessler, 2015). Patients with DSD often report voiding difficulties and incomplete bladder empty. In the setting of a sacral/infrasacral level lesions, voiding dysfunction could arise from lesions affecting the descending bulbospinal pathways resulting in the urodynamic signal of detrusor underactivity (Panicker, Fowler and Kessler, 2015).

Figure 2.2. Patterns of lower urinary tract dysfunction following neurological disease.



The pattern of lower urinary tract dysfunction following neurological disease is determined by the site and nature of the lesion. The blue box denotes the region above the pons and that in green denotes the sacral cord and infrasacral region. Figures on the right show the expected dysfunctional states of the detrusor-sphincter system. PVR, post-void residual. (Panicker, Fowler and Kessler, 2015.)

2.3. Overview of multiple sclerosis

MS is an inflammatory demyelinating disorder affecting the CNS, resulting in a significant impact on patients' quality of life, regardless the MS phenotypes (relapsing remitting MS, RRMS; secondary progressive MS, SPMS; primary progressive MS, PPMS; Lublin, 2014). The condition affects about 2.3 million people worldwide, with most of the onset at young age, and females have markedly increased sex ratio than males (Thompson, Baranzini, *et al.*, 2018). As the commonest progressive inflammatory demyelinating neurological disorder, over 100000 people in the United Kingdom are affected by MS (population ~ 63 million; Leary *et al.*, 2016). The clinically isolated syndrome (CIS) is considered as the first clinical representation of the disease, but still need to fulfil the diagnostic criteria of MS; RRMS, which affects around 85% of MS, is defined as relapses, followed by partial or complete recovery (remission); following the relapsing remitting course, there is a gradual increase in patients number of converting to SPMS (around 25% by 10 years after MS onset, 50% by 20 years, and more than 75% by 30 years; Khurana V and Medin J, 2018), which is a condition with steadier progression of disability and increasing neurodegeneration; and PPMS patients (around 10% of MS) present steady worsening of neurologic function from onset (Thompson, Banwell, *et al.*, 2018). The Expanded Disability Status Scale (EDSS) is a commonly used tool to measure the progression of the disability in MS, and covers different domains, including pyramidal, cerebellar, brainstem, sensory, bowel and bladder, visual, cerebral and other functional system (Kurtzke, 1983). The LUTS evaluation is included in the EDSS. Considering the LUTS evaluation from the EDSS, which investigates the incomplete bladder empty, is not a satisfactory score for LUTS (Panicker and Fowler, 2015), in this thesis, the EDSS score is used to evaluate

the disability from MS and the LUTS are measured by LUTS related questionnaires.

MRI has been accepted widely being a non-invasive tool for disease diagnosis and progress monitoring (Leary *et al.*, 2016). Based on the 2017 revised McDonald's diagnostic criteria, dissemination in space needs presence of two or more lesions in periventricular, juxta-cortical, infra-tentorial and spinal cord (Thompson, Banwell, *et al.*, 2018). Dissemination in time needs presence of a lesion when comparing with a previous scan, and simultaneous presence of gadolinium enhancing and non-enhancing lesion (Thompson, Banwell, *et al.*, 2018). For research, considering the conventional T1-weighted and T2-weighted scans cannot present the full pathophysiological progress of the disease, novel MRI techniques have been developed, such as the DWI (Enzinger *et al.*, 2015). Recent studies using DWI technique with various analysis approaches were reported to study the WM in MS. The DWI data was used to measure the voxel-based characters, such as the fractional anisotropy (FA; see details in **chapter 4**; Enzinger *et al.*, 2015). For example, the DWI was applied to investigate the potential damage in normal-appearing white matter (NAWM), and FA was decreased in corpus callosum in MS compared with healthy cohort (Ciccarelli *et al.*, 2003). The DWI data was also applied to reconstruct the fibre pathways (structural connectivity) to create the structural network (Enzinger *et al.*, 2015). Charalambous *et al.* used the measures, derived from the reconstructed structural network, to explain the pathology of MS disability (Charalambous *et al.*, 2018). In this thesis, the DWI technique was applied to the analysis of WM using both TBSS and structural connectivity. Considering both of the studies compared

WM abnormalities in MS with controls, it would be good to understand well the main findings from previous research, especially the ones involving same concerns included in thesis, for example, the clinical correlation (disability and cognitive dysfunction) with FA value. Table 2.1 and 2.2 concluded some main results from previous studies in MS using TBSS and tractography, correspondingly.

Table 2.1. Main results from previous studies in MS using TBSS.

Authors	Main results
Liu <i>et al.</i> , 2012	The MS patients had significantly decreased FA (9.11%), increased MD (8.26%), AD (3.48%) and RD (13.17%) in their white matter skeletons compared with the controls. The percentage means the extent of diffusion metric changes in patients relative to the mean diffusion metrics of controls. Decreased FA, increased MD and increased RD were involved in whole-brain white matter, while several regions exhibited increased AD, such as inferior temporal and frontal gyrus, external capsule and the regions around the cerebral ventricles.
Bodini <i>et al.</i> , 2009	PPMS patients showed reduced FA compared with controls in normal-appearing WM (NAWM) along the corticospinal tracts bilaterally, in the WM adjacent to the premotor cortex bilaterally and in the entire corpus callosum. Significant reduced FA also observed in bilateral thalamic radiation, optic radiation, fornix,

	<p>fasciculus arcuatus, inferior longitudinal fasciculus and WM of the temporal and frontal lobe. The NAWM FA in each of these regions correlated with disability. The study demonstrated a link between the pathological processes occurring in the NAWM in PPMS in specific, clinically relevant brain areas.</p>
<p>Kern <i>et al.</i>, 2011</p>	<p>Diffusion metrics in both the corticospinal tracts and the transcallosal hand motor (TBHM) fibres were strongly associated with hand motor performance. The TCHM fibres were predictive of declining performance. RD appears to be the most sensitive metric in relation to motor performance, though FA is closely linked. AD may be the least sensitive measure in early RRMS patients, since white matter architecture is relatively preserved.</p>
<p>Dineen <i>et al.</i>, 2009</p>	<p>The study was able to map the anatomical pattern of WM tract involvement in MS brains where ultrastructural fibre integrity predicts impaired performance in specific cognitive domains. There were multiple areas showing significant reduction in skeleton FA in MS versus controls, including corpus callosum, the inferior longitudinal fasciculi and inferior fronto-occipital fasciculi bilaterally, the bodies and tails of the fornices bilaterally, the posterior corona radiata bilaterally and in the left cerebral peduncle.</p>

AD axial diffusivity; FA: fractional anisotropy; MD: mean diffusivity; MS: multiple sclerosis; NAWM: normal-appearing white matter; RD radial diffusivity; RRMS: relapsing remitting multiple sclerosis; TBHM: transcallosal hand motor; WM: white matter.

Table 2.2. Main results from previous studies in MS using tractography.

Authors	Main results
Shu <i>et al.</i> , 2011	The global and local network efficiencies were significantly decreased in the MS patients compared with the controls, with the most pronounced changes observed in the sensorimotor, visual, default-mode, and language areas. The decreased network efficiencies were significantly correlated with the expanded disability status scale scores, the disease durations, and the total WM lesion loads.
Charalambous <i>et al.</i> , 2018	Relative to HC, SPMS had reduced global and local efficiency, PPMS reduced global efficiency while there was no efficiency change in RRMS. There was a decrease in clustering coefficient in RRMS compared with HC. Network metrics, particularly the global efficiency explains disability over and above non-network metrics supporting the relevance of intact long-distance connexions mainly, to maintain normal function.
Fleischer <i>et al.</i> , 2017	In the first year after disease onset, WM networks evolved to a structure of increased modularity, strengthened local connectivity and increased local clustering while no clinical decline occurred. Clinical impairment was associated at later disease stages with a divergence of the network patterns. The study suggested that network functionality in MS is maintained through structural adaptation towards increased local and modular connectivity, patterns linked to adaptability and homeostasis.

Muthuraman <i>et al.</i> , 2016	In comparison to CIS subjects, patients with RRMS were found to have increased modular connectivity and higher local clustering, highlighting increased local processing in both GM and WM. Both groups presented increased modularity and clustering coefficients in comparison to healthy controls.
------------------------------------	---

CIS: clinically isolated syndrome; GM: grey matter; HC: healthy control; MS: multiple sclerosis; RRMS: relapsing remitting multiple sclerosis; SPMS: secondary progressive multiple sclerosis; WM: white matter.

2.4. Lower urinary tract involvement in multiple sclerosis

The prevalence of LUTS in MS varies (32 - 96%), depending upon the stage and duration of disease (Dalton *et al.*, 2010). On average, LUTS begin 6 years into after getting MS and almost all patients complain of LUTS by around 10 years or more (de Seze *et al.*, 2007). Urogenital dysfunction most often results from spinal cord involvement, and LUTS is often related to lower limb symptoms (Fowler, 1998). Moreover, severity of the LUTS increases with the extending duration and progression of the pyramidal symptoms in lower limbs (Leary *et al.*, 2016). There is a correlation between worsening LUTS symptoms and increasing spinal cord lesions, showing deteriorated mobility (Leary *et al.*, 2016).

Patients can report storage and voiding symptoms depending upon the site of lesions within the nervous system. The most common LUTS storage symptoms are urinary urgency, daytime frequency, nocturia and incontinence, whereas the

commonest voiding difficulties are urinary hesitancy and an interrupted stream. The commonest case for storage symptoms is DO (34 - 91% of MS patients), captured by a urodynamic study, which is an precise evaluation of the functional pathophysiology of LUTD (Phé, Chartier-Kastler and Panicker, 2016). Voiding symptoms arising from the detrusor underactivity is found less than 37% of MS patients, and the DSD is presented in 5 – 60% of the MS patients (Phé, Chartier-Kastler and Panicker, 2016). Therefore, the main neural correlates of overactive bladder symptoms in MS are assumed at suprapontine and infrapontine-suprasacral level, and voiding difficulties are related to spinal cord involvement at sacral and infrasacral lesion symptoms (Figure 2.2).

2.5. Strategies to study lower urinary tract symptoms in multiple sclerosis

Considering the commonest LUTS in MS is OAB and the DWI is an advanced non-invasive technique widely applied in MS, investigations into neural correlates to OAB symptoms in MS using DWI is desired. **Chapter 3** will introduce the current understanding of LUTS from MRI studies, and **chapter 4** will provide some basic knowledge of DWI MRI techniques and related methods applied in this thesis.

Bibliography

- Abrams, P. *et al.* (2003) 'The standardisation of terminology in lower urinary tract function: Report from the standardisation sub-committee of the International Continence Society', *Urology*, 61(1), pp. 37–49. doi: 10.1016/S0090-4295(02)02243-4.
- Araki, I. *et al.* (2003) 'Relationship of bladder dysfunction to lesion site in multiple sclerosis.', *The Journal of urology*, 169(4), pp. 1384–1387. doi: 10.1097/01.ju.0000049644.27713.c8.
- Bodini, B. *et al.* (2009) 'Exploring the Relationship Between White Matter and Gray Matter Damage in Early Primary Progressive Multiple Sclerosis : An In Vivo Study With TBSS and VBM', *Human Brain Mapping*, 2861(November 2008), pp. 2852–2861. doi: 10.1002/hbm.20713.
- Charalambous, T. *et al.* (2018) 'Structural network disruption markers explain disability in multiple sclerosis', *Journal of Neurology, Neurosurgery, and Psychiatry*, pp. 219–226. doi: 10.1136/jnnp-2018-318440.
- Ciccarelli, O. *et al.* (2003) 'A study of the mechanisms of normal-appearing white matter damage in multiple sclerosis using diffusion tensor imaging--evidence of Wallerian degeneration.', *Journal of neurology*. Germany, 250(3), pp. 287–292. doi: 10.1007/s00415-003-0992-5.
- Dineen, R. A. *et al.* (2009) 'Disconnection as a mechanism for cognitive dysfunction in multiple sclerosis.', *Brain : a journal of neurology*. England, 132(Pt 1), pp. 239–249. doi: 10.1093/brain/awn275.
- Enzinger, C. *et al.* (2015) 'Nonconventional MRI and microstructural cerebral changes in multiple sclerosis', *Nature Reviews Neurology*. Nature Publishing Group, 11(12), pp. 676–686. doi: 10.1038/nrneurol.2015.194.
- Fleischer, V. *et al.* (2017) 'Increased structural white and grey matter network connectivity compensates for functional decline in early multiple sclerosis', *Multiple Sclerosis Journal*, 23(3), pp. 432–441. doi: 10.1177/1352458516651503.
- Fowler, C. J. (1998) 'The neurology of male sexual dysfunction and its investigation by clinical neurophysiological methods.', *British journal of urology*. England, 81(6), pp. 785–795.
- Fowler, C. J., Griffiths, D. and De Groat, W. C. (2008) 'The neural control of micturition', *Nature Reviews Neuroscience*, 9(6), pp. 453–466. doi: 10.1038/nrn2401.
- Kern, K. C. *et al.* (2011) 'Corpus callosal diffusivity predicts motor impairment in relapsing-remitting multiple sclerosis: A TBSS and tractography study', *NeuroImage*. Elsevier Inc., 55(3), pp. 1169–1177. doi: 10.1016/j.neuroimage.2010.10.077.
- Khurana V and Medin J. 'Time to, and rate of secondary progression in patients with multiple sclerosis: results of a systematic search', [Last accessed on 2018 May 31]. ePoster at ECTRIMS 2017, EP1326. Available from: <https://onlinelibrary.ectrims-congress.eu/ectrims/2017/ACTRIMS-ECTRIMS2017/199347/jennie.medin.time.to.and.rate.of.secondary.progression.in.patients.with.html>
- Kurtzke, J. F. (1983) 'Rating neurologic impairment in multiple sclerosis: An expanded disability status scale (EDSS)', *Neurology*, 33(11), pp. 1444–1444. doi: 10.1212/WNL.33.11.1444.
- Leary, S. *et al.* (2016) 'Multiple Sclerosis and Demyelinating Diseases', *Neurology*. (Wiley Online Books). doi: doi:10.1002/9781118486160.ch11.

- Liu, Y. *et al.* (2012) 'Whole brain white matter changes revealed by multiple diffusion metrics in multiple sclerosis: A TBSS study', *European Journal of Radiology*. Elsevier Ireland Ltd, 81(10), pp. 2826–2832. doi: 10.1016/j.ejrad.2011.11.022.
- Lublin, F. D. (2014) 'New Multiple Sclerosis Phenotypic Classification', 72(suppl 1), pp. 1–5. doi: 10.1159/000367614.
- Muthuraman, M. *et al.* (2016) 'Structural brain network characteristics can differentiate CIS from early RRMS', *Frontiers in Neuroscience*, 10(FEB), pp. 1–12. doi: 10.3389/fnins.2016.00014.
- Onukwugha, E. *et al.* (2009) 'The total economic burden of overactive bladder in the United States: a disease-specific approach.', *The American journal of managed care*. United States, 15(4 Suppl), pp. S90-7.
- Panicker, J. (2016) 'Uroneurology', in *Neurology*. (Wiley Online Books). doi: doi:10.1002/9781118486160.ch25.
- Panicker, J. N. and Fowler, C. J. (2015) 'Lower urinary tract dysfunction in patients with multiple sclerosis.', in *Handbook of clinical neurology*. Netherlands, pp. 371–381. doi: 10.1016/B978-0-444-63247-0.00021-3.
- Panicker, J. N., Fowler, C. J. and Kessler, T. M. (2015) 'Lower urinary tract dysfunction in the neurological patient: Clinical assessment and management', *The Lancet Neurology*. Elsevier Ltd, 14(7), pp. 720–732. doi: 10.1016/S1474-4422(15)00070-8.
- Panicker, J., de Sèze, M. and Fowler, C. (2010) 'Neurogenic lower urinary tract dysfunction and its management.', *Clinical Rehabilitation*, 24(7), pp. 579-589 11p. doi: 10.1177/0269215509353252.
- Phé, V., Chartier-Kastler, E. and Panicker, J. N. (2016) 'Management of neurogenic bladder in patients with multiple sclerosis', *Nature Reviews Urology*. Nature Publishing Group, 13(5), pp. 275–288. doi: 10.1038/nrurol.2016.53.
- de Seze, M. *et al.* (2007) 'The neurogenic bladder in multiple sclerosis: review of the literature and proposal of management guidelines.', *Multiple sclerosis (Houndmills, Basingstoke, England)*. England, 13(7), pp. 915–928. doi: 10.1177/1352458506075651.
- Shu, N. *et al.* (2011) 'Diffusion tensor tractography reveals disrupted topological efficiency in white matter structural networks in multiple sclerosis.', *Cerebral cortex (New York, N.Y. : 1991)*. United States, 21(11), pp. 2565–2577. doi: 10.1093/cercor/bhr039.
- Stewart, W. F. *et al.* (2003) 'Prevalence and burden of overactive bladder in the United States.', *World journal of urology*. Germany, 20(6), pp. 327–336. doi: 10.1007/s00345-002-0301-4.
- Thompson, A. J., Banwell, B. L., *et al.* (2018) 'Diagnosis of multiple sclerosis: 2017 revisions of the McDonald criteria', 17(February). doi: 10.1016/S1474-4422(17)30470-2.
- Thompson, A. J., Baranzini, S. E., *et al.* (2018) 'Multiple sclerosis', *The Lancet*. England, 391(10130), pp. 1622–1636. doi: 10.1016/S0140-6736(18)30481-1.
- Wein, A. J. and Rovner, E. S. (2002) 'Definition and Epidemiology of Overactive Bladder', *Urology*, 60(5), pp. 7–12. doi: [https://doi.org/10.1016/S0090-4295\(02\)01784-3](https://doi.org/10.1016/S0090-4295(02)01784-3).

Chapter 3

3. Current understanding of the higher control of lower urinary tract functions

3.1. Current understanding of neurological correlates of the lower urinary tract functions

Two functions of the LUT are storage of urine and periodic emptying, depending on the amount of volume in the bladder and the social awareness (Griffiths *et al.*, 2007). To regulate the LUT functions between storage and voiding, intact neural pathways distributed across the peripheral nervous system to the CNS act as a switching circuit to maintain the coordinated activity of smooth and striated muscles of the bladder, bladder neck and urethra (Kuhtz-Buschbeck *et al.*, 2009; Griffiths, 2015). Different from the other visceral organs, learned behaviours and social appropriateness influence the LUT functions (Fowler, 2006). The CNS therefore plays a critical role in modulating LUT functions that allows individuals to consciously decide to void at an appropriate time and place (Griffiths *et al.*, 2007; Tadic *et al.*, 2008; Tadic, Griffiths, Murrin, *et al.*, 2010). However, in contrast with the other visceral organs, which could maintain a certain extent of

functioning after damage to the extrinsic innervation, the LUTS is commonly seen in neurological diseases (Panicker, 2016).

The initial idea of modulating LUT functions was from cat experiments by Barrington, indicating that the bladder activities were controlled by a series of reflexes (Barrington, 1931, 1941). With development of functional brain imaging techniques, including single-photon computerized tomography (SPECT), positron emission tomography (PET) and fMRI, functional brain imaging discoveries were made. In the past 20 years, being a non-invasive technique without exposure to radiation, fMRI was increasingly applied to study the brain function, and contributed substantially to the understanding of brain activities and the relationship between central neural control and various functions, including the LUT functions (Griffiths, 2015). At the same time, various of study paradigms were reported during the fMRI, including scanning with full and/or empty bladder, and bladder filling and/or emptying naturally and/or through a catheter.

In view of increasing knowledge contributed from functional brain imaging studies, several brain regions found in studies implicated in neural control of LUT functions, including the frontal lobes, insula and anterior cingulate gyrus, and three circuits were proposed for perception of bladder fullness (circuit 1), urinary urgency (circuit 2) and the perception when the volume in the bladder is small (circuit3; Figure 3.1). The working model of LUT control in Figure 3.1 was concluded from various imaging studies, using fMRI and PET, in different cohorts,

including health and disease, female and male, right and left handedness, and the task paradigms were distinct (Griffiths, 2015).

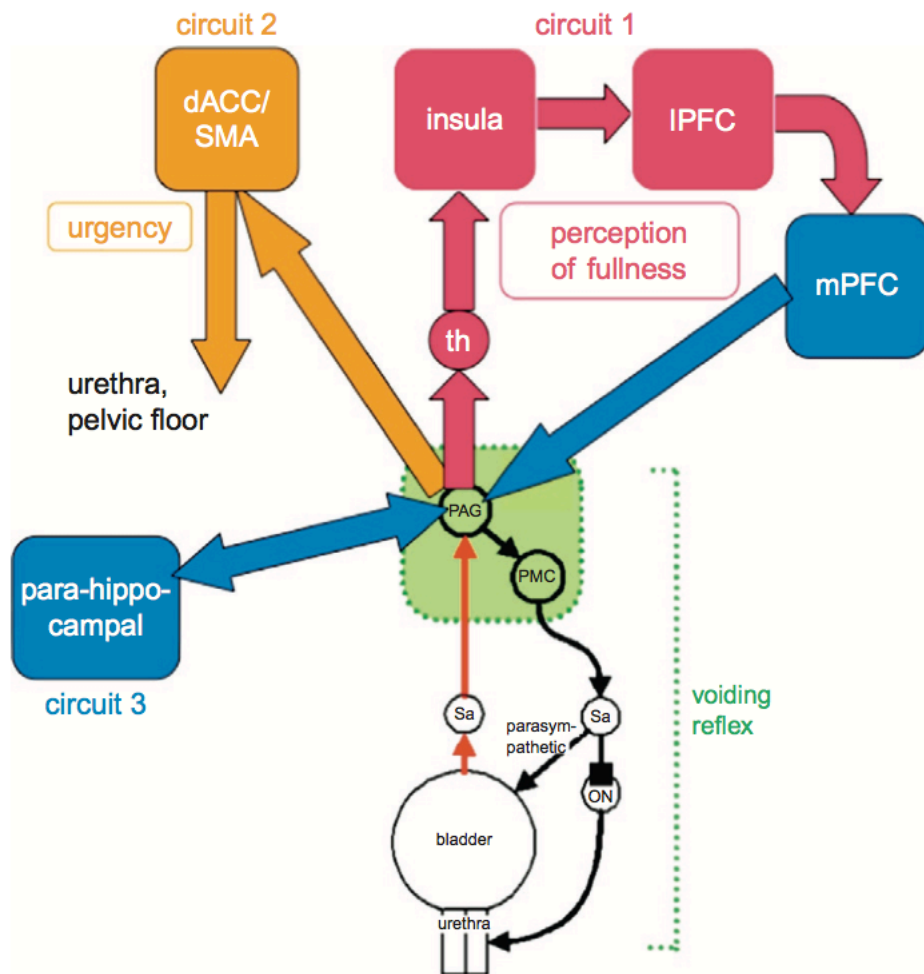
During the storage phase, the midbrain PAG is activated, while the PMC is inactive (Griffiths, 2015). Functional imaging studies show that the signals coming from the PAG inhibit the PMC during bladder filling procedure (Griffiths, 2015). In addition, the anterior cingulate gyrus and the right insula present as activated during bladder filling procedure (Griffiths, 2015). Whereas when it is considered appropriated to void, the PAG no longer exerts tonic inhibition at the PMC, and the increasing bladder afferent signals exceeding a threshold set in the brainstem can trigger the bladder contraction and the urethral sphincter relaxation, followed by an activation of the PMC (Tadic *et al.*, 2013; Griffiths, 2015). That is to say, the PAG is thought to be a relay centre for afferent signals and an informing agency for the level of bladder fullness, and the switch from filling to voiding is combined with increased activation in both the PAG and the PMC (Griffiths, 2015; Panicker, 2016). Besides, the prefrontal cortex is considered to be related to not only voiding, but also social appropriateness and complex cognitive behaviours (Panicker and Fowler, 2010).

There are multiple connections between the PAG and some higher centres, such as the insula, thalamus, cingulate and prefrontal cortex (Tadic *et al.*, 2012). As shown in Figure 3.1, the PAG receives ascending signals from the bladder and projects to the forebrain (including amygdala, hypothalamus and thalamus), and back to the bladder and urethra through the PMC, respectively (Griffiths, 2015).

The insula is considered to be involved in interoceptive awareness of visceral sensations, and the prefrontal cortex is involved in appropriate conscious of social behaviours (Panicker, Fowler and Kessler, 2015; Panicker, 2016). Besides, the anterior cingulate gyrus acts as a monitor controlling during the procedure (Griffiths and Tadic, 2008). Therefore, the prefrontal cortex helps with making decision on where and whether to void.

As discussed, the working model of LUT control is a general functional connectivity network for LUT functions in general cohort without specificity in neurological disease or symptoms of LUTS. Considering this thesis is interested in OAB symptoms in MS, the GM regions regarding LUT functions included in the working model of LUT control are possibly different from the GM regions involved in network for the OAB symptoms in MS. Moreover, as the GM regions were reported with different atlases in various studies, including the Brodmann areas, the Montreal Neurological Institute (MNI) coordinates and Talairach coordinates, it would be challenging to identify the LUT related GM regions by any specific atlas coordinates. Therefore, based on the working model of LUT control, this thesis applied broader GM regions in following analysis, rather than any specific coordinates. Table 3.1 concluded the LUT related GM regions regarding bladder filling paradigm and the coordinates abstracted from several studies involved in Griffiths' review (Kuhntz-Buschbeck *et al.*, 2005; Griffiths *et al.*, 2007; Tadic *et al.*, 2008; Tadic, Griffiths, Schaefer, *et al.*, 2010; Mehnert *et al.*, 2011; Krhut *et al.*, 2014; Griffiths, 2015). Same GM regions are presented with different coordinates in distinct studies.

Figure 3.1. Working model of the lower urinary tract control system.



A simple working model of the lower urinary tract control system, showing the voiding reflex with its rostral terminus in the brainstem (green), and circuits 1, 2, and 3 of the control networks (in red, orange, and blue respectively). The return path of circuit 1 is in blue to signify that medial prefrontal cortex (mPFC) deactivation plays an important role in continence control. dACC, dorsal anterior cingulate cortex; IPFC, lateral prefrontal cortex; ON, Onuf's nucleus; PAG, periaqueductal gray; PMC, pontine micturition center; Sa, sacral parasympathetic area; SMA, supplementary motor area; th, thalamus. (Griffiths, 2015.)

Table 3.1. The LUT related GM regions and the coordinates abstracted from different studies.

GM regions	Coordinates
anterior insula/prefrontal (right)	32, 32, -8
claustrum/insula	36/-36, 0/-6, -2/20
cingulate sulcus, superior frontal gyrus	0/0, 3/-12, 51/60
frontal (right)	38, -6, 54
frontal (right)	40, 42, 12
frontal (right), precentral gyrus	39, -10, 58 (MNI)
frontal (right), precentral gyrus	41, -3, 35 (MNI)
frontal lobe (right)	6, 15, 55 (MNI)
frontal lobe (right), paracentral lobule	15, -44, 62 (MNI)
frontal lobe (subcallosal gyrus)	-12, 26, -10
frontal lobe, medial surface (PMA)	±4, -27, 65
frontal lobe, medial surface (SMA)	±2, 2, 50
frontal operculum (left)	-54, 9, 0
frontal operculum and/or anterior insula (right)	40, 12, 10 (MNI)
inferior frontal gyrus	38, 30, 6
inferior frontal gyrus	42, 24, 0
inferior frontal gyrus	48, 8, 22
inferior frontal gyrus (left)	-39, 34, 5
inferior frontal gyrus (left)	-32, 32, -10 (MNI)
inferior frontal gyrus (right)	44, 18, 6
inferior frontal gyrus (right)	50, 12, 22
inferior frontal gyrus (right)	53, 10, 11 (MNI)
inferior frontal gyrus (right)	54, 6, 32 (MNI)
inferior frontal gyrus (right)	61, 8, 11 (MNI)
insula	-38, 12, 2
insula	32, 20, 4
insula	36, 20, 8
insula	38, 12, 4
insula	48, 6, -3
insula (left)	-52, 0, 8
insula (left)	-46, 0, 4
insula (left)	-42/-51, 3/12, -6/-6
insula (left)	-42, 4, 8

insula (left)	-34, 14, 10
insula (right)	34, 2, 10
insula (right)	34, 8, 16
insula (right)	34, 24, 4
insula (right)	38, 8, 10
insula (right)	40, -3, 14 (MNI)
insula (right)	40, 4, 4
insula (right)	42, 9, -2 (MNI)
insula (right)	47, 9, 0 (MNI)
insula (right)	50, -4, 2
insula (right)	40, 2, -10
insula/frontal operculum (right)	57, 15, -3
insula/temporal pole (right)	60, 9, -6
medial frontal gyrus	-8, -8, 56
medial frontal gyrus	-4, 60, -8
medial frontal gyrus	-2, 46, 30
medial frontal gyrus	2, 0, 58
medial frontal gyrus	4, 12, 48
medial frontal gyrus	6, 2, 58
medial frontal gyrus	10, -12, 56
medial frontal gyrus (frontal lobe)	-12, 52, 14 (MNI)
medial frontal gyrus (left)	-18, -8, 64 (MNI)
medial frontal gyrus (right)	12, -4, 62 (MNI)
medial prefrontal	18, 50, 8
medial prefrontal	6, 62, 24
middle frontal gyrus	-40, 36, 24
middle frontal gyrus	-39, 36, 18
middle frontal gyrus	-26, 28, 28
middle frontal gyrus	20, 32, 38
middle frontal gyrus	34, 40, 10
middle frontal gyrus	38, 22, 34
middle frontal gyrus (left)	-36, 38, -3
middle frontal gyrus (right)	36, 22, 34
medial/superior frontal gyrus (left)	-14, 48, 26
medial/superior frontal gyrus (left)	-8, 52, 22
orbital surface of the inferior frontal lobe, olfactory cortex, bordering the frontal cingulum	-5, 20, -10
orbitofrontal cortex (left)	-42, 48, -6

PAG	2, -30, -6
PAG	3, -27, -12
R frontal lobe, sub-gyrus	25, -6, 61 (MNI)
R frontal operculum	63, 9, 12
R insula	38, -1, 5 (MNI)
R insula	40, 14, 3
R insula	42/60, 15/15, -9/-3
R insular cortex	45, 9, -9
R middle frontal gyrus	39, 39, -2
R precentral gyrus (frontal lobe)	59, -8, 25 (MNI)
R superior frontal gyrus	8, 61, 28 (MNI)
R superior frontal gyrus	23, 25, 55 (MNI)
R thalamus	22, -21, 19
SMA (superior frontal gyrus)	14, -8, 66
subcortical grey matter nuclei of the thalamus bilaterally	±10, -16, 3
superior frontal gyrus	-38, 36, 26
superior frontal gyrus	-20, 54, 10
superior frontal gyrus	-10, 16, 58
superior frontal gyrus	-2, 16, 52
superior frontal gyrus	-2, 18, 52
superior frontal gyrus	2, 30, 52
superior frontal gyrus	6, -18, 57
superior frontal gyrus	6/-10, 50/56, 28/18
superior frontal gyrus	8, 18, 32
superior frontal gyrus (left)	-23, 41, 26
superior frontal gyrus (right)	3, 44, 50 (MNI)
superior medial frontal gyrus	0, 45, 36
thalamus	-22, -28, 2
thalamus	-10, 2, 4
thalamus	2, -2, 8
thalamus	4, -6, 8
thalamus	14, -28, 10
thalamus (left)	-8, -12, 5
Thalamus, medial nuclei, posterolateral thalamus (right)	-3/18, -18/-24, 0/9
ventrolateral thalamus (left)	-12, -12, 9

The coordinates are from Talairach atlas, unless the ones marked MNI in bracket.

MNI: Montreal Neurological Institute. The information is concluded from studies

regarding bladder filling paradigm involved in Griffiths' review (Kuhtz-Buschbeck *et al.*, 2005; Griffiths *et al.*, 2007; Tadic *et al.*, 2008; Tadic, Griffiths, Schaefer, *et al.*, 2010; Mehnert *et al.*, 2011; Krhut *et al.*, 2014; Griffiths, 2015).

In addition, a recent fMRI study compensated our understanding of brain activities during micturition in patients with MS. Regions including frontal gyrus (correlated with executive function), cingulate gyrus and parietal lobules (correlated with emotional regulation) and lentiform nucleus, putamen, cerebellum, and precuneus (correlated with motor control) were reported being activated at a strong desire of voiding (Khavari *et al.*, 2017). At an initial desire of voiding, elevated activity was shown in middle and medial frontal gyrus, supplementary motor areas, cingulate gyrus, insula, parahippocampal gyrus and subcallosal gyrus (Khavari *et al.*, 2017).

3.2. White matter structural changes leading to lower urinary tract dysfunction

Apart from studies on the neural control of LUT in GM via functional brain imaging, recent researches focusing on the cerebral WM compensate our understanding on LUT disorders in WM structural changes. Structural WM change, known as WMH, has been reported associated with urinary urgency and urinary incontinence from longitudinal studies in elder adults (Kuchel *et al.*, 2009; Tadic, Griffiths, Murrin, *et al.*, 2010). Among the WM tracts, two are reported particularly of significance: the anterior thalamic radiation, which connects the thalamus and frontal brain, another one is the superior longitudinal fasciculus, connecting the

lateral and medial parts of each side of the cortex of the superior brain (Tadic, Griffiths, Murrin, *et al.*, 2010). Besides, Kuchel *et al.* pointed that incontinence, incontinence severity and the degree of bother can be predicted by WMH in right inferior frontal regions (Kuchel *et al.*, 2009). Moreover, as the GM, including PAG, PMC, anterior cingulate gyrus, thalamus, insula and the prefrontal cortex, are identified as the areas for bladder control, the WM tracts nearby the relative GM are speculated to be involved, such as anterior corona radiata and superior fronto-occipital fasciculus (Tadic, Griffiths, Murrin, *et al.*, 2010).

In addition to the WM structural studies on LUTD in relatively elderly healthy adults, researches on WMH caused by LUTD were carried out in Alzheimer's disease, dementia, brain vascular diseases, and ischemic white matter disease (WMD; Sakakibara *et al.*, 2012; Ogama *et al.*, 2016). Frontal WM changes show a significant association with LUT dysfunction, especially urinary incontinence (Sakakibara *et al.*, 2012; Ogama *et al.*, 2016). However, geriatric impairment in LUT function, mobility and cognition level are getting notable as the age increases (Griffiths *et al.*, 2009; Wakefield *et al.*, 2010; Sakakibara *et al.*, 2014). Therefore, further LUTD dysfunction researches are expected looking into the WM changes exclusively correlated to LUTD dysfunction.

3.3. Motivation of the design for this thesis

Different brain imaging studies have advanced our understanding of the neural control of LUT functions. However, there is limited information on the role of the WM. Preliminary information suggests association between specific WM tracts

and occurrence of LUTS in small vessel disease. However, very little is understood in WM changes regarding LUT functions in neurological conditions. The non-invasive MRI technique with advanced analysis approaches, like TBSS and structural connectivity network analysis with used of DWI measures, investigating the WM changes could be used. Besides, as the OAB symptoms are the commonest LUTS in MS, the MRI measures could be correlated to clinical scores representing OAB severity. **Chapter 4** will introduce basic principles of DWI, its measures and related concepts involved in following analysis.

Bibliography

- Barrington, F. (1931) 'THE COMPONENT REFLEXES OF MICTURITION IN THE CAT. Part I and II.', *Brain*, 54(2), pp. 177–188.
- Barrington, F. (1941) 'THE COMPONENT REFLEXES OF MICTURITION IN THE CAT. Part III.', *Brain*, 64(4), pp. 239–243.
- Fowler, C. J. (2006) 'Integrated control of lower urinary tract--clinical perspective', *British journal of pharmacology*. Nature Publishing Group, 147 Suppl 2(Suppl 2), pp. S14–S24. doi: 10.1038/sj.bjp.0706629.
- Griffiths, D. *et al.* (2007) 'Cerebral control of the bladder in normal and urge-incontinent women', *Neuroimage*, 37(1), pp. 1–7.
- Griffiths, D. *et al.* (2009) 'Cerebral control of the lower urinary tract: how age-related changes might predispose to urge incontinence', *Neuroimage*, 47(5), pp. 213–223. doi: 10.1007/978-1-62703-673-3.
- Griffiths, D. (2015) *Functional imaging of structures involved in neural control of the lower urinary tract*. 1st edn, *Handbook of clinical neurology*. 1st edn. Elsevier B.V. doi: 10.1016/B978-0-444-63247-0.00007-9.
- Griffiths, D. and Tadic, S. D. (2008) 'Bladder control, urgency, and urge incontinence: evidence from functional brain imaging.', *Neurourology and urodynamics*. United States, 27(6), pp. 466–474. doi: 10.1002/nau.20549.
- Khavari, R. *et al.* (2017) 'Functional Magnetic Resonance Imaging with Concurrent Urodynamic Testing Identifies Brain Structures Involved in Micturition Cycle in Patients with Multiple Sclerosis', *Journal of Urology*. Elsevier Ltd, 197(2), pp. 438–444. doi: 10.1016/j.juro.2016.09.077.
- Krhut, J. *et al.* (2014) 'Brain activity during bladder filling and pelvic floor muscle contractions: A study using functional magnetic resonance imaging and synchronous urodynamics', *International Journal of Urology*. John Wiley & Sons, Ltd (10.1111), 21(2), pp. 169–174. doi: 10.1111/iju.12211.
- Kuchel, G. A. *et al.* (2009) 'Localization of Brain White Matter Hyperintensities and Urinary Incontinence in Community-Dwelling Older Adults', *The Journals of Gerontology Series A: Biological Sciences and Medical Sciences*, 64A(8), pp. 902–909. doi: 10.1093/gerona/glp037.
- Kuhtz-Buschbeck, J. P. *et al.* (2005) 'Cortical representation of the urge to void: A functional magnetic resonance imaging study', *Journal of Urology*, 174(4 I), pp. 1477–1481. doi: 10.1097/01.ju.0000173007.84102.7c.
- Kuhtz-Buschbeck, J. P. *et al.* (2009) 'Control of bladder sensations: an fMRI study of brain activity and effective connectivity.', *NeuroImage*. United States, 47(1), pp. 18–27. doi: 10.1016/j.neuroimage.2009.04.020.
- Mehnert, U. *et al.* (2011) 'The supraspinal neural correlate of bladder cold sensation—An fMRI study', *Human Brain Mapping*. John Wiley & Sons, Ltd, 32(6), pp. 835–845. doi: 10.1002/hbm.21070.
- Ogama, N. *et al.* (2016) 'Frontal white matter hyperintensity predicts lower urinary tract dysfunction in older adults with amnesic mild cognitive impairment and Alzheimer's disease.', *Geriatrics & gerontology international*. Japan, 16(2), pp. 167–174. doi: 10.1111/ggi.12447.
- Panicker, J. (2016) 'Uroneurology', in *Neurology*. (Wiley Online Books). doi: 10.1002/9781118486160.ch25.
- Panicker, J. N. and Fowler, C. J. (2010) 'The bare essentials: Uro-Neurology', *Practical Neurology*, 10(3), pp. 178–185. doi: 10.1136/jnnp.2010.213892.
- Panicker, J. N., Fowler, C. J. and Kessler, T. M. (2015) 'Lower urinary tract dysfunction in the neurological patient: Clinical assessment and

- management', *The Lancet Neurology*. Elsevier Ltd, 14(7), pp. 720–732. doi: 10.1016/S1474-4422(15)00070-8.
- Sakakibara, R. *et al.* (2012) 'Vascular incontinence: incontinence in the elderly due to ischemic white matter changes.', *Neurology international*. Italy, 4(2), p. e13. doi: 10.4081/ni.2012.e13.
- Sakakibara, R. *et al.* (2014) 'Is overactive bladder a brain disease? The pathophysiological role of cerebral white matter in the elderly', *International Journal of Urology*, 21(1), pp. 33–38. doi: 10.1111/iju.12288.
- Tadic, Griffiths, Murrin, *et al.* (2010) 'Brain Activity During Bladder Filling Is Related To White Matter Structural Changes in Older Women with Urinary Incontinence', *Neuroimage*, 51(4), pp. 1294–1302. doi: 10.1016/j.neuroimage.2010.03.016.BRAIN.
- Tadic, Griffiths, Schaefer, W., *et al.* (2010) 'Brain activity measured by functional magnetic resonance imaging (fMRI) is related to patient reports and clinical severity of Urge urinary incontinence', *Neurourology and Urodynamics*, 28(7), pp. 841–842. doi: 10.1002/nau.20808.
- Tadic, S. *et al.* (2013) 'Brain responses to bladder filling in older women without urgency incontinence.', *Neurourology and urodynamics*. United States, 32(5), pp. 435–440. doi: 10.1002/nau.22320.
- Tadic, S. D. *et al.* (2008) 'Abnormal connections in the supraspinal bladder control network in women with urge urinary incontinence.', *Neuroimage*, 39(4), pp. 1647–1653.
- Tadic, S. D. *et al.* (2012) 'Brain activity underlying impaired continence control in older women with overactive bladder', *Neurourology and Urodynamics*, 31(5), pp. 652–658. doi: 10.1002/nau.21240.
- Wakefield, D. B. *et al.* (2010) 'White matter hyperintensities predict functional decline in voiding, mobility, and cognition in older adults', *Journal of the American Geriatrics Society*, 58(2), pp. 275–281. doi: 10.1111/j.1532-5415.2009.02699.x.

Chapter 4

4. Diffusion-weighted imaging and related analysis approaches

4.1. Basic principles of diffusion-weighted imaging in neuroscience research

Unlike the conventional T1-weighted and T2-weighted MRI sequences, DWI, based on the microscopic random motion of water, is a non-conventional MRI tool used to measure the microscopic properties of neural tissues and indicate the pathophysiological basis in neural changes (Newcombe, Das and Cross, 2013; Aliotta *et al.*, 2014). By providing the numerical values of parameters from the imaging, the clinical correlation, such as the cerebral infarction, tumours, axonal integrity and myelin sheaths, can be identified (Newcombe, Das and Cross, 2013).

In recent studies, DWI is used extensively in WM tractography (structural connectivity in brain), because the diffusion of water in WM is highly anisotropic (directional; Mori and Zhang, 2006). Aligning with WM tract, the speed of water

molecules diffusion will be more rapidly, while it will be slowly in the perpendicular directions (Mori and Zhang, 2006). Therefore, water motion is almost not restricted in cerebrospinal fluid (CSF), less restricted in the GM and markedly restricted in WM. Several scalar indices (fractional anisotropy, FA; mean diffusivity, MD; axial diffusivity, AD or Da; radial diffusivity, RD or Dr), quantifying the water diffusion direction, are commonly used to characterize the diffusion tensor (Liu *et al.*, 2012; Aliotta *et al.*, 2014). In this thesis, FA was selected to represent the diffusion tensor as it was the widely accepted index in diffusion imaging analysis and the commonest used one in TBSS studies. However, it is deserved to identify the diffusion tensor by other indices, and this will be one of the future directions.

By measuring the anisotropic water diffusion, FA is calculated from three eigenvalues (λ_1 , λ_2 and λ_3 , known as the length of the axis in the tensor), and gives the degree of directionality of cellular structures in WM tracts (Le Bihan *et al.*, 2001; Alexander *et al.*, 2007; Liu *et al.*, 2012). FA ranges between 0 and 1: 0 means the diffusion is completely isotropic in all directions, and 1 means the diffusion is restricted in all the other directions except one axis (Newcombe, Das and Cross, 2013). MD measures the diffusion in the noncolinear free diffusion, namely the overall water mobility without directionality (Le Bihan *et al.*, 2001; Liu *et al.*, 2012). AD is believed to show information on axonal integrity, which indicates the changes in extra-axonal space (Beaulieu and Allen, 1994; Knake *et al.*, 2010). Different from AD, RD is a parameter giving the degree of myelination (Song *et al.*, 2002, 2003; Davis *et al.*, 2009; Knake *et al.*, 2010). Based on the previous studies, FA and MD are the most frequently used indices in analysis,

whereas AD and RD are more specifically used to identify the integrity of axon and myelin, respectively (Song *et al.*, 2005; Sun *et al.*, 2007; Budde *et al.*, 2008; Liu *et al.*, 2012).

4.2. Common artefacts during MRI acquisition

MRI artefacts, which are not in the original objects, can present during MRI acquisition. The artefacts need to be corrected to improve the research quality. The artefacts involved in this thesis are introduced below.

Bias field

Bias field is caused by the sensitivity of the receiver coil, leading to intensity inhomogeneity occurring in the same physical property (Despotovic, Goossens and Philips, 2015). The variation needs to be mapped out and removed in structural scans.

Motion artefacts

Motion artefacts happens when the subject has voluntary or involuntary movement during MRI acquisition, including respiration, cardiac motion, blood flow, swallowing and movements of head, resulting in blurred images (Zaitsev, Maclaren and Herbst, 2015).

Eddy currents

For DWI, additional strong magnetic field gradients are added, and the magnetic field gradients are changing rapidly, using echo planar imaging (EPI). The additional currents caused by the gradients are named as eddy currents, and it can cause unwanted time-varying gradients leading to image shearing, shading and blurring (Spees *et al.*, 2011). Besides, the EPI, which is sensitive to magnetic field inhomogeneities, can cause image geometric distortion at areas between CSF, brain tissue and skull (Poustchi-Amin *et al.*, 2001).

4.3. Brain network analysis

Network analysis is an approach to study the brain, and the brain network consist of nodes (brain GM regions) and edges linking between edges. A network matrix will be created when nodes and edges are identified, and some measures can be derived from network matrix to represent the network characters.

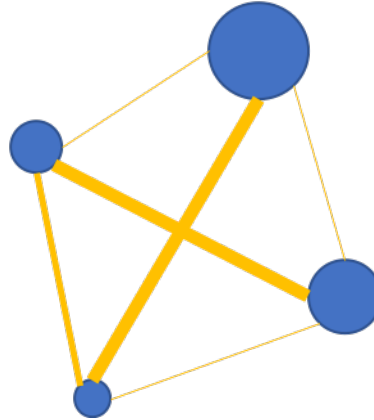
Network nodes

The network nodes are anatomical brain GM regions parcellated on the T1-weighted image. There is no standard parcellation criteria, but ideally, both the structural and functional information should be taken into account (Craddock *et al.*, 2013; Arslan *et al.*, 2018). In this thesis, the Geodesic Information Flows (GIF) software was applied in this thesis to define the network nodes, according to the Desikan-Killiany-Tourville atlas (Cardoso *et al.*, 2015).

Network edges

The network edges are links between each pair of nodes, and ideally, they can represent the biological information of the axons. An approach called constrained spherical deconvolution (CSD), which can estimate fibre orientation, is applied to test the response function, representing the orientation of the fibre bundle (Tournier *et al.*, 2004; Tournier, Calamante and Connelly, 2007). A probabilistic tractography can be reconstructed with the interested GM regions and the edges (streamlines). To give the streamlines anatomical priors, the anatomically constrained tractography (ACT) framework is applied (Smith *et al.*, 2012) and the spherical-deconvolution informed filtering of tractograms (SIFT2) is used to reweight the generated streamlines to correct the density (thickness; Smith *et al.*, 2015a, 2015b).

Figure 4.1. A model graph of tractogram.

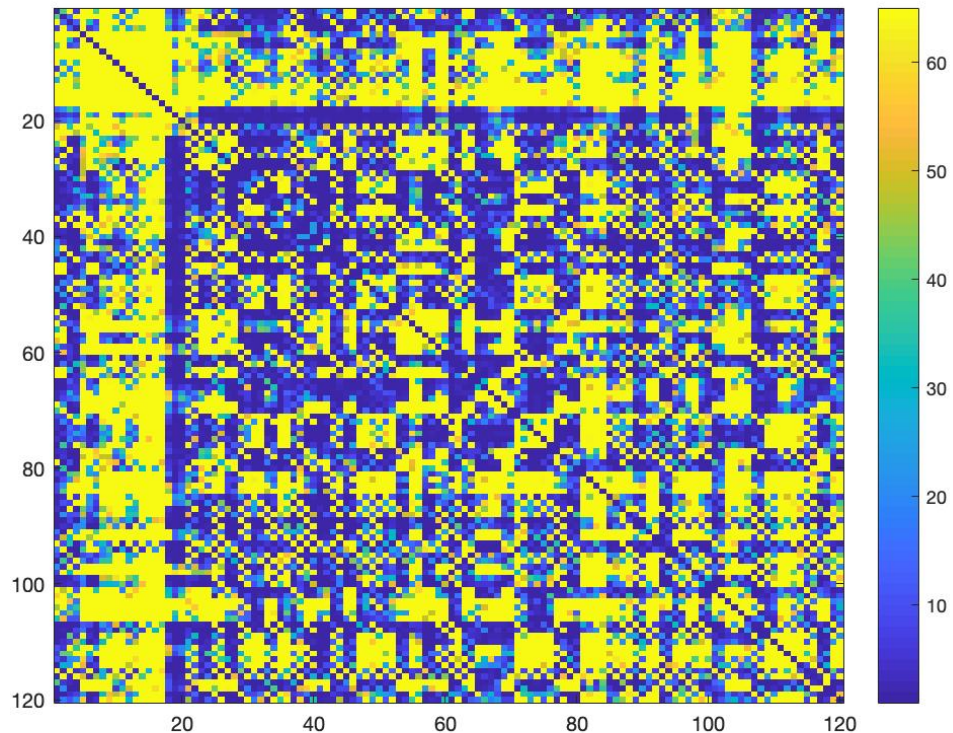


Nodes are in blue and edges are in yellow. Different thickness of the edges represents different weights of the streamlines. The thicker edges, the higher weights.

Network matrix

With the nodes and edges, a connectivity matrix can be drawn with Matlab. Figure 4.2 provides an example of the connectivity matrix.

Figure 4.2. An example of brain connectome matrix.



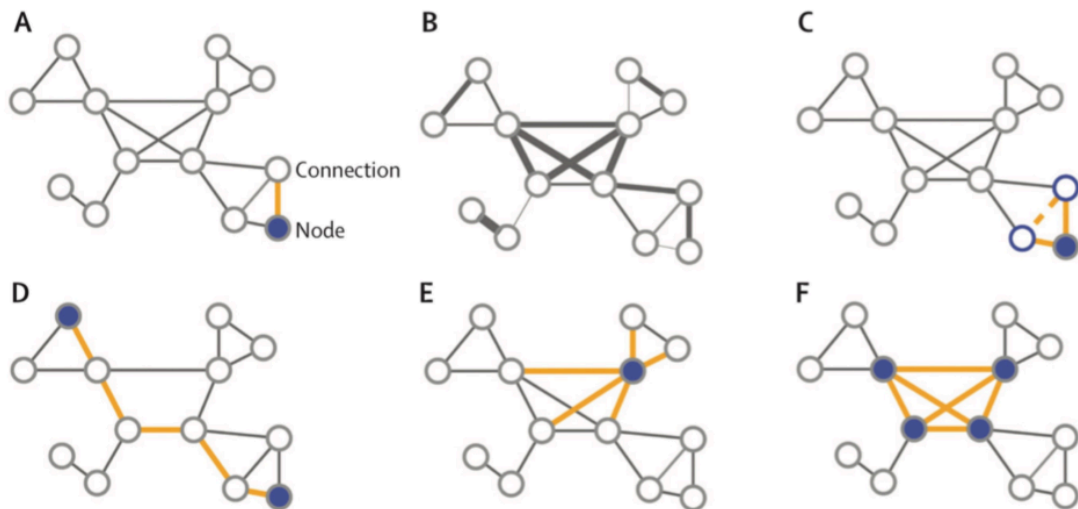
The connectome matrix demonstrates an example of the brain connectivity matrix consisting of nodes and streamlines connecting each pair of nodes. The number on x and y axes refer to the nodes and the elements in the matrix refer to the number of streamlines between a pair of nodes. The main diagonal is zero, meaning that the self-connection is not taken into account.

Measures of the network characters

After network reconstruction, several quantitative measures can be derived representing the characters, such as integration and segregation, of the network (Rubinov and Sporns, 2010). The measures are calculated by the Brain Connectivity Toolbox (BCT; Rubinov and Sporns, 2010) and there are several

network indices measuring network characters. In this thesis, six measures were selected, including degree (DEG), betweenness centrality (BC), cluster coefficient (CC), participation coefficient (PC), local efficiency (LE) and global efficiency (GE). They were the commonest used network measures in previous network studies and could typically represent the basic concept of the nodes, network centrality, integration and segregation (Rubinov and Sporns, 2010). The DEG provides the number of links connected to a node (Rubinov and Sporns, 2010); the BC is the fraction of all shortest paths in the network that contain a given node, and nodes with high values of BC participate in a large number of shortest paths (Rubinov and Sporns, 2010); the PC is a measure of diversity of intermodular connections of individual nodes (Rubinov and Sporns, 2010); the GE offers the average inverse shortest path length in the network, and it is inversely related to the characteristic path length (Latora and Marchiori, 2001); the LE is the global efficiency computed on the neighbourhood of the node, and is related to the clustering coefficient (Rubinov and Sporns, 2010); the CC is the fraction of the triangles around a node (Watts and Strogatz, 1998). Figure 4.3 presents a graphic summary of the connectivity measures.

Figure 4.3. Summary of the main measures estimated with graph analysis.



(A) A graph is composed of nodes and edges (connections). **(B)** A weighted graph provides information regarding the strength of the connection. Higher connection weights are represented by thicker lines **(C)** The clustering coefficient describes the tendency of the nodes to form local triangles and it is a measure of local connectivity. **(D)** The shortest path length describes the minimum number of steps required to communicate between two nodes and it provides insights into the communication efficiency between those nodes. **(E)** The degree of the node describes the number of existing connections of that node. A node with many connections will have a more central role in the network and it may suggest the existence of hub nodes. **(F)** The “rich-club” organization describes the tendency of hub nodes to be more closely connected among themselves. For each metric the node and edge of interest is always highlighted. (Filippi *et al.*, 2013.)

4.4. Applications of diffusion-weighted imaging in multiple sclerosis

The disabling symptoms of MS are caused by inflammatory demyelinating lesions in the WM tracts, and demyelination and axonal loss in GM (Sakakibara *et al.*, 2012; Ogama *et al.*, 2016). MRI researches indicate increasingly knowledge on brain structure and function (Smith *et al.*, 2004, 2006). With a number of MRI investigations and different statistical techniques, the pathophysiological damages in MS patients are able to be investigated. The MRI data analysing techniques, combining the structural and functional imaging data with various sources of clinical information, offer pathophysiological basis of the brain and the spinal cord (Smith *et al.*, 2004). For example, an approach called TBSS is widely used for analysis of the diffusivity in WM via DWI.

DWI indices are sensitive to WM damage in MS and FA is the most commonly used in the relative studies, looking into the voxel-wise results, to identify the areas correlated to brain changes (Smith *et al.*, 2006; Ontaneda *et al.*, 2014). However, the standard registration cannot align all the FA images from multiple subjects in an optimal way to be drawn from the subsequent voxel-wise analysis (Smith *et al.*, 2006). Another obstacle is the arbitrariness choice of spatial smoothing extent (Smith *et al.*, 2006). With the use of TBSS, the nonlinear registration can be tuned carefully by aligning all FA images to a 1x1x1mm standard space, and project onto an alignment-invariant tract representation (the “mean FA skeleton”; Bach *et al.*, 2014). Therefore, TBSS approach helps to make multiple subject DWI studies become sensitive, objective and interpretive.

In WM studies of MS, decreased FA and increased MD have been detected in WM, regardless the clinical subtypes (Sbardella *et al.*, 2013). RD will be increased due to the loss of myelin (Fink *et al.*, 2010). However, either increased or decreased AD has been demonstrated in previous studies (Sbardella *et al.*, 2013). Axonal loss can result in a decreased AD and a compensative mechanism maintaining functionality when there are WM damages can lead to an increased AD (Fink *et al.*, 2010). In general, the pathological damage and the degree of disability is more pronounced in definite MS in adults than in children and CIS (Sbardella *et al.*, 2013). Nevertheless, compared with healthy subjects, research suggests that increased RD and MD, and decreased FA and AD are presented in both paediatric subjects and CIS patients (Gallo *et al.*, 2005; Henry *et al.*, 2009; Preziosa *et al.*, 2011; Tillema, Leach and Pirko, 2012). Those changes can be treated as an early sign of WM damage (Sbardella *et al.*, 2013). Compared with CIS, RRMS, PPMS and SPMS have greater WM diffusion abnormalities (Castriota Scanderbeg *et al.*, 2000; Preziosa *et al.*, 2011; Braley *et al.*, 2012). Moreover, diffusivity change demonstrated in SPMS is greater than in RRMS and PPMS, which can be due to the more pronounced axonal loss and more advanced phase of inflammatory (Castriota Scanderbeg *et al.*, 2000; Rovaris *et al.*, 2002; Sijens *et al.*, 2005; Preziosa *et al.*, 2011). Furthermore, studies on regions of diffusivity changes in MS compared to healthy subjects have been conducted. Contrast to healthy group, significant lower FA and higher MD are identified in a number of brain areas (mostly bilaterally), including most parts of the corpus callosum, the cingulum bundles, the internal capsules, the inferior longitudinal fasciculus, the optic radiation, the left corona radiata and the right

corticospinal tract down to the level cerebral peduncles (Ciccarelli *et al.*, 2003; Roosendaal *et al.*, 2009).

DWI has been applied to explore the pathophysiology of different neurological disabilities in MS, such as motor impairment and cognitive dysfunction. Studies were carried out to show the correlation between diffusivity changes and clinical scores. Factors including disability, bladder and bowel dysfunctions, and cognitive symptoms are reported to be worsening as the progression of the disease and have significant effects on quality of life (Lobentanz *et al.*, 2004). As a characteristic symptom in MS, motor function is concerned as an evidence for the disease severity and provides indication for proper managements (Kurtzke, 1983; Kern *et al.*, 2011). A TBSS study on motor impairment in RRMS reported that decreased FA mainly in corpus callosum was correlated to worse performance in mobility assessment with nine-hole peg test (NHPT) bilaterally (Kern *et al.*, 2011). Moreover, decreased FA in the mid-posterior corona radiata is related to the right-hand performance, and change in the occipital WM is related to the left side (Kern *et al.*, 2011). Regarding the cognitive dysfunctions, SPMS is found with greater degree than RRMS, linking with more severe WM changes (Chiaravalloti and DeLuca, 2008; Francis *et al.*, 2014). Loss of WM integrity was reported widespread in MS group and lower FA in regions including the fornix, superior longitudinal fasciculus and forceps major was observed due to more severe WM damage (Meijer *et al.*, 2016).

In addition to diffusion measures, a recent connectivity study reported the structural network disruption markers explaining disability in MS (Charalambous *et al.*, 2018). The CC, LE and GE were compared between MS and healthy people and they were all decreased in MS group, and the reduction was significantly driven by the decrease of the network measures in SPMS (Charalambous *et al.*, 2018). The network density and GE properly explained the MS disability rather than non-network measures, and highlighted the association between clinical information and network measures (Charalambous *et al.*, 2018).

4.5. Research scheme of this thesis

The advanced MRI techniques and analysis methods, and the successful use of the methods in MS studies, provided possible application to investigate the LUT functions. Keeping the aims of this work in mind, the subsequent chapters in this thesis investigate the WM abnormalities subtending the OAB symptoms in MS using TBSS and brain connectivity network approaches. **Chapter 5** will present the WM changes using TBSS without any prior assumption. **Chapter 6-7** create a structural connectivity network in MS with OAB symptoms by reconstructing a whole brain connectivity network (**chapter 6**), generating the structural network subtending OAB in MS (MS-OAB-network; **chapter 7**) and comparing the MS-OAB-network with the working model of LUT control (**chapter 7**).

Bibliography

- Alexander, A. L. *et al.* (2007) 'Diffusion tensor imaging of the brain.', *Neurotherapeutics: the journal of the American Society for Experimental NeuroTherapeutics*. United States, 4(3), pp. 316–329. doi: 10.1016/j.nurt.2007.05.011.
- Aliotta, R. *et al.* (2014) 'Tract-based spatial statistics analysis of diffusion-tensor imaging data in pediatric- and adult-onset multiple sclerosis', *Human Brain Mapping*, 35(1), pp. 53–60. doi: 10.1002/hbm.22148.
- Arslan, S. *et al.* (2018) 'Human brain mapping: A systematic comparison of parcellation methods for the human cerebral cortex.', *NeuroImage*. United States, 170, pp. 5–30. doi: 10.1016/j.neuroimage.2017.04.014.
- Bach, M. *et al.* (2014) 'Methodological considerations on tract-based spatial statistics (TBSS).', *NeuroImage*. United States, 100, pp. 358–369. doi: 10.1016/j.neuroimage.2014.06.021.
- Beaulieu, C. and Allen, P. S. (1994) 'Determinants of anisotropic water diffusion in nerves.', *Magnetic resonance in medicine*. United States, 31(4), pp. 394–400.
- Le Bihan, D. *et al.* (2001) 'Diffusion tensor imaging: concepts and applications.', *Journal of magnetic resonance imaging: JMRI*. United States, 13(4), pp. 534–546.
- Braley, T. J. *et al.* (2012) 'Differences in diffusion tensor imaging-derived metrics in the corpus callosum of patients with multiple sclerosis without and with gadolinium-enhancing cerebral lesions.', *Journal of computer assisted tomography*. United States, 36(4), pp. 410–415. doi: 10.1097/RCT.0b013e31825c6cee.
- Budde, M. D. *et al.* (2008) 'Axonal injury detected by in vivo diffusion tensor imaging correlates with neurological disability in a mouse model of multiple sclerosis.', *NMR in biomedicine*. England, 21(6), pp. 589–597. doi: 10.1002/nbm.1229.
- Cardoso, M. J. *et al.* (2015) 'Geodesic Information Flows: Spatially-Variant Graphs and Their Application to Segmentation and Fusion.', *IEEE transactions on medical imaging*. United States, 34(9), pp. 1976–1988. doi: 10.1109/TMI.2015.2418298.
- Castriota Scanderbeg, A. *et al.* (2000) 'Demyelinating plaques in relapsing-remitting and secondary-progressive multiple sclerosis: assessment with diffusion MR imaging.', *AJNR. American journal of neuroradiology*. United States, 21(5), pp. 862–868.
- Charalambous, T. *et al.* (2018) 'Structural network disruption markers explain disability in multiple sclerosis', *Journal of Neurology, Neurosurgery, and Psychiatry*, pp. 219–226. doi: 10.1136/jnnp-2018-318440.
- Chiaravalloti, N. D. and DeLuca, J. (2008) 'Cognitive impairment in multiple sclerosis.', *The Lancet. Neurology*. England, 7(12), pp. 1139–1151. doi: 10.1016/S1474-4422(08)70259-X.
- Ciccarelli, O. *et al.* (2003) 'A study of the mechanisms of normal-appearing white matter damage in multiple sclerosis using diffusion tensor imaging--evidence of Wallerian degeneration.', *Journal of neurology*. Germany, 250(3), pp. 287–292. doi: 10.1007/s00415-003-0992-5.
- Craddock, R. C. *et al.* (2013) 'Imaging human connectomes at the macroscale.', *Nature methods*. United States, 10(6), pp. 524–539. doi: 10.1038/nmeth.2482.

- Davis, S. W. *et al.* (2009) 'Assessing the effects of age on long white matter tracts using diffusion tensor tractography.', *NeuroImage*. United States, 46(2), pp. 530–541.
- Despotovic, I., Goossens, B. and Philips, W. (2015) 'MRI segmentation of the human brain: challenges, methods, and applications.', *Computational and mathematical methods in medicine*. United States, 2015, p. 450341. doi: 10.1155/2015/450341.
- Filippi, M. *et al.* (2013) 'Assessment of system dysfunction in the brain through MRI-based connectomics.', *The Lancet. Neurology*. England, 12(12), pp. 1189–1199. doi: 10.1016/S1474-4422(13)70144-3.
- Fink, F. *et al.* (2010) 'Comparison of diffusion tensor-based tractography and quantified brain atrophy for analyzing demyelination and axonal loss in MS.', *Journal of neuroimaging : official journal of the American Society of Neuroimaging*. United States, 20(4), pp. 334–344. doi: 10.1111/j.1552-6569.2009.00377.x.
- Francis, P. L. *et al.* (2014) 'Extensive white matter dysfunction in cognitively impaired patients with secondary-progressive multiple sclerosis.', *AJNR. American journal of neuroradiology*. United States, 35(10), pp. 1910–1915. doi: 10.3174/ajnr.A3974.
- Gallo, A. *et al.* (2005) 'Diffusion-tensor magnetic resonance imaging detects normal-appearing white matter damage unrelated to short-term disease activity in patients at the earliest clinical stage of multiple sclerosis.', *Archives of neurology*. United States, 62(5), pp. 803–808. doi: 10.1001/archneur.62.5.803.
- Henry, R. G. *et al.* (2009) 'Connecting white matter injury and thalamic atrophy in clinically isolated syndromes.', *Journal of the neurological sciences*. Netherlands, 282(1–2), pp. 61–66. doi: 10.1016/j.jns.2009.02.379.
- Kern, K. C. *et al.* (2011) 'Corpus callosal diffusivity predicts motor impairment in relapsing-remitting multiple sclerosis: A TBSS and tractography study', *NeuroImage*. Elsevier Inc., 55(3), pp. 1169–1177. doi: 10.1016/j.neuroimage.2010.10.077.
- Knake, S. *et al.* (2010) 'In vivo demonstration of microstructural brain pathology in progressive supranuclear palsy: a DTI study using TBSS.', *Movement disorders : official journal of the Movement Disorder Society*. United States, 25(9), pp. 1232–1238. doi: 10.1002/mds.23054.
- Kurtzke, J. F. (1983) 'Rating neurologic impairment in multiple sclerosis: An expanded disability status scale (EDSS)', *Neurology*, 33(11), pp. 1444–1444. doi: 10.1212/WNL.33.11.1444.
- Latora, V. and Marchiori, M. (2001) 'Efficient behavior of small-world networks.', *Physical review letters*. United States, 87(19), p. 198701. doi: 10.1103/PhysRevLett.87.198701.
- Liu, Y. *et al.* (2012) 'Whole brain white matter changes revealed by multiple diffusion metrics in multiple sclerosis: A TBSS study', *European Journal of Radiology*. Elsevier Ireland Ltd, 81(10), pp. 2826–2832. doi: 10.1016/j.ejrad.2011.11.022.
- Lobentanz, I. S. *et al.* (2004) 'Factors influencing quality of life in multiple sclerosis patients: disability, depressive mood, fatigue and sleep quality.', *Acta neurologica Scandinavica*. Denmark, 110(1), pp. 6–13. doi: 10.1111/j.1600-0404.2004.00257.x.
- Meijer, K. A. *et al.* (2016) 'White matter tract abnormalities are associated with cognitive dysfunction in secondary progressive multiple sclerosis.', *Multiple sclerosis (Houndmills, Basingstoke, England)*. England, 22(11),

- pp. 1429–1437. doi: 10.1177/1352458515622694.
- Mori, S. and Zhang, J. (2006) 'Principles of Diffusion Tensor Imaging and Its Applications to Basic Neuroscience Research', *Neuron*, 51(5), pp. 527–539. doi: 10.1016/j.neuron.2006.08.012.
- Newcombe, V. F. J., Das, T. and Cross, J. J. (2013) 'Diffusion imaging in neurological disease', *Journal of Neurology*, 260(1), pp. 335–342. doi: 10.1007/s00415-012-6769-y.
- Ogama, N. *et al.* (2016) 'Frontal white matter hyperintensity predicts lower urinary tract dysfunction in older adults with amnesic mild cognitive impairment and Alzheimer's disease.', *Geriatrics & gerontology international*. Japan, 16(2), pp. 167–174. doi: 10.1111/ggi.12447.
- Ontaneda, D. *et al.* (2014) 'Identifying the start of multiple sclerosis injury: a serial DTI study.', *Journal of neuroimaging : official journal of the American Society of Neuroimaging*. United States, 24(6), pp. 569–576. doi: 10.1111/jon.12082.
- Poustchi-Amin, M. *et al.* (2001) 'Principles and applications of echo-planar imaging: a review for the general radiologist.', *Radiographics : a review publication of the Radiological Society of North America, Inc.* United States, 21(3), pp. 767–779. doi: 10.1148/radiographics.21.3.g01ma23767.
- Preziosa, P. *et al.* (2011) 'Intrinsic damage to the major white matter tracts in patients with different clinical phenotypes of multiple sclerosis: a voxelwise diffusion-tensor MR study.', *Radiology*. United States, 260(2), pp. 541–550. doi: 10.1148/radiol.11110315.
- Roosendaal, S. D. *et al.* (2009) 'Regional DTI differences in multiple sclerosis patients.', *NeuroImage*. United States, 44(4), pp. 1397–1403. doi: 10.1016/j.neuroimage.2008.10.026.
- Rovaris, M. *et al.* (2002) 'Assessment of normal-appearing white and gray matter in patients with primary progressive multiple sclerosis: a diffusion-tensor magnetic resonance imaging study.', *Archives of neurology*. United States, 59(9), pp. 1406–1412.
- Rubinov, M. and Sporns, O. (2010) 'NeuroImage Complex network measures of brain connectivity : Uses and interpretations', *NeuroImage*. Elsevier Inc., 52(3), pp. 1059–1069. doi: 10.1016/j.neuroimage.2009.10.003.
- Sakakibara, R. *et al.* (2012) 'Vascular incontinence: incontinence in the elderly due to ischemic white matter changes.', *Neurology international*. Italy, 4(2), p. e13. doi: 10.4081/ni.2012.e13.
- Sbardella, E. *et al.* (2013) 'DTI Measurements in Multiple Sclerosis: Evaluation of Brain Damage and Clinical Implications', *Multiple Sclerosis International*, 2013, pp. 1–11. doi: 10.1155/2013/671730.
- Sijens, P. E. *et al.* (2005) 'Analysis of the human brain in primary progressive multiple sclerosis with mapping of the spatial distributions using 1H MR spectroscopy and diffusion tensor imaging.', *European radiology*. Germany, 15(8), pp. 1686–1693. doi: 10.1007/s00330-005-2775-0.
- Smith, R. E. *et al.* (2012) 'Anatomically-constrained tractography: improved diffusion MRI streamlines tractography through effective use of anatomical information.', *NeuroImage*. United States, 62(3), pp. 1924–1938. doi: 10.1016/j.neuroimage.2012.06.005.
- Smith, R. E. *et al.* (2015a) 'SIFT2: Enabling dense quantitative assessment of brain white matter connectivity using streamlines tractography.', *NeuroImage*. United States, 119, pp. 338–351. doi: 10.1016/j.neuroimage.2015.06.092.

- Smith, R. E. *et al.* (2015b) 'The effects of SIFT on the reproducibility and biological accuracy of the structural connectome.', *NeuroImage*. United States, 104, pp. 253–265. doi: 10.1016/j.neuroimage.2014.10.004.
- Smith, S. M. *et al.* (2004) 'Advances in functional and structural MR image analysis and implementation as FSL.', *NeuroImage*. United States, 23 Suppl 1, pp. S208-19. doi: 10.1016/j.neuroimage.2004.07.051.
- Smith, S. M. *et al.* (2006) 'Tract based spatial statistics: voxelwise analysis of multi-subjects diffusion data', *NeuroImage*, 31(4), pp. 1487–1505. doi: 10.1016/j.neuroimage.2006.02.024.
- Song, S.-K. *et al.* (2002) 'Dysmyelination revealed through MRI as increased radial (but unchanged axial) diffusion of water.', *NeuroImage*. United States, 17(3), pp. 1429–1436.
- Song, S.-K. *et al.* (2003) 'Diffusion tensor imaging detects and differentiates axon and myelin degeneration in mouse optic nerve after retinal ischemia.', *NeuroImage*. United States, 20(3), pp. 1714–1722.
- Song, S.-K. *et al.* (2005) 'Demyelination increases radial diffusivity in corpus callosum of mouse brain.', *NeuroImage*. United States, 26(1), pp. 132–140. doi: 10.1016/j.neuroimage.2005.01.028.
- Spees, W. M. *et al.* (2011) 'Quantification and compensation of eddy-current-induced magnetic-field gradients.', *Journal of magnetic resonance (San Diego, Calif. : 1997)*. United States, 212(1), pp. 116–123. doi: 10.1016/j.jmr.2011.06.016.
- Sun, S.-W. *et al.* (2007) 'Selective vulnerability of cerebral white matter in a murine model of multiple sclerosis detected using diffusion tensor imaging.', *Neurobiology of disease*. United States, 28(1), pp. 30–38. doi: 10.1016/j.nbd.2007.06.011.
- Tillema, J. M., Leach, J. and Pirko, I. (2012) 'Non-lesional white matter changes in pediatric multiple sclerosis and monophasic demyelinating disorders.', *Multiple sclerosis (Houndmills, Basingstoke, England)*. England, 18(12), pp. 1754–1759. doi: 10.1177/1352458512447527.
- Tournier, J.-D. *et al.* (2004) 'Direct estimation of the fiber orientation density function from diffusion-weighted MRI data using spherical deconvolution.', *NeuroImage*. United States, 23(3), pp. 1176–1185. doi: 10.1016/j.neuroimage.2004.07.037.
- Tournier, J.-D., Calamante, F. and Connelly, A. (2007) 'Robust determination of the fibre orientation distribution in diffusion MRI: non-negativity constrained super-resolved spherical deconvolution.', *NeuroImage*. United States, 35(4), pp. 1459–1472. doi: 10.1016/j.neuroimage.2007.02.016.
- Watts, D. J. and Strogatz, S. H. (1998) 'Collective dynamics of "small-world" networks.', *Nature*. England, 393(6684), pp. 440–442. doi: 10.1038/30918.
- Zaitsev, M., Maclaren, J. and Herbst, M. (2015) 'Motion artifacts in MRI: A complex problem with many partial solutions.', *Journal of magnetic resonance imaging: JMRI*. United States, 42(4), pp. 887–901. doi: 10.1002/jmri.24850.

Chapter 5

5. Exploring association between white matter changes and overactive bladder symptoms in multiple sclerosis with diffusion MRI

Summary

This chapter internally validates the application of TBSS analysis in our study, establishes the association between OAB symptoms and WM changes using diffusion MRI, adds further understanding to the working model of LUT control proposed by Griffiths (see details in **chapter 3**), identifies the WM tracts connecting different GM regions involved in the proposed working model of LUT control, and offers fundamental idea exploring brain network subtending OAB symptoms in MS. Although the findings are limited to a cohort of women in MS, the application is highly reproducible and can be generalised to other neurological conditions and other domains of LUTS.

5.1. Introduction

Following the introduction **chapters 2 - 4**, we understand that depending on different part and level of the nervous system being affected, LUTS manifest as OAB/storage problems and/or voiding problems such as hesitancy, poor stream and retaining urine (Araki *et al.*, 2003; Fowler and Griffiths, 2009). The OAB/storage symptoms defined as the presence of urinary urgency, with or without urgency urinary incontinence and usually associated with frequency and nocturia (Wein and Rovner, 2002; Abrams *et al.*, 2003) is a source of considerable distress, affecting quality of life. In MS, the LUTS are described in more than 80% of the patients, and the most common LUT complaints are OAB symptoms, including bladder urgency, frequency and incontinence (Phé, Chartier-Kastler and Panicker, 2016). There is, however, limited information on the neural underpinnings and how supraspinal activity and connectivity is altered in different LUT conditions in MS.

Functional brain imaging has been successful in providing insight into the central control of LUT functions in health and diseases. Responses in bilateral insula, the PAG, the anterior cingulate gyrus, as well as the prefrontal cortex bilaterally are described for bladder control (Griffiths, 2015). Recent research focusing on the structural changes through WMH, has been reported linking with urinary urgency and urinary incontinence (Kuchel *et al.*, 2009; Tadic *et al.*, 2010). However, the previous researches on WMH associated with LUTS were carried out in relatively elderly people, including healthy adults, Alzheimer's disease, dementia, brain vascular diseases, and ischemic WM diseases. The geriatric impairments in LUT function, mobility and cognition level are getting notable as

the age increases (Griffiths *et al.*, 2009; Wakefield *et al.*, 2010; Sakakibara *et al.*, 2014). Therefore, further researches on LUTS are expected looking into the WM changes exclusively.

DWI, as a non-conventional MRI tool, was widely used to measure the microscopic properties of neural tissues and indicate the pathophysiological basis in neural changes. The TBSS approach offers advanced methods to illustrate the WM changes using diffusion indices and associate the WM changes with the clinical presentations.

With these in mind, the aims of this chapter are:

1. to identify the WM changes in MS by the HC and MS patients;
2. to determine the association between the OAB symptoms and the WM changes using diffusion MRI through:
 - 1) microstructural WM difference between MS with OAB (MS-OAB) and MS without LUTS (MS-no-LUTS) patients;
 - 2) whether there are associations between microstructural indices and clinical scores of the OAB symptoms in MS.

5.2. Methods

5.2.1. Participants

Thirty female patients were recruited from National Hospital for Neurology and Neurosurgery (NHNN), with a diagnosis of MS according to McDonald criteria (Polman *et al.*, 2011). Exclusion criteria were designed from neurological, urological and MRI aspects, including left-handed, pregnancy, breast feeding, any contraindications to having MRI, craniocerebral injuries or surgeries, other known neurological diseases, cognitive impairment assessed by a Mini-Mental State Examination (MMSE; <23; see **Appendix 1**), the EDSS score (Kurtzke, 1983) more than 6.5, MS relapses in the previous 3 months, LUT treatments within the previous 6 months, presence of additional active urological diseases, surgeries of LUT or genitalia which is related to the LUT symptoms, any anatomical anomaly of LUT or genitalia, active LUT malignancy or metabolic disease. Detailed inclusion and exclusion criteria are described in **Appendix 2**. The study was designed to study on female participants to avoid prostate effects, such as the benign prostatic hyperplasia (BPH), affecting LUT symptoms in male patients. After the initial screening assessments, participants underwent clinical tests and MRI imaging. Subsequently, 29 patients completed the clinical assessments and MRI imaging sessions. As a control group, fourteen female healthy participants were recruited as a group of HC. The difference in age between patients and HC was adjusted in later imaging and statistical analysis. Patients' and HC's characteristics are shown in Table 5.1. All participants were fully informed and consented before research assessments. Two research protocols were involved in this study. One research protocol, covering two of the HC, was approved by The Joint UCL/UCLH committees on the Ethics of Human

Research, and the REC reference is 05/Q0502/101 (05/N053-PHTSICS01). The protocol was used to test the MRI protocols at the beginning, then the study was covered by the main research protocol, which included all the other participants. The main research protocol was approved by The Joint Medical Ethics Committee of the National Hospital for Neurology and Neurosurgery and the Institute of Neurology, London (protocol No. is 13/0523; REC reference is 14/LO/1636). Informed consent forms were signed by all participants. Participants in the following chapters (Chapter 6 - 7) were recruited under the same inclusion and exclusion criteria, research protocol and ethics approval, with an increase in participants number.

The MS patients were divided into two groups based on their OAB score evaluated by a sub score in the Urinary Symptom Profile (USP) questionnaire (**Appendix 3**): one group includes MS patients reporting predominant OAB symptoms (MS-OAB), another group includes MS patients who were free of LUTS (MS-no-LUTS).

5.2.2. Clinical assessments

Participants were assessed at their screening visit, using both uro-neurological investigations and questionnaires as following:

1. Patients' clinical history was recorded based on clinical record in the hospital;

2. The MMSE (De Marchis *et al.*, 2010) was assessed for cognitive impairment in all participants, and people were excluded if the score was less than 23;
3. Physical examinations, including neurological and urological examinations, were given out by one Consultant Neurologist at NHNN, helping to offer more clinical details;
4. The EDSS (Kurtzke, 1983) was assessed by experienced Consultant Neurologists at NHNN and patients' EDSS more than 6.5, or who had relapse in the previous 3 months, were excluded from this study. The EDSS score was only assessed in MS participants;
5. The urodynamic test was performed in MS patients, to give detailed information on patients' bladder functions;
6. A set of questionnaires (see **Appendix 3 - 8**):
 - 1) USP (Haab *et al.*, 2008) questionnaire, providing a comprehensive evaluation of urinary symptoms and their severity in males and females. Stress urinary incontinence (USP-SUI), overactive bladder (USP-OAB) and low stream (USP-LS) are three domains of the questionnaire;
 - 2) International consultation on Incontinence Questionnaire – Overactive bladder (ICIQ-OAB);
 - 3) International Consultation on Incontinence questionnaire for female lower urinary tract symptoms (ICIQ_FLUTS). ICIQ_FLUTS - frequency (ICIQ_FLUTS-f), ICIQ_FLUTS - voiding (ICIQ_FLUTS-v) and ICIQ_FLUTS - incontinence (ICIQ_FLUTS-i) are three sub scores in the questionnaire;

- 4) International consultation on Incontinence Questionnaire – quality of life (ICIQ-LUTSqol, was King’s Health Questionnaire previously), assessing quality of life with regard to bladder function;
 - 5) International Prostate Symptom Score (IPSS) questionnaire. This questionnaire was used to provide an indicator of severity of bladder symptoms. Though it was initially developed to assess voiding symptoms in male with benign prostatic hyperplasia (BPH), it is neither prostate nor gender specific (Chai *et al.*, 1993; Chancellor and Rivas, 1993; Lepor and Machi, 1993);
 - 6) SF-Qualiveen questionnaire (Bonniaud *et al.*, 2008), providing health related quality of life for urinary disorders.
7. A three-day bladder diary (BD, see **Appendix 9**). Three parameters, including day time frequency (BD-dayf), night time frequency (BD-nightf) and maximum voided volume (ml; BD-max), were abstracted to be used as covariates in data analysis (van Brummen, Heintz and Vaart, 2004);
 8. Somatosensory evoked potential (SSEP) was carried out on both of the tibial nerves and the pudendal nerve (N50 and P40), but the relative parameters were not used in current study analysis.

For the whole research protocol, including resting states, task fMRI and spinal cord protocol for MS and MSA cohorts, other clinical assessments were carried out but not included for the analysis in this chapter. Full lists and details of clinical assessments are in **Appendix 1 - 10**.

5.2.3. MRI Imaging acquisition

All the imaging was carried out at the NMR Research Unit, using a 3.0 Tesla scanner (Philips Achieva, Philips Medical Systems, Best, The Netherlands). Proton density (PD) and T2-weighted images were acquired in the axial-oblique plane parallel to the anterior-posterior callosal line using the following parameters: TE1/TE2 = 19/85ms, TR = 3500ms, FOV 240×180mm², NEX = 1, voxel size = 1×1×3mm³, 50 slices and scan time = 4:01 min. DWI was also performed in the axial-oblique plane, with 32 distributed diffusion encoding directions (b = 0 and b = 1000 s/mm²) and the following parameters: TE = 92ms, TR = 9714ms, FOV 248×248mm², NEX = 1, voxel size = 2×2 ×2mm³, 70 slices and scan time = 6:46min.

5.2.4. MRI imaging processing and Tract-Based Spatial Statistics analysis

Imaging processing and TBSS were performed using the FMRIB Software Library (FSL, Oxford, UK, <https://fsl.fmrib.ox.ac.uk/fsl>) on Linux-based systems. The WM lesions were manually identified on PDT2 images using Jim version 6 (<http://www.xinapse.com/j-im-7-software/>). The diffusion-weighted image was corrected for eddy current-induced distortions and subject movements using FSL (Andersson and Sotiropoulos, 2016). DWI fitting and calculation of FA, MD, AD and RD maps were performed using the NiftyFit toolbox (Melbourne *et al.*, 2016).

The TBSS tool firstly pre-processed the FA images by slightly eroding and zeroing the end slices to remove likely outliers from the tensor fitting. Then, the

nonlinear registration helps all FA images align to a $1 \times 1 \times 1 \text{ mm}^3$ MNI152 space (MNI, McConnell Brain Imaging Centre) using the FMRIB58_FA as the target image (Hickman *et al.*, 2002). The next step was to apply the nonlinear transforms found in the previous step to all FA images to bring them into standard space, and merge into a single 4D image file (skeletonized). This 4D mean FA skeletonized image was then thresholded at 0.2 to include only voxels indicative of WM. One of the advantages of TBSS method is that though the WM fibre centres may not be perfectly aligned, the maximum DWI measurements of each subjects, such as the FA values, could be compared at each point of the skeleton (Kern *et al.*, 2011). Moreover, this way of skeleton projection could minimize the effects from WM lesions (Kern *et al.*, 2011). The JHU ICBM-DTI-81 White-Matter atlas and the JHU White-Matter Tractography atlas were used to provide a map of regions of interest (Wakana *et al.*, 2007; Mori, Oishi and Faria, 2009). The JHU ICBM-DTI-81 White-Matter atlas was created from averaged 81 subjects' DWI maps (mean age 39, M: 42, F: 39). 48 WM tracts were labelled in the JHU ICBM-DTI-81 White-Matter atlas. The JHU White-Matter Tractography atlas was created from the averaging results of 28 subjects (M: 17, F:11; mean age 29), and 20 structures were identified.

5.2.5. Statistical analysis

Descriptive statistics of age, EDSS, disease duration, lesion load, USP-OAB score are expressed as mean and standard deviation (see Table 5.1). All variables were checked for skewness and presence of outliers. SPSS version 24 was used for the basic statistical analysis. A p value < 0.05 was considered

statistically significant, and p value < 0.1 was considered a favourable statistical trend.

The design matrix and contrast files were created by the General Linear Model (GLM) tool (<https://fsl.fmrib.ox.ac.uk/fsl/fslwiki/GLM>) and passed to the Randomise tool (<https://fsl.fmrib.ox.ac.uk/fsl/fslwiki/Randomise>) for nonparametric permutation inference (5000 permutations). The FA parameters were adjusted for age in analysis of MS patients plus HC, and adjusted for age, EDSS, lesion load and disease duration in analysis among MS patients, using a linear regression model. Any single regressor added into the regression model were mean centred, across all subjects rather than within group, by subtracting the overall mean value from each individual variable. The Threshold-Free Cluster Enhancement (TFCE) option was adopted for all tests in Randomise, and it is generally more robust and avoids the need for the arbitrary initial cluster forming threshold ($p < 0.05$ as statistical significant, $P < 0.1$ as statistical trend; Smith and Nichols, 2009).

Group difference analysis was firstly carried out between HC and MS, and the results were compared with previous literatures. Comparisons between the two MS sub-groups (MS-no-LUTS and MS-OAB) were performed to identify WM changes potentially responsible for LUTS in MS, adjusting for age and EDSS. Correlation analysis (f-tests using GLM) was performed to explore any associations between diffusion measures (FA) and clinical scores of OAB (USP-

OAB) in MS. All regressors added to the regression model were mean centred across all subjects.

5.2.6. Bullseye representation

Differences of the frequency of lesion volume in terms of median and interquartile range (IQR, measuring statistical dispersion) value, and differences of distribution and frequency of WM changes were plotted in a bullseye plot of WM regions (Figure 5.2 and 5.3; Sudre *et al.*, 2018). The regional representation is based on the division of the WM and deep GM volume into sector (representing the lobes) and radial regions (representing the distance from the ventricles; Sudre *et al.*, 2018). Aggregation of cortical regions obtained from GIF parcellation algorithm (Cardoso *et al.*, 2015) applied to the brain in MNI space was used to obtain cortical lobes (or deep GM regions), and WM voxels were allocated to the closest cortical lobe. The lobes were illustrated as FRONT (frontal lobe), PAR (parietal lobe), TEMP (temporal lobe), OCC (occipital lobe) and BGIT (the basal ganglia, thalami and infratentorial regions from both sides; Sudre *et al.*, 2018). Radially, the application of the Laplace equation between ventricular and cortical surface enabled the creation of a normalised distance measure, that was divided into four equal parts providing the four equidistant radial layers (Sudre *et al.*, 2018). Overall, this systematic division of the volume of interest results in thirty-six regions (four layers and nice lobar separations; Sudre *et al.*, 2018).

This regional division of the WM volume allows for a local representation of the whole brain results. In this study, distribution plots reflect the ratio between the

number of voxels of interest (significant values) located in the specific region and the overall number of significant voxels, while the frequency plots were drawn as the ratio between number of significant voxels in a given region and volume of this region. Figure 5.2 represented the frequency plots of the lesion volume regarding median and IQR value, while Figure 5.3 showed the distribution and frequency plots of significant results from TBSS group difference analysis and correlation analysis.

5.3. Results

5.3.1. Participants

Thirty right-handed MS patients, fulfilling recruitment inclusion criteria, participated in the study and fourteen people were recruited as a HC group. One MS participants were excluded from all data analysis procedure because another neurological diagnosis, rather than MS, was made after the MRI scanning. Considering the potential effects from voiding difficulties, three of MS patients reporting voiding problems were excluded from data analysis for OAB symptoms in MS. In the end, twenty-nine female MS patients (mean age = 43.3 ± 9.4 , range 27.3-56.7 years) and fourteen female healthy participants (mean age = 48.5 ± 20.0 , range 25.7-73.7 years) were included in data analysis for all participants, including HC and MS; twenty-six female MS patients were included in data analysis for MS groups, excluding three patients with voiding difficulties. Considering this study focus on DWI imaging analysis, age was calculated at the

DWI imaging scanning day. Detailed demographic participants characteristics are shown in Table 5.1.

The MS patients were then divided into two subgroups, including nine MS with OAB symptoms (MS-OAB) and seventeen MS without LUTS (MS-no-LUTS), based on the OAB sub-score from USP-OAB questionnaire (USP-OAB), representing degree of OAB symptoms. The cut off value (mean + 2SD) was calculated from the USP-OAB sub-score of the HC. Participants scoring below or equal to the cut off value (3, range 0 - 21) were treated as the MS-no-LUTS group (mean age = 37.5 ± 8.9 , range 27.5-50.4 years), and those scoring above the value were included in the MS-OAB group (mean age = 46.1 ± 8.6 , range 27.3-56.7 years). The demographic data are summarized in Table 5.1.

Table 5.1. Demographic characteristics of HC and MS patients.

	HC	MS	MS-no-LUTS	MS-OAB	P-value	
n	14	29	9	17	N/A^a	N/A^b
Mean age, years (SD)	48.5 (20.0)	43.3 (9.4)	37.5 (8.9)	46.1 (8.6)	0.641^a	0.026^{b,*}
Mean EDSS (SD)	N/A	2.3 (1.8)	0.9 (0.9)	2.9 (2.0)	N/A^a	0.004^{b,**}
Median lesion volume, $\times 10^3$ml (range)	N/A	7.7 (0.2-69.6)	1.9 (0.2-13.7)	8.8 (1.0-69.6)	N/A^a	0.055^{b,*}
Median disease duration, years (range)	N/A	10.0 (0.8-42.0)	4.0 (1.0-14.0)	12.3 (0.8-42.0)	N/A^a	0.029^{b,*}
Mean USP-OAB (SD)	1.1 (1.7)	5.9 (4.7)	1.0 (1.0)	8.8 (3.7)	<0.001^{a,**}	<0.001^{b,**}

EDSS: Expanded Disability Status Scale; HC: healthy control; LUTS: lower urinary tract symptoms; MS: multiple sclerosis; MS-no-LUTS: MS patients without LUTS; MS-OAB: MS patients with OAB; N/A: not applicable; OAB: overactive bladder; USP: Urinary Symptom Profile; USP-OAB: USP OAB sub-score. Statistical difference between HC and MS, MS-no-LUTS and MS-OAB were tested using Chi Square test, student's t-test, and Mann-Whitney U test. ^a: statistical difference between HC and MS; ^b: statistical difference between MS-no-LUTS and MS_OAB. *: p < 0.05; **: p < 0.01.

5.3.2. Clinical assessments characteristics

Table 5.1 described the characteristics of the clinical assessments. The EDSS score and the lesion volume were only assessed among MS participants and was adjusted as covariates in MRI data analysis within MS group. So, the EDSS score, lesion load and the disease duration are not applicable in HC and they were not used as covariates in imaging analysis among HC and MS.

Urodynamic testing was useful for evaluating bladder functions. Fourteen out of twenty-nine MS patients refused to have the test as they were afraid of catheter and worried about getting UTI after the test. With help from an experienced neuro-urologist, we checked all urodynamic reports. However, as we already knew, there could be a mismatch between clinical presentation (OAB symptoms) and test results (DO). In our study, we could not identify any correlation between DO and OAB symptoms. Thus, we only treat urodynamic as a clinical test, rather than a research measure, providing information about the bladder functions.

The parameters indicating OAB symptoms (the BD-dayf, BD-nightf and BD-max) from the three-day BD was initially planned to be analysed. Among twenty-nine MS patients, only twenty-three filled the diary. We tested the correlation between BD parameters and FA value, followed by the group difference analysis on the BD parameters between MS-no-LUTS and MS-OAB group. However, there was no significant correlation or group difference. Therefore, we did not apply the BD parameters in the following TBSS analysis.

5.3.3. Group difference analysis

The group difference analysis was carried out in both the HC versus MS, and the MS-no-LUTS versus MS-OAB. Age and LUTS score were mean centred and adjusted. The EDSS score, lesion load and the disease duration were not added as a covariate in group difference between HC and MS, but between MS-no-LUTS and MS-OAB.

In group difference analysis between HC and MS, the statistical analysis illustrates significant group difference in the FA value. Compared with the HC group, the FA value shows significant reduction in the WM skeleton in the MS group ($p < 0.05$), after adjusting for age. The voxels that showed significant reduction in FA were spread out in different WM regions, especially the corpus callosum, which kept consistent with the findings from previous studies (Gean-Marton *et al.*, 1991; Evangelou *et al.*, 2000).

Between the MS-no-LUTS and the MS-OAB, there was no significant reduction of FA in the MS-OAB group, after adjusting for age, but there was a trend for significance after adjusting for age and the EDSS score ($p < 0.08$). After adjusting for the EDSS score alone, there was a significant reduction in FA value in the MS-OAB group ($p < 0.05$). Table 5.2 presents the results of the group difference analysis.

Table 5.2. FA values of mean skeleton in HC, MS and MS sub-groups.

	FA of mean skeleton	P-value	P-value	P-value
	(median, range)	(adjusted for age)	(adjusted for EDSS)	(adjusted for age + EDSS)
HC (n=14)	0.4590268 (0.4404533, 0.4853403)	0.004**	N/A	N/A
MS (n=29)	0.4338049 (0.3303200, 0.4874299)			
MS-no-LUT (n=9)	0.4446728 (0.4288627, 0.4740112)	0.159	0.047*	0.072
MS-OAB (n=17)	0.4299469 (0.3305743, 0.4859033)			

FA: fractional anisotropy; HC: healthy controls; MS: multiple sclerosis; MS-no-LUTS: MS patients without LUTS; MS-OAB: MS patients with OAB; N/A: not applicable. Statistical difference between HC and MS, MS-no-LUTS and MS-OAB were tested using Mann-Whitney U test. *: $p < 0.05$; **: $p < 0.01$.

5.3.4. Correlation analysis

Correlation analysis was carried out across all the subjects ($n = 43$), including HC and MS patients, and extended to the MS subgroups. All the covariates added into analysis were mean centred. Age and LUTS score were adjusted in both of the correlation analysis in all subjects and MS subjects. However, the EDSS

score, lesion load and the disease duration were only added in analysis within MS group.

Among all the participants (n = 43), age and USP-OAB score present negative correlation with FA ($p < 0.05$, $p < 0.1$, respectively), which means the higher the age, or the USP-OAB score, the lower the FA value. Other LUTS scores correlation tests did not present significant or broadly significant results. Within the MS subgroups, considering there are three MS patient presenting significant voiding difficulties, with or without OAB symptoms, the correlation analysis was carried out in the subjects without voiding problems (26 subjects, including 9 presenting OAB problems and 17 without OAB). Table 5.3 illustrates the significant results and the threshold used in correlation analysis. The negative correlation between the FA value and age presents the age effects on WM. The FA value decreases as the age increases. In addition, there is a negative correlation between the FA value and the USP-OAB score, presenting that the lower FA value gives a higher USP-OAB score. In another word, MS-OAB symptoms are reported to have reduced FA value, compared with MS-no-LUTS. That is to say, the reduced FA value would indicate more severe OAB symptoms.

Additionally, Table 5.4 summarizes the analysis without relative significance.

Table 5.3. Correlations between FA values and clinical scores.

	Age	EDSS	USP-OAB
FA of mean skeleton of all subjects (n=43)	r = -0.36* p = 0.018	N/A	r = -0.493** p = 0.001
FA of mean skeleton of MS (n=26)	r = -0.51** p = 0.008	r = -0.271 p = 0.181	r = -0.449* p = 0.021

Spearman's correlations between FA value and age, EDSS and USP-OAB sub-score were tested, in HC and MS subjects. EDSS: Expanded Disability Status Scale; FA: fractional anisotropy; MS: multiple sclerosis; N/A: not applicable; p: p-value of correlation; r: Spearman's correlation coefficient (two-tailed); USP-OAB: Urinary Symptom Profile OAB sub-score. *: $p < 0.05$; **: $p < 0.01$.

Table 5.4. Analysis results without relative significance.

Correlation Analysis in MS Subjects (n = 26)

Positive and negative correlation between FA and EDSS, lesion load, disease duration, ICIQ-OAB, ICIQ_FLUTS-f, ICIQ_FLUTS-v, ICIQ_FLUTS-I, ICIQ-QoL, USP-SUI, USP-LS, IPSS, SF-Qualiveen, BD-dayf*, BD-nightf*, and BD-max*, respectively.

Group difference analysis between MS without LUTS (n = 9) and MS with OAB (n = 17)

Group difference adjusting for age/EDSS/lesion load/disease duration (combined and separately) and a LUT score, including ICIQ-OAB, ICIQ_FLUTS-f, ICIQ_FLUTS-v, ICIQ_FLUTS-I, ICIQ-QoL, USP-SUI, USP-OAB, USP-LS, IPSS, SF-Qualiveen, BD-dayf**, BD-nightf**, and BD-max**, respectively. Except analysis adjusting for EDSS alone, and age plus EDSS.

*. The analysis was run among twenty-three subjects; **. The analysis was run among seven MS without LUTS and sixteen MS with OAB.

5.3.5. WM abnormalities subtending OAB symptoms in MS

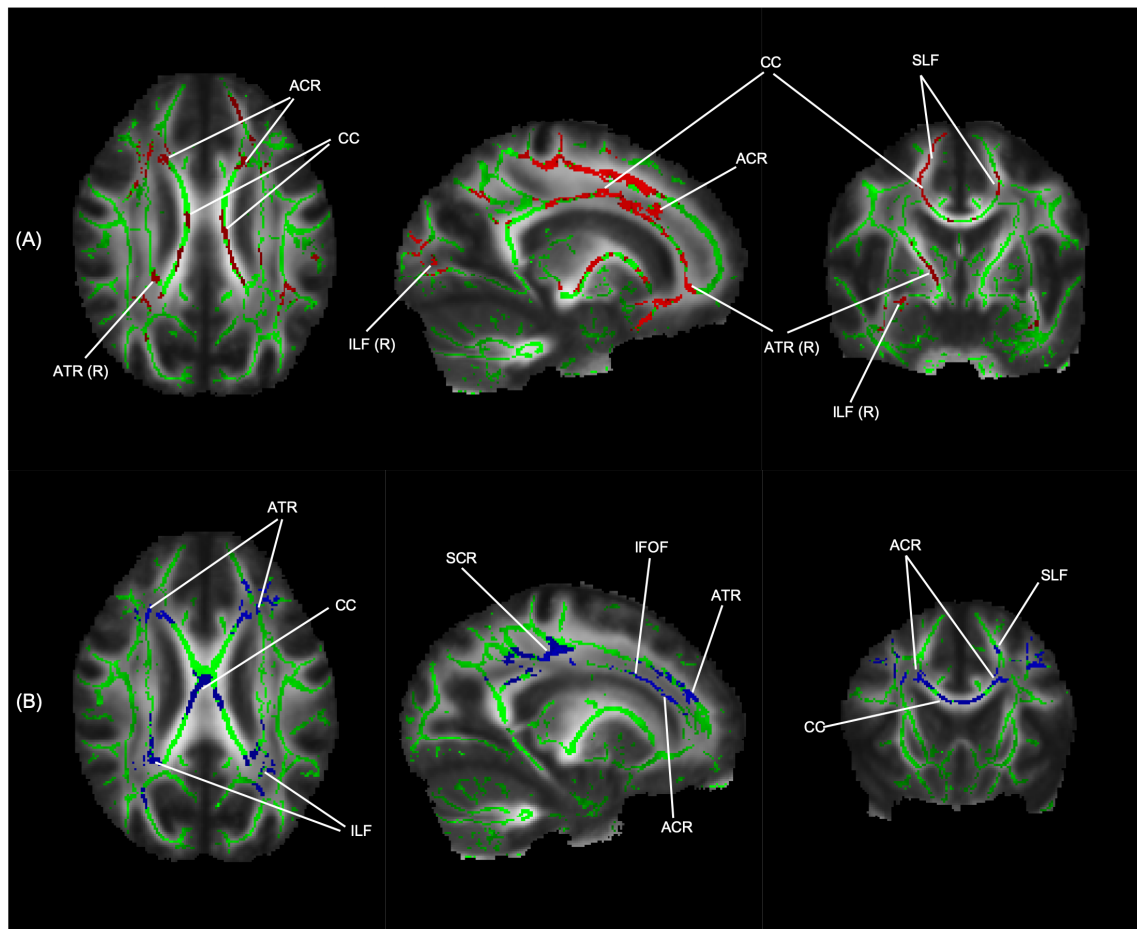
The WM changes caused by OAB symptoms were identified based on two atlases provided in FSL: one is JHU ICBM-DTI-81 White-Matter atlas, and another one is JHU White-Matter Tractography atlas.

In group difference analysis, the lower FA value was found in MS with OAB, compared with MS without LUTS, and the corresponding regions included: corpus callosum, anterior corona radiata bilaterally, right anterior thalamic radiation, superior longitudinal fasciculus bilaterally, right inferior longitudinal fasciculus (Figure 5.1A). The red voxels represent the regions showing lower FA in MS-OAB than MS-no-LUTS group. Figure 5.2 shows clear difference of lesion volume in terms of median and IQR between MS-no-LUTS and MS-OAB, indicating more lesion volume in MS-OAB. Figure 5.3a presents the bullseye plots of the significant difference in FA value between MS-no-LUTS and MS-OAB groups.

In correlation analysis, decreasing FA with increasing USP-OAB score was identified widespread in white matter regions bilaterally. Several regions showed significant decreased FA, such as corpus callosum, anterior corona radiata bilaterally, superior corona radiata bilaterally, superior longitudinal fasciculus bilaterally, inferior longitudinal fasciculus bilaterally and inferior fronto-occipital fasciculus bilaterally (Figure 5.1B). The voxels in red showed a significant correlation between decreasing FA and increasing USP-OAB. Figure 5.3b gives the correlation result map using bullseye plots. The plots show that the significant

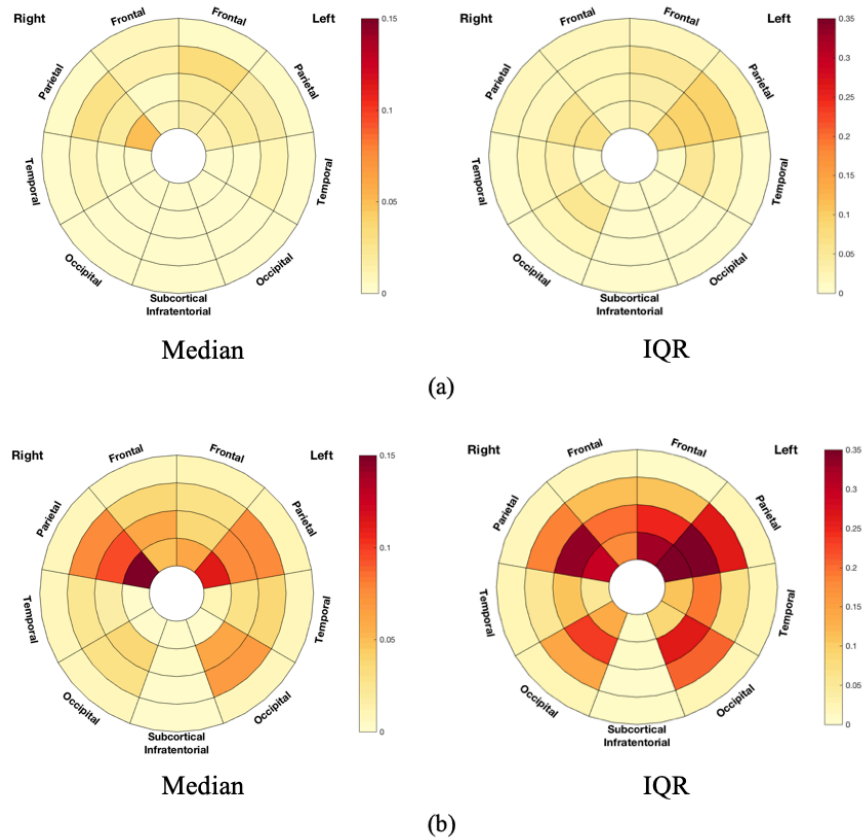
correlation analysis is primarily in the frontal lobe bilaterally, followed by the left parietal lobes. That is to say, among all the decreased FA voxels, majority of them are distributed in the frontal lobes bilaterally, and compared with other regions, the frontal lobes have a higher percentage of the decreased FA voxel volume. Therefore, a higher USP-OAB score (more severe OAB symptoms) was correlated with a decreased FA in the frontal lobes. Moreover, more severe WM changes were seen in the frontal lobes that correlated higher USP-OAB scores. Besides, the percentage of the decreased FA volume, indicating WM changes, is showing similar in the frontal lobes and the parietal lobes.

Figure 5.1. Significant results from TBSS (A) group difference analysis and (B) correlation analysis.



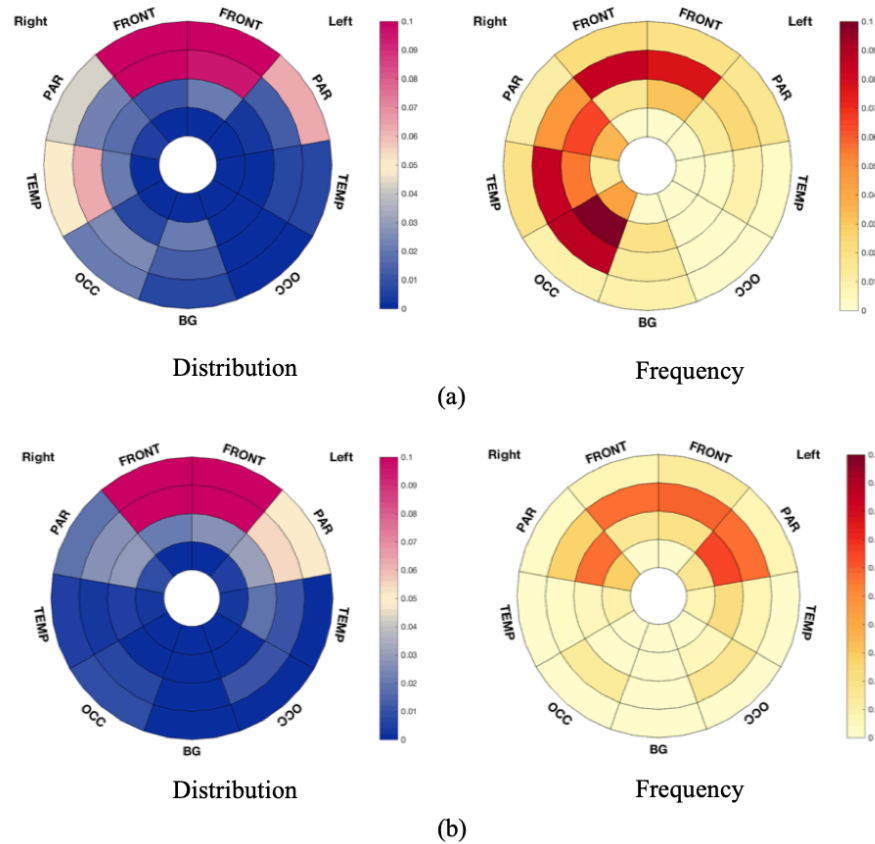
The WM skeleton in green is created based on voxels indicative of WM across MS participants ($n = 26$). (A) Voxels in red show a significant FA reduction in MS-OAB compared to MS-no-LUTS, adjusting for age and EDSS ($p = 0.072$). (B) Voxels in red show significant negative correlation between FA and USP-OAB sub-score ($p = 0.021$). ACR: anterior corona radiata; ATR: anterior thalamic radiation; CC: corpus callosum; IFOF: inferior fronto-occipital fasciculus; ILF: inferior longitudinal fasciculus; R: right-sided; SCR: superior corona radiata; SLF: superior longitudinal fasciculus.

Figure 5.2. Frequency plots of lesion volume in terms of median and IQR in (a) MS-no-LUTS and (b) MS-OAB.



The frequency plots were drawn as the ratio between number of significant voxels in a given region and volume of this region. The colour bars from bottom to top indicate the lesion volume from less to more. IQR: interquartile range.

Figure 5.3. Bullseye plots showing significant results from TBSS.



(a) Bullseye plots showing reduced FA in MS-OAB, compared with MS-no-LUTS, adjusting for age and EDSS ($p = 0.072$). (b) Bullseye plots showing negative correlation between FA and USP-OAB sub-score across MS patients ($n = 26$, $p = 0.021$). The distribution plots reflect the ratio between the number of voxels of interest (significant values) located in the specific region and the overall number of significant voxels, while the frequency plots were drawn as the ratio between number of significant voxels in a given region and volume of this region. The colour bars from bottom to top indicate the number of voxels from less to more at the significant level. FRONT: frontal lobe; BG: the basal ganglia, thalami and infratentorial regions from both sides; OCC: occipital lobe; PAR: parietal lobe; TEMP: temporal lobe.

5.4. Discussions

We explored differences in WM changes in MS-OAB and MS-no-LUTS by evaluating changes in FA using diffusion MRI, and, to the best of our knowledge, this is the first study establishing the WM changes subtending OAB in MS. Current understanding of the central neural network controlling LUT functions is informed by positron-emission tomography (PET) and fMRI studies of the GM which suggests a network involving different regions including thalamus, insula, anterior cingulate cortex, medial prefrontal cortex and lateral prefrontal cortex (Griffiths, 2015). The involvement of WM tracts in determining the function/dysfunction of this network is currently only speculative (Griffiths, 2015), therefore this study aimed to evaluate the extent of WM tracts damage, specifically in MS. The scenario is very much complicated in MS given the mixture of disability in motor, sensory, autonomic and visual functions. The current study compensates our understanding of WM changes related to OAB in MS by two major findings:

1. There are FA reductions in the MS-OAB group, compared with MS-no-LUTS (Table 5.2), in regions consistent with the literature, which include corpus callosum, anterior corona radiata, anterior thalamic radiation, superior longitudinal fasciculus and inferior longitudinal fasciculus (Kuchel *et al.*, 2009; Tadic *et al.*, 2010). Among the identified tracts, WM changes in corpus callosum have been widely reported in MS, accounting for all sorts of functions; WM changes in anterior thalamic radiation, superior longitudinal fasciculus and inferior longitudinal fasciculus have also been reported in MS, accounting for cognitive functions (Enzinger *et al.*, 2015). While specificity to LUTS may be

difficult to claim, it is true that when we controlled for age and EDSS (as a measure of overall motor and functional disability), a significant FA reduction in the identified WM tracts in the MS-OAB group continued to be seen. Taking into account the working model of LUT system built up by Griffiths based on previous GM studies (Griffiths, 2015), the present findings suggest the presence of a potential suprapontine structural circuit for the LUT functional network, building up the connections involving thalamus, insula, anterior cingulate cortex and the prefrontal cortex. In addition, WM studies assessing WMH in a cohort of elderly community-dwelling women from Kuchel et al. and Tadic et al. speculate the involvement of cingulum, anterior corona radiata, anterior thalamic radiation superior longitudinal fasciculus, and superior frontal-occipital fasciculus for urinary incontinence, which could be due to OAB symptoms (Kuchel *et al.*, 2009; Tadic *et al.*, 2010). Our study confirms the presence of FA reductions in these specific WM tracts, with an advanced MRI technique - diffusion MRI – and statistical analysis of the whole WM skeleton, without imposing *a priori* hypothesis.

Differences subtending OAB symptoms were observed particularly in the frontal lobe as expected. In previous studies, Andrew and Nathan (1964) pointed out that GM lesions in medial prefrontal cortex resulted in dysfunction in short-term incontinence (Andrew and Nathan, 1964). The orbitofrontal or lateral prefrontal cortex have been established to have extensive connections with the limbic system, including insula, which was found as the homeostatic afferent area projecting the sensation of bladder filling (Griffiths *et al.*, 2005; Kuhtz-Buschbeck *et al.*, 2005), and the anterior cingulate cortex, which mediated LUT functions together with the supplementary motor area (SMA) by arousing the sensation of

urgency and contracting the urethral sphincter (Seseke *et al.*, 2006; Kuhtz-Buschbeck *et al.*, 2007). Moreover, one unexpected finding of the present study is the clear difference between the left and the right hemisphere involvement, particularly clear when looking at the Frequency bullseye plot in Figure 3a. In another words, more WM changes associated with the group presenting OAB symptoms are found in the right hemisphere. In view of the fact that this study only recruited right-handed candidates, it is clear that, compared with MS-no-LUTS people, the MS-OAB group presents a significant FA reduction in WM tracts not only in both frontal lobes, but also in extensive WM regions of the right (non-dominant) hemisphere. Based on previous studies looking into the cerebral control network of the bladder function, activations were reported with a preference of the insula and prefrontal cortex, with a predominance for the right insula and right lateral prefrontal cortex (Griffiths, 2015). There is a non-dominant hemisphere prevalence presented in the median lesion volume plot in Figure 2b and lesions of the right hemisphere would be consistent with the expected findings in the literature (Kuchel *et al.*, 2009). Considering the findings between interoceptive awareness, food craving and dyspepsia and right GM regions from previous studies, including right insula and right thalamus (Critchley *et al.*, 2004; Contreras-Rodríguez *et al.*, 2018; Liu *et al.*, 2018), the right hemisphere WM tracts alteration could lead to the visceral responses change, such as LUTS.

2. There is a negative correlation between FA and the USP-OAB sub-score, suggesting that a lower FA was associated with more severe OAB symptoms (Table 3). Considering that an important role for WM changes in anterior corona radiata was shown to predict urinary incontinence severity in elderly women with

small vessel disease (Kuchel *et al.*, 2009), this study confirms the importance of this tract in the neural control of LUT functions; moreover, our results suggest that there are additional WM tracts that when affected by microstructure alterations can contribute to LUT dysfunction (OAB) in neurological diseases (MS). It is fundamental for later studies to assess these tracts and the possible LUT network in associations to other specific symptoms of OAB, like urgency and frequency, and in other neurological conditions.

There are some limitations of this study. In the group difference analysis, a trend towards a significantly reduced FA ($p = 0.072$) was observed in MS-OAB compared with MS-no-LUTS, after adjusting for age and EDSS. These two groups, though, are not matched for number of subjects and reflect the expected disease distribution where LUTS is common in 80% of MS and therefore a cohort of MS-no-LUTS is unusual and very difficult to recruit. Additionally, LUT dysfunctions in MS arises due to suprapontine and spinal lesions, as well as GM lesions (Phé, Chartier-Kastler and Panicker, 2016), while only the suprapontine subcortical WM changes were considered in this study. Moreover, worth considering that the EDSS score, used for assessing MS disability, has a LUTS component, hence it could be a reason that regressing EDSS for LUT studies in MS decreases of significance of findings in LUTS. On the other hand, not correcting for EDSS would make any finding non-specific given that there is a natural correlation between LUTS and increased disability.

5.5. Remaining question and further direction

This chapter investigated the brain WM without prior assumption of OAB related WM changes. Recent connectivity study in MS generated the structural brain network (see details in **chapter 4**) and the connectivity measures were used to explain the MS disability. So, the connectivity approaches are potential to explore the OAB symptoms in MS. **Chapter 6 - 7** will explore the WM network underlying OAB in MS by reconstructing the whole brain structural network, generating of the structural network for OAB in MS, and explaining the structural network combined with the functional network for LUT functions.

Bibliography

- Abrams, P. *et al.* (2003) 'The standardisation of terminology in lower urinary tract function: Report from the standardisation sub-committee of the International Continence Society', *Urology*, 61(1), pp. 37–49. doi: 10.1016/S0090-4295(02)02243-4.
- Andersson, J. L. R. and Sotiropoulos, S. N. (2016) 'An integrated approach to correction for off-resonance effects and subject movement in diffusion MR imaging', *NeuroImage*. The Authors, 125, pp. 1063–1078. doi: 10.1016/j.neuroimage.2015.10.019.
- Andrew, J. and Nathan, P. W. (1964) 'Lesions on the anterior frontal lobes and disturbances of micturition and defaecation.', *Brain*, 87(2), pp. 233–262. Available at: <http://dx.doi.org/10.1093/brain/87.2.233>.
- Araki, I. *et al.* (2003) 'Relationship of bladder dysfunction to lesion site in multiple sclerosis.', *The Journal of urology*, 169(4), pp. 1384–1387. doi: 10.1097/01.ju.0000049644.27713.c8.
- Bonniaud, V. *et al.* (2008) 'Development and validation of the short form of a urinary quality of life questionnaire: SF-Qualiveen.', *The Journal of urology*. United States, 180(6), pp. 2592–2598. doi: 10.1016/j.juro.2008.08.016.
- van Brummen, H. J., Heintz, A. P. M. and Vaart, C. H. van der (2004) 'The association between overactive bladder symptoms and objective parameters from bladder diary and filling cystometry', *Neurourology and Urodynamics*, 23(1), pp. 38–42. doi: 10.1002/nau.10162.
- Cardoso, M. J. *et al.* (2015) 'Geodesic Information Flows: Spatially-Variant Graphs and Their Application to Segmentation and Fusion', *IEEE Transactions on Medical Imaging*. IEEE, 34(9), pp. 1976–1988. doi: 10.1109/TMI.2015.2418298.
- Chai, T. C. *et al.* (1993) 'Specificity of the American Urological Association voiding symptom index: comparison of unselected and selected samples of both sexes.', *The Journal of urology*. United States, 150(5 Pt 2), pp. 1710–1713.
- Chancellor, M. B. and Rivas, D. A. (1993) 'American Urological Association symptom index for women with voiding symptoms: lack of index specificity for benign prostate hyperplasia.', *The Journal of urology*. United States, 150(5 Pt 2), pp. 1706–1709.
- Contreras-Rodríguez, O. *et al.* (2018) 'Visceral adiposity and insular networks: associations with food craving', *International Journal of Obesity*. doi: 10.1038/s41366-018-0173-3.
- Critchley, H. D. *et al.* (2004) 'Neural systems supporting interoceptive awareness', *Nature Neuroscience*. Nature Publishing Group, 7, p. 189. Available at: <https://doi.org/10.1038/nn1176>.
- Enzinger, C. *et al.* (2015) 'Nonconventional MRI and microstructural cerebral changes in multiple sclerosis', *Nature Reviews Neurology*. Nature Publishing Group, 11(12), pp. 676–686. doi: 10.1038/nrneurol.2015.194.
- Evangelou, N. *et al.* (2000) 'Regional axonal loss in the corpus callosum correlates with cerebral white matter lesion volume and distribution in multiple sclerosis', *Brain*, 123(9), pp. 1845–1849. doi: 10.1093/brain/123.9.1845.
- Fowler, C. J. and Griffiths, D. J. (2009) 'A decade of functional brain imaging applied to bladder control', *Neurourology and Urodynamics*. Wiley Subscription Services, Inc., A Wiley Company, 29(1), p. n/a-n/a. doi:

10.1002/nau.20740.

- Gean-Marton, A. D. *et al.* (1991) 'Abnormal corpus callosum: a sensitive and specific indicator of multiple sclerosis.', *Radiology*. United States, 180(1), pp. 215–221. doi: 10.1148/radiology.180.1.2052698.
- Griffiths, D. *et al.* (2005) 'Brain control of normal and overactive bladder', *Journal of Urology*, 174(5), pp. 1862–1867. doi: 10.1097/01.ju.0000177450.34451.97.
- Griffiths, D. *et al.* (2009) 'Cerebral control of the lower urinary tract: how age-related changes might predispose to urge incontinence', *Neuroimage*, 47(5), pp. 213–223. doi: 10.1007/978-1-62703-673-3.
- Griffiths, D. (2015) *Functional imaging of structures involved in neural control of the lower urinary tract*. 1st edn, *Handbook of clinical neurology*. 1st edn. Elsevier B.V. doi: 10.1016/B978-0-444-63247-0.00007-9.
- Haab, F. *et al.* (2008) 'Comprehensive Evaluation of Bladder and Urethral Dysfunction Symptoms: Development and Psychometric Validation of the Urinary Symptom Profile (USP) Questionnaire', *Urology*, 71(4), pp. 646–656. doi: 10.1016/j.urology.2007.11.100.
- Hickman, S. J. *et al.* (2002) 'Technical note: The comparison of hypointense lesions from "pseudo-T1" and T1-weighted images in secondary progressive multiple sclerosis', *Multiple Sclerosis*, 8(5), pp. 433–435. doi: 10.1191/1352458502ms824xx.
- Kern, K. C. *et al.* (2011) 'Corpus callosal diffusivity predicts motor impairment in relapsing-remitting multiple sclerosis: A TBSS and tractography study', *NeuroImage*. Elsevier Inc., 55(3), pp. 1169–1177. doi: 10.1016/j.neuroimage.2010.10.077.
- Kuchel, G. A. *et al.* (2009) 'Localization of Brain White Matter Hyperintensities and Urinary Incontinence in Community-Dwelling Older Adults', *The Journals of Gerontology Series A: Biological Sciences and Medical Sciences*, 64A(8), pp. 902–909. doi: 10.1093/gerona/glp037.
- Kuhtz-Buschbeck, J. P. *et al.* (2005) 'Cortical representation of the urge to void: A functional magnetic resonance imaging study', *Journal of Urology*, 174(4 I), pp. 1477–1481. doi: 10.1097/01.ju.0000173007.84102.7c.
- Kuhtz-Buschbeck, J. P. *et al.* (2007) 'Activation of the supplementary motor area (SMA) during voluntary pelvic floor muscle contractions-An fMRI study', *NeuroImage*. Elsevier Inc., 35(2), pp. 449–457. doi: 10.1016/j.neuroimage.2006.12.032.
- Kurtzke, J. F. (1983) 'Rating neurologic impairment in multiple sclerosis: An expanded disability status scale (EDSS)', *Neurology*, 33(11), pp. 1444–1444. doi: 10.1212/WNL.33.11.1444.
- Lepor, H. and Machi, G. (1993) 'Comparison of AUA symptom index in unselected males and females between fifty-five and seventy-nine years of age.', *Urology*. United States, 42(1), pp. 31–36.
- Liu, P. *et al.* (2018) 'Altered structural and functional connectivity of the insula in functional dyspepsia', *Neurogastroenterology and Motility*, 30(9), pp. 1–9. doi: 10.1111/nmo.13345.
- De Marchis, G. M. *et al.* (2010) 'Mild cognitive impairment in medical inpatients: the Mini-Mental State Examination is a promising screening tool.', *Dementia and geriatric cognitive disorders*. Switzerland, 29(3), pp. 259–264. doi: 10.1159/000288772.
- Melbourne, A. *et al.* (2016) 'NiftyFit: a Software Package for Multi-parametric Model-Fitting of 4D Magnetic Resonance Imaging Data', *Neuroinformatics*. Neuroinformatics, 14(3), pp. 319–337. doi:

- 10.1007/s12021-016-9297-6.
- Mori, S., Oishi, K. and Faria, A. V (2009) 'White matter atlases based on diffusion tensor imaging', *Curr Opin Neurol*, 22(4), pp. 362–369. doi: 10.1097/WCO.0b013e32832d954b.White.
- Phé, V., Chartier-Kastler, E. and Panicker, J. N. (2016) 'Management of neurogenic bladder in patients with multiple sclerosis', *Nature Reviews Urology*. Nature Publishing Group, 13(5), pp. 275–288. doi: 10.1038/nrurol.2016.53.
- Polman, C. H. *et al.* (2011) 'Diagnostic criteria for multiple sclerosis: 2010 Revisions to the McDonald criteria', *Annals of Neurology*, 69(2), pp. 292–302. doi: 10.1002/ana.22366.
- Sakakibara, R. *et al.* (2014) 'Is overactive bladder a brain disease? The pathophysiological role of cerebral white matter in the elderly', *International Journal of Urology*, 21(1), pp. 33–38. doi: 10.1111/iju.12288.
- Seseke, S. *et al.* (2006) 'Voluntary pelvic floor muscle control-an fMRI study', *NeuroImage*, 31(4), pp. 1399–1407. doi: 10.1016/j.neuroimage.2006.02.012.
- Smith, S. M. and Nichols, T. E. (2009) 'Threshold-free cluster enhancement: Addressing problems of smoothing, threshold dependence and localisation in cluster inference', *NeuroImage*. Elsevier Inc., 44(1), pp. 83–98. doi: 10.1016/j.neuroimage.2008.03.061.
- Sudre, C. H. *et al.* (2018) 'Bullseye's representation of cerebral white matter hyperintensities.', *Journal of neuroradiology. Journal de neuroradiologie*. France, 45(2), pp. 114–122. doi: 10.1016/j.neurad.2017.10.001.
- Tadic *et al.* (2010) 'Brain Activity During Bladder Filling Is Related To White Matter Structural Changes in Older Women with Urinary Incontinence', *Neuroimage*, 51(4), pp. 1294–1302. doi: 10.1016/j.neuroimage.2010.03.016.BRAIN.
- Wakana, S. *et al.* (2007) 'Reproducibility of quantitative tractography methods applied to cerebral white matter', *NeuroImage*. Elsevier Inc., 36(3), pp. 630–644. doi: 10.1016/j.neuroimage.2007.02.049.
- Wakefield, D. B. *et al.* (2010) 'White matter hyperintensities predict functional decline in voiding, mobility, and cognition in older adults', *Journal of the American Geriatrics Society*, 58(2), pp. 275–281. doi: 10.1111/j.1532-5415.2009.02699.x.
- Wein, A. J. and Rovner, E. S. (2002) 'Definition and Epidemiology of Overactive Bladder', *Urology*, 60(5), pp. 7–12. doi: [https://doi.org/10.1016/S0090-4295\(02\)01784-3](https://doi.org/10.1016/S0090-4295(02)01784-3).

Chapter 6

6. Whole brain structural connectome reconstruction

Summary

This chapter presents the procedure of whole brain structural network reconstruction and provides the structural connectivity matrix for subsequent analysis focusing on OAB symptoms in MS (see **chapters 7**). We applied the latest algorithm for connectome reconstruction, including response function estimation, the constrained spherical deconvolution (CSD) approach, anatomically constrained tractography (ACT) framework and the spherical-deconvolution informed filtering of tractograms (SIFT2) approach improving the quantitative nature of the structural reconstructed network in order to minimize connectivity biases. The reconstruction methods and algorithm are also validated in this chapter by comparing the network measures between HC and MS, with previous studies.

6.1. Introduction

Following TBSS analysis in **Chapter 5**, we identified the difference of WM changes between MS-no-LUTS and MS-OAB group and established the association between OAB symptoms and WM changes in MS cohort. With the working model of LUT control proposed by Griffiths (see details in **chapter 3**; Griffiths, 2015), a WM network for LUTS could compensate the current understanding of the neural pathway of LUT functions. With the diffusion MRI technique and a specific method, such as tractography, the structural network could be created and used for further analysis combined with functional working model identified by fMRI. Together with the findings from TBSS analysis, **chapter 6 - 7** would gradually explore the WM network subtending OAB symptoms in MS starting from the reconstruction of the whole brain structural network, to the comparison of the network between MS-no-LUTS and MS-OAB, and extend to explore the similarities and differences between the network proposed from MS cohort and the one from the working model of LUT control.

Current anatomical methods investigating regions of interest can provide localized pathological basis (Bodini *et al.*, 2009). To gain a better understanding of a widespread pathology, the network approach is considered as a possible method. As discussed in **chapter 4**, the reconstructed brain network can provide biologically relevant information, such as the thickness of WM tracts (Sporns, Tononi and Ko, 2005). However, there are possibilities that the quantitative figures of the streamline from reconstructed network might offer unreliable information of the connectivity, which do not fully match the biological connections, such as the crossing fibres. In order to reconstruct a biological

meaningful network, we need to eliminate the plausible streamlines and improve the reliability of the reconstruction. Therefore, the aims of this chapter are:

1. to reconstruct the whole brain connectome network using recent published pipelines;
2. to describe the characters of the streamlines using the Brain Connectivity Toolbox (BCT);
3. to validate the reconstruction methods by comparing the network measures between HC and MS;
4. to provide a whole brain connectivity matrix for subsequent studies on OAB symptoms in MS.

6.2. Methods

6.2.1. Participants

Thirty-three right-handed female MS patients with a diagnosis of MS according to McDonald criteria (Polman *et al.*, 2011) were recruited from NHNN. Thirteen right-handed female healthy participants were recruited as a control group. Inclusion and exclusion criteria, research protocol and ethics approval were same as the items introduced in **chapter 5** for TBSS study.

6.2.2. Clinical assessments

Participants were assessed at their screening visit, using both uro-neurological investigations and questionnaires as following:

9. Patients' clinical history was recorded based on clinical record in the hospital;
10. The MMSE (De Marchis *et al.*, 2010) was assessed for cognitive impairment in all participants, and people were excluded if the score was less than 23 (see details in **Appendix 1**);
11. Physical examinations, including neurological and urological examinations, were given out by two Consultant Neurologists (JNP and ATT) at NHNN, helping to offer more clinical details;
12. The EDSS (Kurtzke, 1983) was assessed by experienced Consultant Neurologists (JNP and ATT) at NHNN and patients' EDSS more than 6.5, or who had relapse in the previous 3 months, were excluded from this study. The EDSS score was only assessed in MS participants (see details in **Appendix 2**).

6.2.3. MRI imaging acquisition

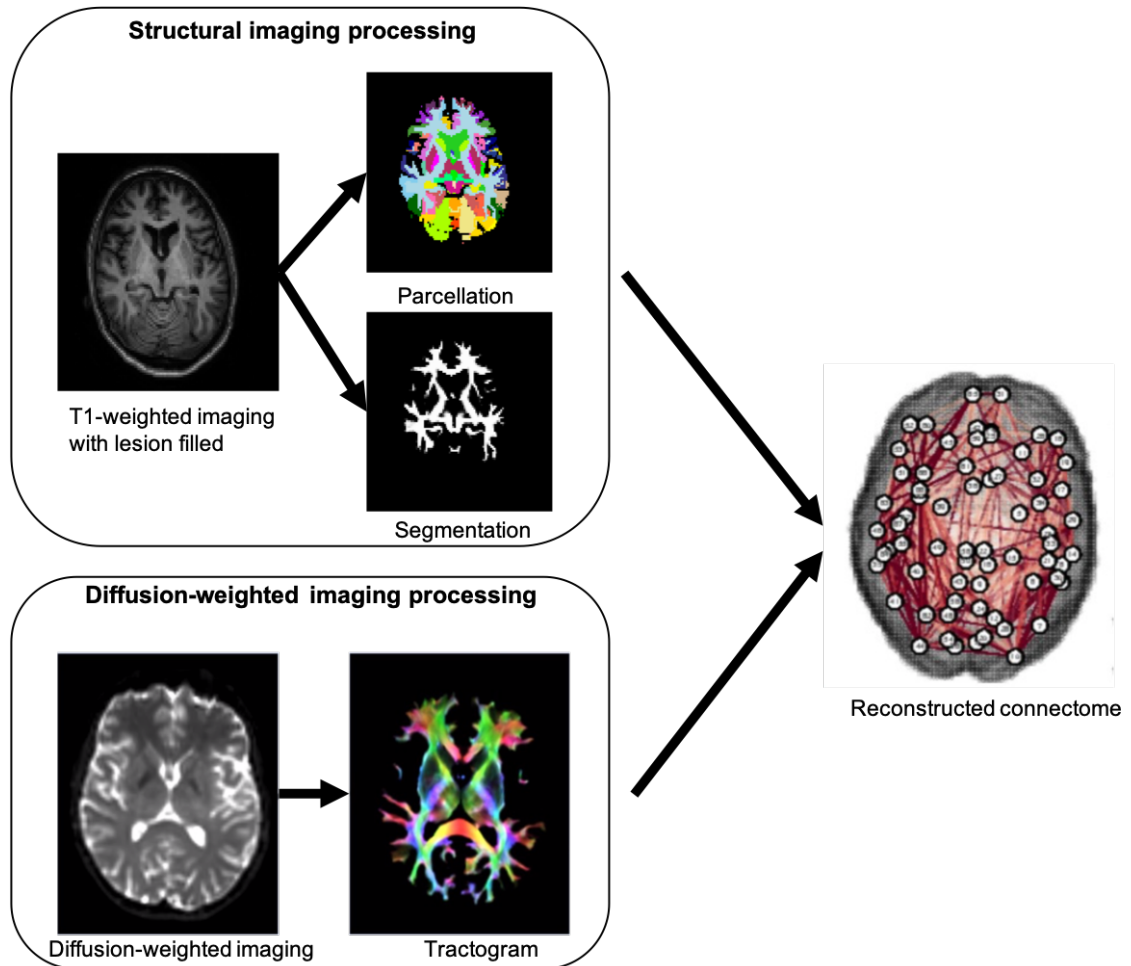
MRI scanning was carried out using a 3.0 Tesla scanner (Philips Achieva, Philips Medical Systems, Best, The Netherlands). Clinical scans were acquired in the axial-oblique plane parallel to the anterior-posterior callosal line using the following parameters: 1) T1-weighted images: TE = 10 ms, TR = 625 ms, FOV 240×180 mm², NEX = 1, voxel size = 1×1×1 mm³, 50 slices and scan time = 5:43 min; 2) PD-weighted and T2-weighted images: TE1/TE2 = 19/85 ms, TR = 3500

ms, FOV 240×180 mm², NEX = 1, voxel size = 1×1×3 mm³, 50 slices and scan time = 4:01 min. DTI was also performed in the axial-oblique plane, with 32 distributed diffusion encoding directions (b = 0 and b = 1000 s/mm²) and the following parameters: TE = 92 ms, TR = 9714 ms, FOV 248×248 mm², NEX = 1, voxel size = 2×2×2 mm³, 70 slices and scan time = 6:46 min.

6.2.4. MRI imaging processing

Briefly, there are three parts in MRI imaging processing: DWI pre-processing, structural imaging pre-processing, and connectome reconstruction (see Figure 6.1).

Figure 6.1. MRI processing procedure for whole brain connectivity reconstruction.



The MRI processing was applied for each participant and the diagram briefly presented the workflow for the whole brain connectivity reconstruction.

Diffusion-weighted imaging pre-processing

The motion and eddy current correction were performed using the FSL (<https://fsl.fmrib.ox.ac.uk/fsl>; Andersson and Sotiropoulos, 2016). The geometric distortion correction was performed using BrainSuite (Bhushan *et al.*, 2012).

Structural imaging pre-processing

The bias field correction was performed using the N4 algorithm (Tustison *et al.*, 2010). The participants' T1-weighted images were registered to the corresponding DWI images using BrainSuite (Bhushan *et al.*, 2012), so that the resolution of structural images turned to be $2 \times 2 \times 2 \text{ mm}^3$ (Smith *et al.*, 2012). As a result, the voxel dimensions and positions of T1-weighted images are matched to the DWI scans, and the images derived from structural images by subsequent steps could be aligned to the DWI.

WM lesions were identified on both PD-weighted and T2-weighted images and manually drew on PD-weighted images, using Jim 6.0 (<http://www.xinapse.com/Manual/index.html>), and the PD-weighted lesion masks were then registered to T1-weighted images (Hickman *et al.*, 2002). The segmentation and parcellation were then performed on the lesion filled T1-weighted images.

The brain was segmented to cortical grey matter (CGM), deep grey matter (DGM), WM, brainstem and cerebrospinal fluid (CSF), and WM and brainstem were joined as one image for subsequent anatomically constrained tractography (ACT) framework, which could improve the accuracy when reconstructing the tractography streamlines by giving the anatomical prior (Smith *et al.*, 2012). The brain was parcellated to distinct brain regions (120 anatomical GM regions were selected in this study) according to Desikan-Killiany-Tourville atlas using GIF algorithm, which is freely available online at <http://cmictig.cs.ucl.ac.uk/niftyweb> (Cardoso *et al.*, 2015; Prados *et al.*, 2016), which was applied to different neurological conditions previously, including MS (Eshaghi *et al.*, 2018). The 120 GM regions used in this study are listed in Table 6.1.

Table 6.1. List of 120 GM regions used in whole brain connectivity reconstruction.

1	Right Accumbens Area	61	Right middle occipital gyrus
2	Left Accumbens Area	62	Left middle occipital gyrus
3	Right Amygdala	63	Right medial orbital gyrus
4	Left Amygdala	64	Left medial orbital gyrus
5	Pons and Brain Stem	65	Right postcentral gyrus medial segment
6	Right Caudate	66	Left postcentral gyrus medial segment
7	Left Caudate	67	Right precentral gyrus medial segment
8	Right Cerebellum Exterior	68	Left precentral gyrus medial segment
9	Left Cerebellum Exterior	69	Right superior frontal gyrus medial segment
10	Right Hippocampus	70	Left superior frontal gyrus medial segment
11	Left Hippocampus	71	Right middle temporal gyrus
12	Right Pallidum	72	Left middle temporal gyrus
13	Left Pallidum	73	Right occipital pole
14	Right Putamen	74	Left occipital pole
15	Left Putamen	75	Right occipital fusiform gyrus
16	Right Thalamus Proper	76	Left occipital fusiform gyrus
17	Left Thalamus Proper	77	Right opercular part of the inferior frontal gyrus
18	Cerebellar Vermal Lobules I-V	78	Left opercular part of the inferior frontal gyrus

19	Cerebellar Vermal Lobules VI-VII	79	Right orbital part of the inferior frontal gyrus
20	Cerebellar Vermal Lobules VIII-X	80	Left orbital part of the inferior frontal gyrus
21	Left Basal Forebrain	81	Right posterior cingulate gyrus
22	Right Basal Forebrain	82	Left posterior cingulate gyrus
23	Right anterior cingulate gyrus	83	Right precuneus
24	Left anterior cingulate gyrus	84	Left precuneus
25	Right anterior insula	85	Right parahippocampal gyrus
26	Left anterior insula	86	Left parahippocampal gyrus
27	Right anterior orbital gyrus	87	Right posterior insula
28	Left anterior orbital gyrus	88	Left posterior insula
29	Right angular gyrus	89	Right parietal operculum
30	Left angular gyrus	90	Left parietal operculum
31	Right calcarine cortex	91	Right postcentral gyrus
32	Left calcarine cortex	92	Left postcentral gyrus
33	Right central operculum	93	Right posterior orbital gyrus
34	Left central operculum	94	Left posterior orbital gyrus
35	Right cuneus	95	Right planum polare
36	Left cuneus	96	Left planum polare
37	Right entorhinal area	97	Right precentral gyrus
38	Left entorhinal area	98	Left precentral gyrus

39	Right frontal operculum	99	Right planum temporale
40	Left frontal operculum	100	Left planum temporale
41	Right frontal pole	101	Right subcallosal area
42	Left frontal pole	102	Left subcallosal area
43	Right fusiform gyrus	103	Right superior frontal gyrus
44	Left fusiform gyrus	104	Left superior frontal gyrus
45	Right gyrus rectus	105	Right supplementary motor cortex
46	Left gyrus rectus	106	Left supplementary motor cortex
47	Right inferior occipital gyrus	107	Right supramarginal gyrus
48	Left inferior occipital gyrus	108	Left supramarginal gyrus
49	Right inferior temporal gyrus	109	Right superior occipital gyrus
50	Left inferior temporal gyrus	110	Left superior occipital gyrus
51	Right lingual gyrus	111	Right superior parietal lobule
52	Left lingual gyrus	112	Left superior parietal lobule
53	Right lateral orbital gyrus	113	Right superior temporal gyrus
54	Left lateral orbital gyrus	114	Left superior temporal gyrus
55	Right middle cingulate gyrus	115	Right temporal pole
56	Left middle cingulate gyrus	116	Left temporal pole
57	Right medial frontal cortex	117	Right triangular part of the inferior frontal gyrus
58	Left medial frontal cortex	118	Left triangular part of the inferior frontal gyrus

59	Right middle frontal gyrus	119	Right transverse temporal gyrus
60	Left middle frontal gyrus	120	Left transverse temporal gyrus

Connectome reconstruction

This step, previously applied in HC and MS participants (Charalambous *et al.*, 2019), included response function estimation, followed by estimating the voxel-wise fibre orientation distribution (FOD) function, tractogram generation, reweighting the streamlines, and the connectome reconstruction. MRtrix3 v0.3.14 package (<http://www.mrtrix.org>) was used throughout this step.

The Tax algorithm (Tax *et al.*, 2014) was applied to estimate the response function, which represented the signal of a single coherent fibre bundle. To estimate the voxel-wise FOD function, the constrained spherical deconvolution (CSD) was applied on DWI images (Tournier *et al.*, 2004; Tournier, Calamante and Connelly, 2007).

A probabilistic tractography was then generated with ACT framework (Smith *et al.*, 2012) to make sure that there was no streamlines terminating at the WM incorrectly due to the lesions. 10^7 streamlines were created using the “dynamic seeding mechanism” and spherical-deconvolution informed filtering of tractograms (SIFT2) approach was applied to reweight the streamlines, which

could ensure the number of streamlines matches the WM density (Smith *et al.*, 2015a).

In the end, connectome was reconstructed with the 120 GM nodes, which derived from the brain GM parcellation, and the edges were the sum of weights of streamlines between each pair of nodes (Smith *et al.*, 2015a, 2015b). Finally, a connectivity matrix was created to summarise the connectome including both nodes and edges. Figure 6.1 briefly presents the key steps of connectome reconstruction. Matlab R2017b was used to create connectivity matrix.

6.2.5. Brain connectivity toolbox

Based on the connectivity matrix, several measurements could be derived to represent different characters of connectivity strength. The brain connectivity toolbox (BCT; <http://www.brain-connectivity-toolbox.net>) was applied to calculate the global efficiency and mean local efficiency to represent the connectivity integration and segregation (see details in **chapter 4**; Rubinov and Sporns, 2010). The global efficiency and mean local efficiency were compared between HC and MS participant to validate the methods.

6.2.6. Statistical analysis

Descriptive statistics of age, EDSS, and lesion load are expressed as mean and standard deviation (see Table 6.2). SPSS version 24 was used for basic statistical analysis.

6.3. Results

6.3.1. Participants

Thirty-three MS participants (mean age (SD) = 42.1 (9.5) years, range 24.7-56.7 years) and thirteen HC (mean age (SD) = 48.2 (19.3) years, range 25.7-73.6 years) underwent MRI scanning. Considering this study focus on DWI imaging analysis, age was calculated at the DWI imaging scanning day. Detailed demographic participants characteristics are shown in Table 6.2.

Table 6.2. Demographic and network characteristics of HC and MS participants.

	HC	MS	P values
n	13	33	N/A
Gender	female	female	N/A
Age (year)	48.2 (\pm 19.4)	42.1 (\pm 9.5)	0.158
EDSS	N/A	2.1 (\pm 1.7)	N/A
Lesion load, $\times 10^3$ml	N/A	11.9 (\pm 18.3)	N/A
Global efficiency, $\times 10^3$	4.00 (\pm 0.12)	3.98 (\pm 0.18)	0.419
Mean local efficiency, $\times 10^3$	5.05 (\pm 0.17)	5.09 (\pm 0.19)	0.167
Mean clustering coefficient, $\times 10^3$	3.27 (\pm 0.12)	3.30 (\pm 0.14)	0.265

Mean and standard deviation are shown for the data. The EDSS score and lesion volume were not assessed in HC group. Age and lesion load were adjusted between HC and MS. P values < 0.05 are statistically significant. EDSS: Expanded Disability Status Scale; HC: healthy controls; MS: multiple sclerosis; N/A: not applicable.

6.3.2. Whole brain connectome reconstruction

The structural images were bias field corrected and the DWI images were motion, eddy current and geometric distortion corrected. WM lesions were drawn on the PD-weighted images and the lesion masks were registered to T1-weighted images. Figure 6.2 shows the PD-weighted image with lesions and T1-weighted image with lesion filled.

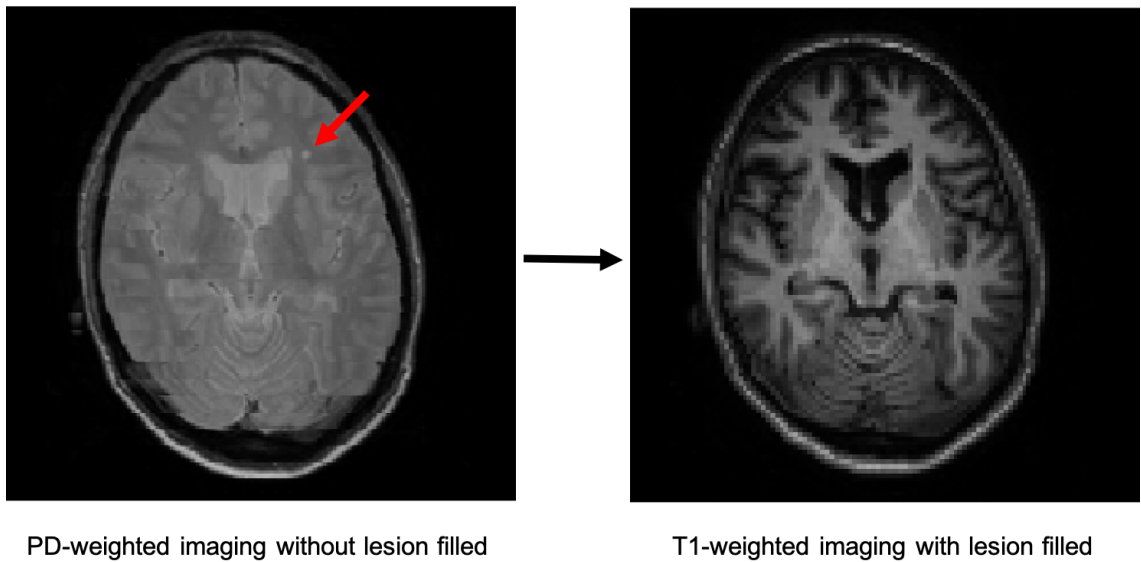
The brain was parcellated, and 120 GM regions (see Table 6.1) were used as nodes for connectivity reconstruction. The brain was segmented to CGM, DGM, WM, brainstem and CSF. Figure 6.3 and 6.4 show an example of the brain parcellation and segmentation.

After response function estimation, the whole brain probabilistic tractography for each participant was generated with ACT framework, followed by streamlines reweighting and connectome reconstruction. Each participant's connectome was represented in a connectivity matrix. Figure 6.5 demonstrates an example of the whole brain tractography comprising 120 nodes on the x and y axis and the number of streamlines connecting between each two of the nodes. In the connectivity matrix, the main diagonal is zero, meaning that the self-connection is not taken into account. Besides, all images from each step were visually checked.

6.3.3. Validation of the connectome reconstruction methods

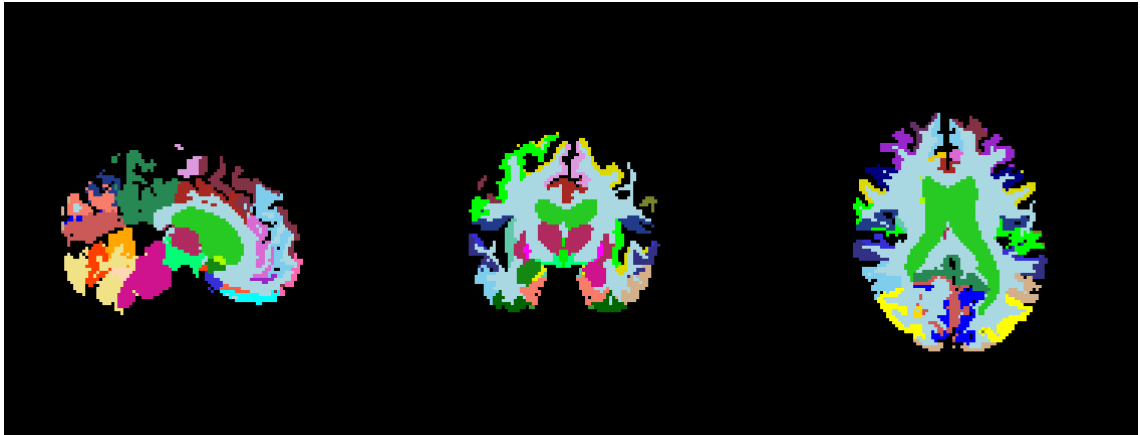
The connectome reconstruction methods were validated by comparing the network measures between HC and MS participant. The global efficiency was reduced in MS group, compared with HC, and the mean local efficiency and the mean clustering coefficient were higher in MS group. Table 6.2 shows the detailed figures of the connectome measures. The results share the same outcome with previous MS study (Charalambous *et al.*, 2019).

Figure 6.2. Lesion masking on PD-weighted image and T1-weighted imaging with lesion filled.



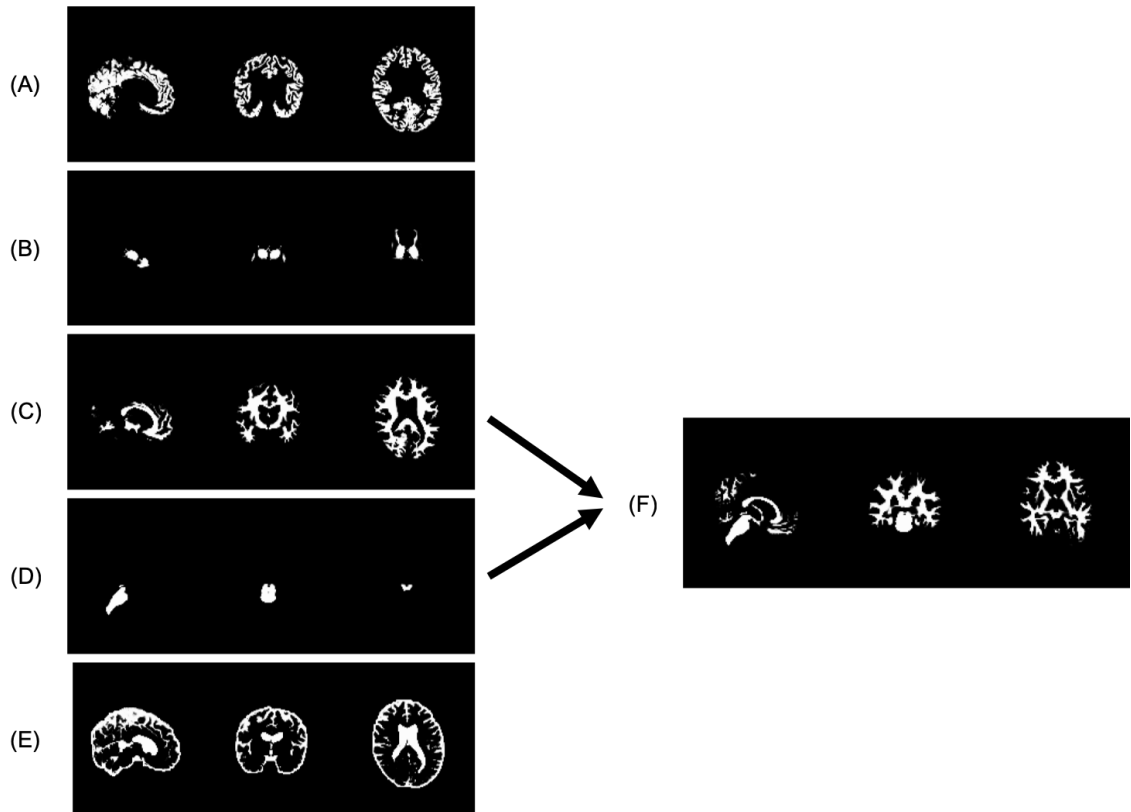
The red arrow on the left pointed out one lesion on the PD-weighted image. The WM lesions were drawn on the PD-weighted images and the lesion masks were registered to T1-weighted images on the right.

Figure 6.3. Brain parcellation.



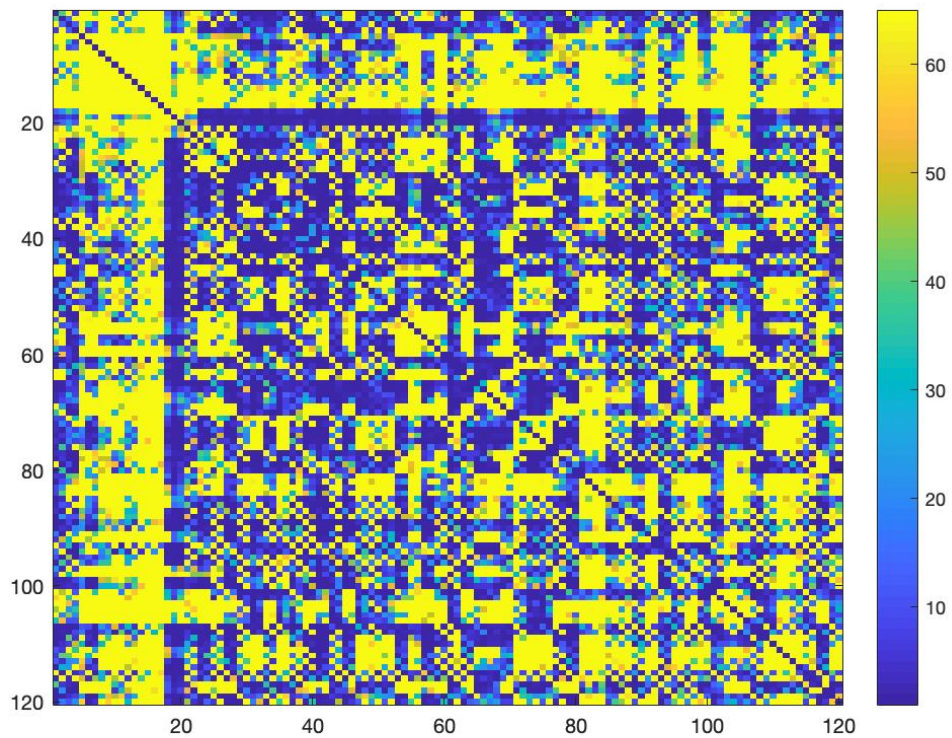
Brain parcellation was performed on the lesion filled T1-weighted images, and the brain was parcellated into distinct anatomical GM regions according to Desikan-Killiany-Tourville atlas using GIF algorithm.

Figure 6.4. Brain segmentation.



Brain segmentation was performed on the lesion filled T1-weighted images, and the brain was segmented into (A) cortical GM, (B) deep GM, (C) WM, (D) brain stem and (E) CSF. The (C) WM and (D) brain stem were then joined as one image (F) for subsequent ACT framework.

Figure 6.5. Whole brain connectome matrix.



The connectome matrix demonstrates an example of the whole brain connectivity matrix comprising 120 nodes and the number of streamlines connecting between each two of the nodes. The number on x and y axes refer to the nodes and the elements in the matrix refer to the streamlines. The main diagonal is zero, meaning that the self-connection is not taken into account.

6.4. Discussion

The connectome reconstruction is a multistep task based on structural images, DWI images and several advanced imaging processing toolboxes and algorithms. Keeping those in mind, each step of imaging processing for every participant needs a careful quality check to make sure the images are properly processed with as little as bias. For the current study, we did the connectome reconstruction with carefully assessment of the quality of all processed images and compared the final results with previous study. There is a reduced global efficiency in MS group, compared with HC, and higher mean local efficiency and mean clustering coefficient. From Charalambous et al. study, there is a significant reduction in global efficiency in MS group, compared with HC, and the reduction was significantly driven by the value from the SPMS patients (Charalambous *et al.*, 2019). Considering the MS patients in our study are mainly RRMS patients with mean EDSS score at 2.1, the reduction of global efficiency in MS group is less significant. Regarding the mean local efficiency and mean clustering coefficient, there were studies reporting reduced and increased value in MS, when comparing to HC, and Fleischer et al. pointed that the increased efficiency at early stage of MS may suggest of structural adaptations to maintain normal function (Fleischer *et al.*, 2017).

After structural images and DWI images pre-processing, several validated imaging processing pipelines were used in this study to improve the accuracy and efficiency of the reconstructed streamlines, including response function estimation, CSD, ACT framework and SIFT2 approach. The approaches equipped the connectome with anatomical and biological meaning by: 1)

estimating response function: modelling a voxel containing a single, coherently oriented bundle of axons (Tournier *et al.*, 2004; Tournier, Calamante and Connelly, 2007; Tax *et al.*, 2014); 2) the CSD approach: estimating a WM FOD function based on the response function (Tournier, Calamante and Connelly, 2007; Raffelt *et al.*, 2012); 3) the ACT framework: improving the accuracy of the reconstructed connectome by giving the anatomical priors (Smith *et al.*, 2012); 4) the SIFT2 approach: a novel approach to improve the quantitative nature of the whole brain connectome reconstruction by improving the streamline density (Smith *et al.*, 2013).

Based on the connectivity matrix, several measures describing the characters of the brain network were calculated by the BCT approach. It could be used to provide better understanding of the brain network integration and segregation by giving the global efficiency and local efficiency (Rubinov and Sporns, 2010). The use of the measures from the BCT approach was validated in this study by comparing the results from previous study in HC and MS patients (Fleischer *et al.*, 2017; Charalambous *et al.*, 2019), and could be spread to further analysis for OAB symptoms in MS.

6.5. Conclusion

In conclusion, this chapter introduced the methods of reconstructing the whole brain connectome network, based on structural images and DWI images, using

the recent published approaches with advanced pipelines improving the accuracy of the streamlines; selected proper BCT measures and described the characters of the connectivity network using the measures derived from the BCT approach; validated the reconstruction methods by comparing the global efficiency, mean local efficiency and mean clustering coefficient between HC and MS; created the connectivity matrix and the structural network for MS patients, which could be compared with the network for OAB symptoms in MS in **Chapter 7**; and provide a whole brain connectivity matrix for subsequent studies on OAB symptoms in MS, for example, selecting OAB related GM regions from the whole matrix. As a result, the well validated whole brain connectome for MS patients, together with the BCT approach calculating different measures of the connectivity matrix, could be properly used for subsequent analysis for OAB symptoms in MS cohort.

6.6. Remaining question and further direction

In this chapter, the whole brain connectome was reconstructed, and the connectivity matrix was obtained. With the use of the BCT approach, several network measures were provided to describe the characters of the whole brain connectivity network and identify differences between HC and MS patients. Considering the successful use of the methods, and the main aim of the whole study which is to investigate the WM abnormalities subtending OAB symptoms in MS cohort, the methods and approaches could be explored to learn the network of OAB symptoms in MS and compensate the current understanding of LUTS in neurological conditions. Therefore, the further direction is to apply the methods from this chapter to MS patients and describe the characters of the structural network subtending OAB symptoms in MS.

Bibliography

- Andersson, J. L. R. and Sotiropoulos, S. N. (2016) 'An integrated approach to correction for off-resonance effects and subject movement in diffusion MR imaging', *NeuroImage*. The Authors, 125, pp. 1063–1078. doi: 10.1016/j.neuroimage.2015.10.019.
- Bhushan, C. *et al.* (2012) 'Correcting Susceptibility-Induced Distortion in Diffusion-Weighted MRI using Constrained Nonrigid Registration.', *Signal and Information Processing Association Annual Summit and Conference (APSIPA), ... Asia-Pacific. Asia-Pacific Signal and Information Processing Association Annual Summit and Conference*. United States, 2012.
- Bodini, B. *et al.* (2009) 'Exploring the Relationship Between White Matter and Gray Matter Damage in Early Primary Progressive Multiple Sclerosis : An In Vivo Study With TBSS and VBM', *Human Brain Mapping*, 2861(November 2008), pp. 2852–2861. doi: 10.1002/hbm.20713.
- Cardoso, M. J. *et al.* (2015) 'Geodesic Information Flows: Spatially-Variant Graphs and Their Application to Segmentation and Fusion', *IEEE Transactions on Medical Imaging*. IEEE, 34(9), pp. 1976–1988. doi: 10.1109/TMI.2015.2418298.
- Charalambous, T. *et al.* (2019) 'Structural network disruption markers explain disability in multiple sclerosis.', *Journal of neurology, neurosurgery, and psychiatry*. England, 90(2), pp. 219–226. doi: 10.1136/jnnp-2018-318440.
- Eshaghi, A. *et al.* (2018) 'Deep gray matter volume loss drives disability worsening in multiple sclerosis.', *Annals of neurology*. United States, 83(2), pp. 210–222. doi: 10.1002/ana.25145.
- Fleischer, V. *et al.* (2017) 'Increased structural white and grey matter network connectivity compensates for functional decline in early multiple sclerosis', *Multiple Sclerosis Journal*, 23(3), pp. 432–441. doi: 10.1177/1352458516651503.
- Griffiths, D. (2015) *Functional imaging of structures involved in neural control of the lower urinary tract*. 1st edn, *Handbook of clinical neurology*. 1st edn. Elsevier B.V. doi: 10.1016/B978-0-444-63247-0.00007-9.
- Hickman, S. J. *et al.* (2002) 'Technical note: The comparison of hypointense lesions from "pseudo-T1" and T1-weighted images in secondary progressive multiple sclerosis', *Multiple Sclerosis*, 8(5), pp. 433–435. doi: 10.1191/1352458502ms824xx.
- Kurtzke, J. F. (1983) 'Rating neurologic impairment in multiple sclerosis: An expanded disability status scale (EDSS)', *Neurology*, 33(11), pp. 1444–1444. doi: 10.1212/WNL.33.11.1444.
- De Marchis, G. M. *et al.* (2010) 'Mild cognitive impairment in medical inpatients: the Mini-Mental State Examination is a promising screening tool.', *Dementia and geriatric cognitive disorders*. Switzerland, 29(3), pp. 259–264. doi: 10.1159/000288772.
- Polman, C. H. *et al.* (2011) 'Diagnostic criteria for multiple sclerosis: 2010 Revisions to the McDonald criteria', *Annals of Neurology*, 69(2), pp. 292–302. doi: 10.1002/ana.22366.
- Prados, F. *et al.* (2016) 'NiftyWeb : web based platform for image processing on the cloud', *24th Scientific Meeting and Exhibition of the International Society for Magnetic Resonance in Medicine (ISMRM)*, (ISMRM).
- Raffelt, D. *et al.* (2012) 'Apparent Fibre Density: a novel measure for the analysis

- of diffusion-weighted magnetic resonance images.', *NeuroImage*. United States, 59(4), pp. 3976–3994. doi: 10.1016/j.neuroimage.2011.10.045.
- Rubinov, M. and Sporns, O. (2010) 'NeuroImage Complex network measures of brain connectivity : Uses and interpretations', *NeuroImage*. Elsevier Inc., 52(3), pp. 1059–1069. doi: 10.1016/j.neuroimage.2009.10.003.
- Smith, R. E. *et al.* (2012) 'Anatomically-constrained tractography: improved diffusion MRI streamlines tractography through effective use of anatomical information.', *NeuroImage*. United States, 62(3), pp. 1924–1938. doi: 10.1016/j.neuroimage.2012.06.005.
- Smith, R. E. *et al.* (2013) 'SIFT: Spherical-deconvolution informed filtering of tractograms.', *NeuroImage*. United States, 67, pp. 298–312. doi: 10.1016/j.neuroimage.2012.11.049.
- Smith, R. E. *et al.* (2015a) 'SIFT2: Enabling dense quantitative assessment of brain white matter connectivity using streamlines tractography.', *NeuroImage*. United States, 119, pp. 338–351. doi: 10.1016/j.neuroimage.2015.06.092.
- Smith, R. E. *et al.* (2015b) 'The effects of SIFT on the reproducibility and biological accuracy of the structural connectome.', *NeuroImage*. United States, 104, pp. 253–265. doi: 10.1016/j.neuroimage.2014.10.004.
- Sporns, O., Tononi, G. and Ko, R. (2005) 'The Human Connectome : A Structural Description of the Human Brain', *PLoS Computational Biology*, 1(4). doi: 10.1371/journal.pcbi.0010042.
- Tax, C. M. W. *et al.* (2014) 'Recursive calibration of the fiber response function for spherical deconvolution of diffusion MRI data.', *NeuroImage*. United States, 86, pp. 67–80. doi: 10.1016/j.neuroimage.2013.07.067.
- Tournier, J.-D. *et al.* (2004) 'Direct estimation of the fiber orientation density function from diffusion-weighted MRI data using spherical deconvolution.', *NeuroImage*. United States, 23(3), pp. 1176–1185. doi: 10.1016/j.neuroimage.2004.07.037.
- Tournier, J.-D., Calamante, F. and Connelly, A. (2007) 'Robust determination of the fibre orientation distribution in diffusion MRI: non-negativity constrained super-resolved spherical deconvolution.', *NeuroImage*. United States, 35(4), pp. 1459–1472. doi: 10.1016/j.neuroimage.2007.02.016.
- Tustison, N. J. *et al.* (2010) 'N4ITK: improved N3 bias correction.', *IEEE transactions on medical imaging*. United States, 29(6), pp. 1310–1320. doi: 10.1109/TMI.2010.2046908.

Chapter 7

7. Brain structural network for overactive bladder in multiple sclerosis

Summary

This chapter includes two sections. **Section A** proposes the structural connectivity network for the OAB symptoms in MS patients (MS-OAB-network) based on the whole brain structural connectome reconstructed in **chapter 6**, and **section B** generates the structural connectivity network based on working model of LUT control and compares it with the MS-OAB-network created in **section A**. The MS-OAB-network is created by: 1) calculating six commonly used connectivity measures using the BCT approach, including degree (DEG), betweenness centrality (BC), cluster coefficient (CC), participation coefficient (PC), local efficiency (LE) and global efficiency (GE); 2) ranking the GM regions representing OAB symptoms among 120 GM regions parcellated by GIF pipelines (see details in **chapter 6**); 3) comparing the connectivity network between the MS-OAB and MS-no-LUTS group. **Section A** introduces six commonly used local measures of the connectivity matrix from the BCT approach and identifies the GM regions subtending OAB symptoms by classification

analysis. The proposed structural connectivity network for OAB symptoms compensates the current understanding of OAB symptoms in MS, and it is the first structural connectivity network for LUTS in neurological conditions. Different from the MS-OAB-network, the LUT working model network in **section B** is created with the GM regions involved in the working model of LUT control, rather than the GM regions selected by classification analysis. The streamlines showing statistical significance between MS-OAB and MS-no-LUTS are included in the LUT working model network. The LUT working model network confirms the structural connectivity between insula and frontal lobe, as the functional circuit showing in the working model of LUT control. The LUT working model network does not include temporal lobe and occipital lobe, whereas the MS-OAB-network presents a widespread connectivity in the brain including key regions involved in working model of LUT control. The similarities and the differences between two networks illustrate the importance of research on structural connectivity network in neurological conditions with different aspects of LUTS.

Section A. Structural network subtending overactive bladder symptoms in multiple sclerosis

7.1. Introduction

Following the reconstruction of the whole brain structural connectivity network in **chapter 6**, the methods and approaches providing characters of the brain connectome could be explored to study the OAB symptoms in MS patients. Based on the current understanding of the LUT functions from PET and fMRI studies, several GM regions specifically including frontal cortex (especially prefrontal cortex), cingulate, insula, and thalamus were identified significance in working model of LUT control (Griffiths, 2015). However, regarding the WM findings for the neural pathway for the LUTS, there were limited studies suggesting some possible relationship between LUTS and WM tracts.

A WMH study reported the right inferior frontal areas and the potential involvement of the nearby WM tracts, including the anterior corona radiata and the superior fronto-occipital fasciculus could predict incontinence, incontinence severity and degree of bother in community-dwelling older adults (age range 75-89 years; Kuchel *et al.*, 2009). In an fMRI study in older adults (mean age (SD) = 71.5 (7.5) years), WMH was investigated to analyse whether the presence of the WMH correlated with brain activity during the bladder filling phase, and the anterior thalamic radiation, uncinate fasciculus, Inferior fronto-occipital fasciculus, inferior longitudinal fasciculus and superior longitudinal fasciculus were positively

or negatively correlated with brain activities, delivering activation or deactivation signals in regard to bladder filling phase (Tadic *et al.*, 2010). The incontinence, urinary urgency and frequency in older adults were not only reported as age-related changes in bladder itself, but also considered as vascular incontinence caused by white matter disease (WMD), which was described as WMH, WM ischemia and multiple cerebral infarction, corresponding to aging (Sakakibara *et al.*, 2012). However, except the knowledge of incontinence, urinary urgency and frequency corresponding to aging, understanding of LUTS in neurological conditions were limited.

The TBSS analysis in **chapter 5** discovered the general WM changes for the OAB symptoms in MS in the whole brain, through the correlation analysis between the OAB severity and the FA value in MS cohort and the group difference analysis of FA values between MS-OAB and MS-no-LUTS, without any pre-proposed brain regions or WM networks. For a better understanding of the OAB symptoms in MS, analysis on WM could be explored in more relevant regions, rather than the whole brain. Based on the knowledge from **chapter 6**, the brain structural connectivity network analysis is considered to be a possible approach to provide the WM network for the OAB symptoms in MS. With the whole brain connectivity network created in **chapter 6**, several GM areas corresponding to the OAB symptoms in MS could be selected for further analysis in more relevant regions, and the BCT approach could be applied to describe the characters of the connectivity network. Functional connectivity refers to the statistical dependencies between the activity of different brain regions, and

structural connectivity studies the physical connections between brain regions. Ideally, both structural and functional information should be taken into account.

Therefore, the objectives of this section are:

1. to calculate the six commonly used BCT measures, derived from the whole brain connectivity matrix created in **chapter 6**;
2. to identify the GM regions, which are more relevant to the OAB symptoms in MS, from the 120 parcellated GM areas using GIF algorithm in **chapter 6**, using classification analysis;
3. to propose the structural network for the MS patients with OAB relevant GM regions (MS-network) and the structural network subtending OAB symptoms in MS (MS-OAB-network);
4. to explain how the MS-OAB-network compensates the current understanding of the working model of LUT control proposed by Griffiths (LUT working model network; discussed in **chapter 3**).

7.2. Methods

7.2.1. Participants

Thirty-three right-handed female MS patients with a diagnosis of MS according to McDonald criteria (Polman *et al.*, 2011) were recruited from NHNN, including seventeen MS patients reporting predominant OAB symptoms (MS-OAB) and sixteen MS patients without any LUTS (MS-no-LUTS). Detailed inclusion and exclusion criteria, research protocol and ethics approval were introduced in **chapter 5**. The LUTS were evaluated by the USP-OAB sub-score from the USP questionnaire (Haab *et al.*, 2008), and the cut off value (mean + 2SD) was calculated from the USP-OAB sub-score of the HC (see details in **chapter 5**). Participants scoring below or equal to the cut off value (3, range 0 - 21) were treated as the MS-no-LUTS group, and those scoring above the value were included in the MS-OAB group. Thirteen right-handed female healthy participants were recruited as a control group.

7.2.2. Clinical assessments

Participants were assessed at their screening visit, using both uro-neurological investigations and questionnaires as following:

13. Patients' clinical history was recorded based on clinical record in the hospital;
14. The MMSE (De Marchis *et al.*, 2010) was assessed for cognitive impairment in all participants, and people were excluded if the score was less than 23 (see details in **Appendix 1**);

15. Physical examinations, including neurological and urological examinations, were given out by two Consultant Neurologists (JNP and ATT) at NHNN, helping to offer more clinical details;
16. The EDSS (Kurtzke, 1983) was assessed by experienced Consultant Neurologists at NHNN and patients' EDSS more than 6.5, or who had relapse in the previous 3 months, were excluded from this study (see details in **Appendix 2**);
17. The USP (Haab *et al.*, 2008) questionnaire, providing a comprehensive evaluation of urinary symptoms and their severity in males and females. The USP-OAB sub-score was used to evaluate the OAB symptoms;
18. A three-day bladder diary (BD, see details in **Appendix 9**), providing more information of the participants' bladder habit.

7.2.3. MRI imaging acquisition

MRI scanning was carried out using a 3.0 Tesla scanner (Philips Achieva, Philips Medical Systems, Best, The Netherlands). Clinical scans were acquired in the axial-oblique plane parallel to the anterior-posterior callosal line using the following parameters: 1) T1-weighted images: TE = 10 ms, TR = 625 ms, FOV 240×180 mm², NEX = 1, voxel size = 1×1×1 mm³, 50 slices and scan time = 5:43 min; 2) PD-weighted and T2-weighted images: TE1/TE2 = 19/85 ms, TR = 3500 ms, FOV 240×180 mm², NEX = 1, voxel size = 1×1×3 mm³, 50 slices and scan time = 4:01 min. DTI was also performed in the axial-oblique plane, with 32 distributed diffusion encoding directions (b = 0 and b = 1000 s/mm²) and the following parameters: TE = 92 ms, TR = 9714 ms, FOV 248×248 mm², NEX = 1, voxel size = 2×2×2 mm³, 70 slices and scan time = 6:46 min.

7.2.4. MRI imaging processing

In this section, all analyses were based on the whole brain structural connectivity network reconstructed for the thirty-three MS patients in **chapter 6**. The connectivity matrices for the MS patients were generated through: 1) diffusion-weighted imaging pre-processing, including the motion and eddy current correction by the FSL v5.0.9 (<https://fsl.fmrib.ox.ac.uk/fsl>; Andersson and Sotiropoulos, 2016), and the geometric distortion correction by the BrainSuite (Bhushan *et al.*, 2012); 2) structural imaging pre-processing, including the bias field correction by N4 algorithm (Tustison *et al.*, 2010), registration T1-weighted images to the DWI images using BrainSuite (Bhushan *et al.*, 2012), lesion masking on PD-weighted images using Jim 6.0 (<http://www.xinapse.com/Manual/index.html>), and brain segmentation and parcellation according to Desikan-Killiany-Tourville atlas using GIF algorithm (<http://cmictig.cs.ucl.ac.uk/niftyweb>; Cardoso *et al.*, 2015; Prados *et al.*, 2016); 3) whole brain structural connectome reconstruction using MRtrix3 v0.3.14 package (<http://www.mrtrix.org>), including response function estimation using Tax algorithm (Tax *et al.*, 2014), fibre orientation distribution (FOD) function estimation using the constrained spherical deconvolution (CSD; Tournier *et al.*, 2004; Tournier, Calamante and Connelly, 2007), a probabilistic tractogram generation with ACT framework (Smith *et al.*, 2012), reweighting the streamlines with SIFT2 approach (Smith *et al.*, 2015), and connectome reconstruction with 120 GM nodes derived from the brain parcellation. All details of MRI imaging processing steps, the reconstructed whole brain structural connectivity network,

and the connectivity matrix were described in **chapter 6**. Matlab R2017b was used to create connectivity matrix.

7.2.5. Selection of GM regions for the OAB symptoms in MS

Six commonly used connectivity measures were derived from the connectivity matrix to represent different characteristics of connectivity network, including local and global metrics, such as degree (DEG), betweenness centrality (BC), cluster coefficient (CC), participation coefficient (PC), local efficiency (LE) and global efficiency (GE). The definition of the six measures were described in **chapter 4**. The BCT (<http://www.brain-connectivity-toolbox.net>) was applied to calculate the six features (DEG, BC, CC, PC, LE, GE) that overall represented network centrality, integration and segregation (see details in **chapter 4**; Rubinov and Sporns, 2010).

The six measures were then used in a classification task to identify the GM regions likely to be responsible for the OAB symptoms in our cohort of MS patients; this was achieved by selecting the best features between the MS-OAB and MS-no-LUTS group. 720 features (120 GM regions \times 6 measures for each GM region) were entered in the classification task performed using the k-nearest neighbours (kNN) algorithm and random tree algorithm, which are non-parametric methods in a supervised machine learning for classification (Altman, 1992; Ho, 1998). All the 720 features were first adjusted for age and EDSS score by calculating the residuals of the BCT features using Stata 14. The statistics measures, including area under receiver operating characteristic (ROC) curve

(AUC), classification accuracy (CA), F1 score, precision and recall, were used to identify the top percentage of features able to classify MS-OAB versus MS-no-LUTS. The GM regions included in the top 10% ranked figures were then selected as forming the LUTS classifying nodes for MS patients with OAB symptoms (MS-OAB-nodes). Orange v3.11.0 (<https://orange.biolab.si>; Demšar *et al.*, 2013) was applied in classification analysis.

7.2.6. Statistical analysis

Descriptive statistics of age, EDSS, disease duration, and lesion load are expressed as mean and standard deviation (see Table 7.1). All variables were checked for skewness and presence of outliers. SPSS version 24 was used for basic statistical analysis and the group difference analysis between HC and MS patients, and the MS-OAB and MS-no-LUTS group on the streamlines between each two nodes selected from the previous step. Stata 14 was used to calculate the residuals of the streamlines adjusted for age and EDSS score. The Student's t test and Mann-Whitney U test were applied. A p value < 0.05 was considered statistically significant, and p value < 0.1 was considered a favourable statistical trend.

7.2.7. Structural connectivity network visualization

A structural network for MS patients (MS-network) was created starting from the whole brain connectivity matrix and selecting the MS-OAB-nodes and corresponding edges whose number of streamlines was statistically significantly

different ($p < 0.05$), when comparing HC and MS patients. Similarly, a structural network subtending OAB symptoms in MS (MS-OAB-network) was created with selected nodes and streamlines showing statistically significant difference ($p < 0.05$) between the MS-OAB and MS-no-LUTS group. The BrainNet Viewer (<https://www.nitrc.org/projects/bnv/>; Xia, Wang and He, 2013) was applied to draw the generated structural connectivity for a better visualization of the results.

7.3. Results

7.3.1. Participants

Sixteen MS-no-LUTS (mean age (SD) = 37.9 (8.8) years, range 24.7-51.1 years), seventeen MS-OAB participants (mean age (SD) = 46.1 (8.6) years, range 27.3-56.7 years), and thirteen HC (mean age (SD) = 48.2 (19.3) years, range 25.7-73.6 years) underwent MRI scanning. Considering this study focus on DWI imaging analysis, age was calculated at the DWI imaging scanning day. Detailed demographic participants characteristics are shown in Table 7.1.

Table. 7.1. Demographic characteristics of MS-no-LUT and MS-OAB participants.

	HC	MS	P values	MS-no-LUTS	MS-OAB	P values
n	13	33	N/A	16	17	N/A
Gender	female	female	N/A	female	female	N/A
Age (year)	48.2 (\pm 19.4)	42.1 (\pm 9.5)	0.158	37.9 (\pm 8.8)	46.1 (\pm 8.6)	0.011
EDSS	N/A	2.1 (\pm 1.7)	N/A	1.3 (\pm 0.9)	2.9 (\pm 2.0)	0.005
Lesion load, $\times 10^3$ml	N/A	11.9 (\pm 18.3)	N/A	5.5 (\pm 6.1)	18.0 (\pm 23.6)	0.048

Mean and standard deviation are shown for the data. The EDSS score and lesion volume were not assessed in HC group. Age and lesion load were adjusted between HC and MS. Age, EDSS and lesion load were adjusted between MS-no-LUTS and MS-OAB. P values in bold are statistically significant at $p < 0.05$. EDSS: Expanded Disability Status Scale; HC: healthy controls; MS: multiple sclerosis; MS-no-LUTS: MS without LUTS; MS-OAB: MS with OAB; N/A: not applicable.

7.3.2. GM regions for the OAB symptoms in MS

With the classification analysis, forty-one GM regions listed at the top 10% of the 720 features (120 GM regions \times 6 features for each GM region). Table 7.2 listed the selected GM regions. The streamlines between each two nodes in the forty-one GM regions were used for further group difference analysis to generate the structural connectivity networks for the OAB symptoms in MS and the MS patients.

Table 7.2. The GM regions selected for the OAB symptoms in MS.

1	Right Accumbens Area	22	Left middle cingulate gyrus
2	Right Amygdala	23	Right medial frontal cortex
3	Left Thalamus Proper	24	Left medial frontal cortex
4	Cerebellar Vermal Lobules VI-VII	25	Right middle frontal gyrus
5	Cerebellar Vermal Lobules VIII-X	26	Right middle occipital gyrus
6	Right anterior cingulate gyrus	27	Left middle occipital gyrus
7	Right anterior insula	28	Right medial orbital gyrus
8	Left anterior insula	29	Right superior frontal gyrus medial segment
9	Right anterior orbital gyrus	30	Right occipital pole
10	Left anterior orbital gyrus	31	Right precuneus
11	Left calcarine cortex	32	Right posterior orbital gyrus
12	Right central operculum	33	Left posterior orbital gyrus
13	Left central operculum	34	Right planum temporale
14	Left cuneus	35	Left planum temporale
15	Left entorhinal area	36	Left subcallosal area
16	Right frontal pole	37	Left supramarginal gyrus
17	Left fusiform gyrus	38	Left superior temporal gyrus
18	Right inferior occipital gyrus	39	Left temporal pole
19	Right inferior temporal gyrus	40	Right triangular part of the inferior frontal gyrus
20	Right lingual gyrus	41	Left transverse temporal gyrus
21	Left lingual gyrus		

7.3.3. The structural connectivity network for the MS patients

With the same selected GM regions and the streamlines showing statistically significant group difference between HC and MS patients, the MS-network was created. Table 7.3 presented the streamlines between the two GM regions showing statistically significant difference between HC and MS patients. Figure 7.1 provided the visualized pictures of the MS-network and MS-OAB-network.

7.3.4. The structural connectivity network for the OAB symptoms in MS

With the selection of the GM regions for the OAB symptoms and the group difference between MS-OAB and MS-no-LUTS group on the streamlines, the MS-OAB-network was generated (Figure 7.1). Table 7.4 presented the streamlines between the two GM regions showing statistically significant difference between MS-no-LUTS and MS-OAB.

Table 7.3. List of GM regions having statistically significant streamlines in between, in group difference between HC and MS.

Two GM regions showing statistically significant streamlines in between		P-value
Right Accumbens	Cerebellar Vermal Lobules VIII-X	0.012
Right Accumbens	Right anterior cingulate gyrus	0.039
Right Accumbens	Left entorhinal area	0.053
Right Accumbens	Left lingual gyrus	0.012
Right Accumbens	Right occipital pole	0.018
Right Amygdala	Left middle cingulate gyrus	0.049
Right Amygdala	Right medial orbital gyrus	0.019
Left Thalamus Proper	Cerebellar Vermal Lobules VI-VII	0.028
Left Thalamus Proper	Right anterior cingulate gyrus	0.008
Left Thalamus Proper	Left lingual gyrus	0.045
Left Thalamus Proper	Right occipital pole	0.043
Cerebellar Vermal Lobules VI-VII	Right inferior temporal gyrus	0.002
Cerebellar Vermal Lobules VIII-X	Left middle cingulate gyrus	0.018
Right anterior cingulate gyrus	Left central operculum	0.022
Right anterior cingulate gyrus	Right occipital pole	0.019
Right anterior insula	Right occipital pole	0.01
Left anterior insula	Right inferior temporal gyrus	0.05
Left anterior orbital gyrus	Left posterior orbital gyrus	0.035
Left calcarine cortex	Right central operculum	0.035
Left central operculum	Left middle cingulate gyrus	0.041
Left central operculum	Left medial frontal cortex	0.074
Left entorhinal area	Left middle cingulate gyrus	0.016
Left fusiform gyrus	Left posterior orbital gyrus	0.032
Right inferior occipital gyrus	Left middle cingulate gyrus	0.046
Right inferior temporal gyrus	Left middle cingulate gyrus	0.044
Right inferior temporal gyrus	Right occipital pole	0.02
Right inferior temporal gyrus	Left planum temporale	0.109
Right lingual gyrus	Right middle occipital gyrus	0.042
Left middle cingulate gyrus	Right middle occipital gyrus	0.03
Right superior frontal gyrus medial segment	Right precuneus	0.03
Right occipital pole	Right posterior orbital gyrus	0.008
Right precuneus	Left planum temporale	0.016
Right precuneus	Left superior temporal gyrus	0.041
Right precuneus	Left transverse temporal gyrus	0.02
Left posterior orbital gyrus	Left supramarginal gyrus	0.013
Left posterior orbital gyrus	Left superior temporal gyrus	0.013
Left posterior orbital gyrus	Left temporal pole	0.044
Right planum temporale	Left subcallosal area	0.025

Right planum temporale	Left superior temporal gyrus	0.091
Right planum temporale	Left transverse temporal gyrus	0.044
Left superior temporal gyrus	Left transverse temporal gyrus	0.012

Statistical difference between HC and MS were tested using Student's t test and Mann-Whitney U test. A p value < 0.05 was considered statistically significant.

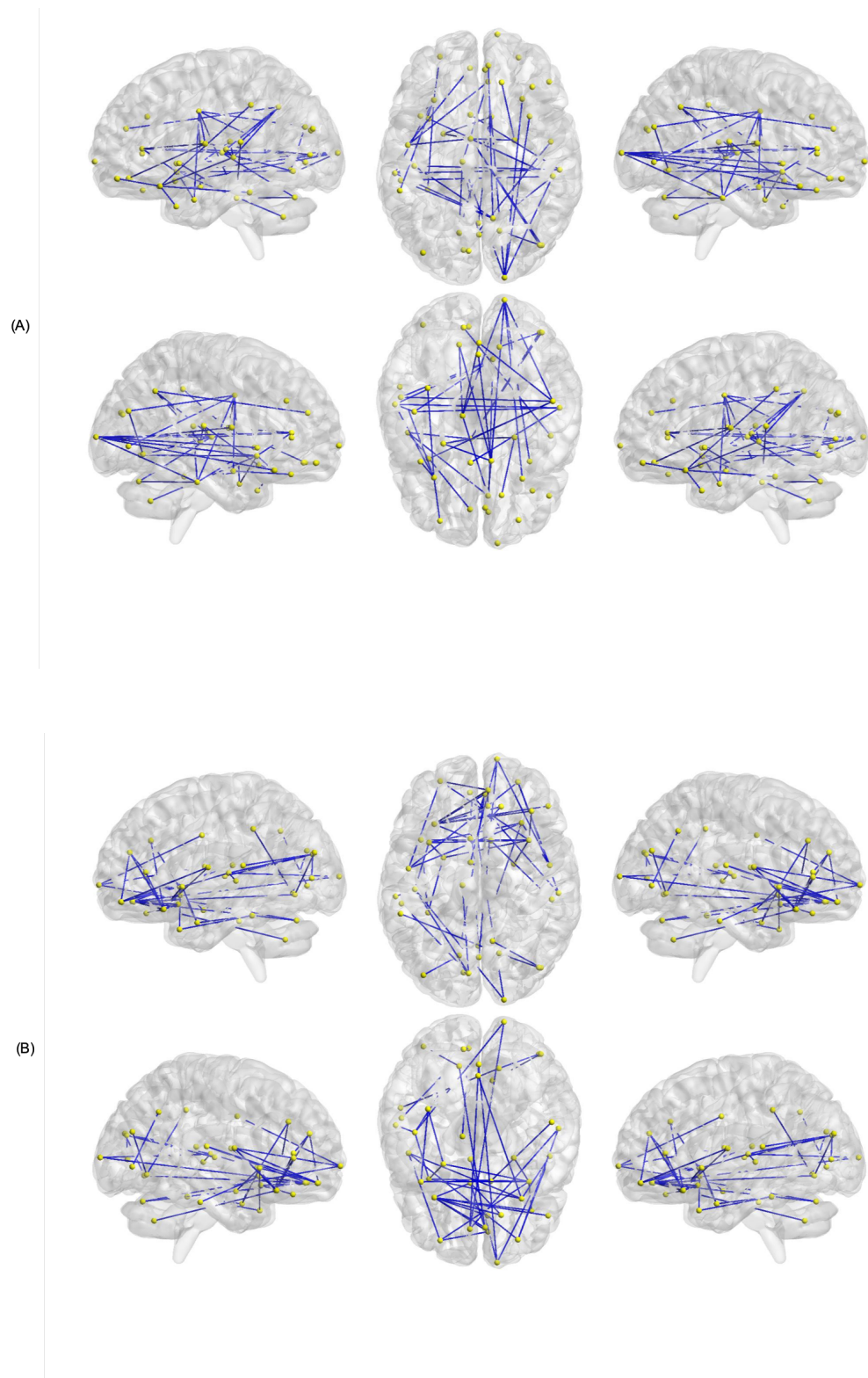
Table 7.4. List of GM regions having statistically significant streamlines in between, in group difference between MS-no-LUT and MS-OAB.

Two GM regions showing statistically significant streamlines in between		P-value
Right Accumbens Area	Right anterior cingulate gyrus	0.042
Right Accumbens Area	Right inferior temporal gyrus	0.038
Right Accumbens Area	Left middle cingulate gyrus	0.038
Right Amygdala	Left cuneus	0.04
Right Amygdala	Right medial orbital gyrus	0.021
Right Cerebellum Exterior	Left temporal pole	0.008
Cerebellar Vermal Lobules VI-VII	Right inferior temporal gyrus	0.004
Cerebellar Vermal Lobules VI-VII	Right middle temporal gyrus	0.029
Cerebellar Vermal Lobules VIII-X	Left superior temporal gyrus	0.005
Right anterior cingulate gyrus	Right medial frontal cortex	0.046
Right anterior cingulate gyrus	Right superior frontal gyrus medial segment	0.045
Right anterior insula	Left calcarine cortex	0.01
Right anterior insula	Right lingual gyrus	0.039
Right anterior insula	Right planum temporale	0.014
Left anterior insula	Right lingual gyrus	0.012
Left anterior insula	Right middle occipital gyrus	0.03
Left anterior orbital gyrus	Left planum temporale	0.036
Left calcarine cortex	Left cuneus	0.018
Left calcarine cortex	Right posterior insula	0.038
Left calcarine cortex	Left transverse temporal gyrus	0.043
Right central operculum	Left entorhinal area	0.029
Right central operculum	Left medial frontal cortex	0.025
Right central operculum	Left posterior orbital gyrus	0.027
Right central operculum	Right planum temporale	0.001
Left central operculum	Right frontal pole	0.004
Left central operculum	Left planum temporale	0.035
Left central operculum	Left superior temporal gyrus	0.015
Left cuneus	Left lingual gyrus	0.009
Left cuneus	Right subcallosal area	0.036
Left cuneus	Left transverse temporal gyrus	0.031
Left entorhinal area	Right superior frontal gyrus medial segment	0.041
Left entorhinal area	right posterior orbital gyrus	0.026
Right frontal pole	Left middle cingulate gyrus	0.018
Right frontal pole	Right planum polare	0.045
Right frontal pole	Left superior temporal gyrus	0.028
Right inferior occipital gyrus	Left posterior orbital gyrus	0.046
Right lingual gyrus	Right subcallosal area	0.017

Left lingual gyrus	Left middle cingulate gyrus	0.026
Left lingual gyrus	Right posterior insula	0.029
Left lingual gyrus	Right subcallosal area	0.014
Left middle cingulate gyrus	Right medial orbital gyrus	0.026
Left middle cingulate gyrus	Right occipital pole	0.004
right medial frontal cortex	Left superior temporal gyrus	0.003
right middle occipital gyrus	Right occipital pole	0.007
Right medial orbital gyrus	Left subcallosal area	0.027
right precuneus	Right subcallosal area	0.017
Right posterior orbital gyrus	Right planum polare	0.027
Right posterior orbital gyrus	Left transverse temporal gyrus	0.049
right planum temporale	Right subcallosal area	0.041
Left superior temporal gyrus	Left transverse temporal gyrus	0.004

Statistical difference between MS-no-LUTS and MS-OAB were tested using Student's t test and Mann-Whitney U test. A p value < 0.05 was considered statistically significant.

Figure 7.1. MS-network and MS-OAB-network.



The connectivity networks, (A) MS-network and (B) MS-OAB-network, created by the BrainNet Viewer. Nodes are in yellow and edges are in blue.

7.4. Discussion

The MS-network and MS-OAB-network were generated based on the whole brain connectivity network reconstructed in **chapter 6**, with relevant GM regions selected by classification task and the streamlines showing statistically significant differences between the HC and MS patients, and MS-no-LUTS and MS-OAB group. It is the first study providing network evidence on WM pathways for LUTS in neurological conditions.

The six commonly used BCT measures derived from the whole brain connectivity matrix provided connectome information from multiple ways on the brain structural network centrality, integration and segregation, and helped with a better understanding on the characters of each GM regions (Rubinov and Sporns, 2010). As discussed in **chapter 4**, the DEG offered basic concepts of the network by giving the number of links connected to a node (Rubinov and Sporns, 2010); the BC was the fraction of all shortest paths in the network that contain a given node (Rubinov and Sporns, 2010); the PC gave a measure of diversity of intermodular connections of individual nodes (Rubinov and Sporns, 2010); the GE provided the average inverse shortest path length in the network (Latora and Marchiori, 2001); the LE was the global efficiency computed on the neighbourhood of the node, and was related to the clustering coefficient (Rubinov and Sporns, 2010); the CC was the fraction of the triangles around an individual node (Watts and Strogatz, 1998). All the measures were calculated on the 120 nodes, helped to express the characters of the network from various prospects, and used to improve the probability of the relevant GM regions for the OAB symptoms, indicating best classifiers between the MS-OAB and MS-no-LUTS group. The

identification of the relevant GM regions for the OAB symptoms led to a proper reconstruction of the MS-OAB-network. With age and EDSS score as covariates adjusted in the analysis, the study provided the MS-OAB-network with minimized effects from aging and mobility impairments on the bladder habits.

As showed in Table 7.4 and Figure 7.1, several streamlines in the MS-OAB-network presented the same trend of the brain WM tracts, including the ones between frontal lobe and cingulate, frontal lobe and temporal lobe, frontal lobe and occipital lobe, temporal lobe and occipital lobe, temporal lobe and insula, and occipital lobe and insula. Compared with the working model of LUT control (see details in **chapter 3**; Griffiths, 2015), the results confirmed the working model, and identified the structural connectivity between importance of insula and the prefrontal lobe. Moreover, the results from MS-OAB-network provided a probability of the underlying structural damage leading to functional alterations. Taking into consideration of working model of LUT control, the MS-OAB-network speculated that there were possibilities of indirect WM damages between GM regions resulting in changes of functional activities. For example, the functional alterations (the activation or deactivation for perception of bladder fullness) in insula and prefrontal cortex may due to the direct WM pathway between them, but also could be the indirect structural pathways from insula to prefrontal lobe through temporal lobe and/or occipital lobe. However, considering the analysis methods used for fMRI, those regions without a significant functional activity could be underestimated due to: firstly, depending on the threshold set in the fMRI analysis, the signal changes may not be captured in temporal and occipital lobe, so the circuit from insula to frontal lobe through temporal and/or occipital

lobe was not observed from the fMRI studies; secondly, the signal could not be conveyed due to the damages in a specific GM region, such as temporal lobe and occipital lobe in this study. In addition, a recent study of neuroanatomical correlates with female sexual dysfunction demonstrated the correlation between female sexual arousal and WM lesions in occipital lobe in MS, and the correlation between bladder symptoms and lubrication scores, which is related to sexual arousal score (Winder *et al.*, 2016). Therefore, the importance for LUTS resulted from occipital lobe and the GM regions not appearing in working model of LUT control could not be neglected. In addition, cerebellum was identified in the MS-OAB-network, which could lead to a possible association between cerebellum damage and OAB symptoms, and it was reported that the cerebellum could be one of the regions contributing to LUTD (Sugiyama *et al.*, 2009).

Besides, the thalamus seemed not significant for the OAB symptoms as there were no WM pathways identified between thalamus and any GM regions in the MS-OAB-network. However, in the MS-network, there were networks between thalamus, cingulate and cerebellum, pointing out the possible damage in the thalamus due to the MS pathology. Thus, the thalamus could not be a valid node in reconstructing the structural connectivity network. In another word, the connectome could be disrupted due to the damages in the thalamus. The pathological correlates between thalamus atrophy and MS were reported in previous studies (Bodini *et al.*, 2009; Eshaghi *et al.*, 2018).

7.5. Conclusion

This section successfully provided the structural connectivity network subtending OAB symptoms in MS cohort based on the whole brain connectivity network created in **chapter 6**. It is the first WM network generated for LUTS in neurological condition by identifying the OAB relevant GM regions from the BCT measures and proposing the structural connectivity network with statistically significant streamlines. The MS-OAB-network connected regions known to be involved in the neural control of LUT functions, and we identified connectivity between insula, and frontal lobe and cingulate. The connectivity between insula and temporal lobe, and insula and occipital lobe, may underpin changes seen in fMRI. Taking into account the working model of LUT control, the MS-network and MS-OAB-network provided explanations of the reconstructed WM pathways based on current understanding of LUTS from MRI studies on GM regions. The methods and approaches in this section could be further explored to study LUTS in other neurological conditions.

7.6. Remaining question and further direction

As discussed in **chapter 3**, various of studies for LUTS on GM were reported, providing kinds of fMRI task phases, distribution of age, gender and health condition, and atlas used to identify the involved GM areas. All above variety made the confirmation of detailed GM regions for OAB symptoms difficult. Therefore, this section selected the relevant GM regions from the original study data, rather than from the identified regions from previous literatures. However, considering the working model of LUT control proposed the principle circuit containing key GM regions for LUTS concluded from previous PET and fMRI studies, it is necessary to reconstruct a brain structural connectivity network with the regions included in the LUT working model, and compare the LUT working model network with the MS-OAB-network created in this section.

Section B. Structural network based on the working model of LUT control

7.7. Introduction

Following the discussion in **section A**, the MS-OAB-network compensated our current understanding of the OAB symptoms from structural prospects in MS. Keeping the working model of LUT control in mind, there were differences between the GM regions involved in MS-OAB-network and the LUT working model, but both networks shared several GM areas. The GM areas included in MS-OAB-network presented widespread in the brain, containing the key regions involved in the LUT working model, whereas LUT working model provided a functional brain network centred on the frontal part of the brain, including regions such as lateral and medial prefrontal cortex.

The working model of LUT control was derived from several previous studies of LUT functions using PET and fMRI (Griffiths, 2015). The participants involved included healthy people and disease, regardless of gender, handedness and paradigms of the task designed during imaging (Griffiths, 2015). For example, Blok et al. reported that brainstem contained specific nuclei, predominantly on the right side, responsible for micturition control in seventeen right-handed HC (age range 21-50 years), with task phases including holding urine, natural micturition and 30 mins after micturition, using PET scans (Blok, Willemsen and Holstege, 1997). One fMRI study from Griffiths et al. investigated ten incontinent

healthy women (age range 30-79 years) using fMRI task including 20 ml fluid repeatedly infused into and withdrawn from the bladder (Griffiths *et al.*, 2009). Another fMRI study reported patients with prostate cancer shared same LUT control with HC, but impaired pelvic floor muscle function after retropubic radical prostatectomy, by analysing the data from twenty-two prostate cancer patients (age range 41-76 years) with fMRI task including mimic voiding and mimic the interruption of voiding during scanning (Seseke *et al.*, 2013). The results from above were all taken into account in working model of LUT control, leading to a general LUT working modelling comprising the common GM regions from kinds of studies as the key regions. As a result, the working model of LUT control provided the functional network for LUT functions with broader conditions in the participants, whereas the MS-OAB-network focused on the OAB symptoms in MS. Therefore, a structural connectivity network with the GM regions from the working model of LUT control is desired to see the similarity and differences between the general network for LUTS and the one subtending OAB symptoms in MS.

So, the objectives of this section are:

1. to identify the GM regions involved in working model of LUT control;
2. to create the structural connectivity network based on the working model of LUT control (LUT working model network);
3. to explore the similarity and differences between the LUT working model network and the MS-OAB-network created in **section A**.

7.8. Methods

7.8.1. Participants

Participants with a diagnosis of MS according to McDonald criteria (Polman *et al.*, 2011) recruited in this section were the same cohort with the MS patients in **section A**, including seventeen right-handed female MS patients reporting predominant OAB symptoms (MS-OAB) and sixteen right-handed female MS patients without any LUTS (MS-no-LUTS). As discussed in **chapter 5**, the LUTS were evaluated by the USP-OAB sub-score from the USP questionnaire (Haab *et al.*, 2008), and the cut off value (mean + 2SD) was calculated from the USP-OAB sub-score of the HC.

7.8.2. Clinical assessments

Detailed clinical assessments were introduced in **section A**, including:

1. Patients' clinical history was recorded based on clinical record in the hospital;
2. The MMSE (De Marchis *et al.*, 2010) was assessed for cognitive impairment (see details in **Appendix 1**);
3. Physical examinations, including neurological and urological examinations, were given out by two Consultant Neurologists (JNP and ATT) at NHNN, helping to offer more clinical details;
4. The EDSS (Kurtzke, 1983) score was assessed by experienced Consultant Neurologists at NHNN;

5. The USP (Haab *et al.*, 2008) questionnaire, providing a comprehensive evaluation of urinary symptoms and their severity in males and females (see details in **Appendix 6**);
6. A three-day bladder diary (see details in **Appendix 9**).

7.8.3. MRI imaging acquisition

MRI scanning was carried out using a 3.0 Tesla scanner (Philips Achieva, Philips Medical Systems, Best, The Netherlands). Clinical scans were acquired in the axial-oblique plane parallel to the anterior-posterior callosal line using the following parameters: 1) T1-weighted images: TE = 10 ms, TR = 625 ms, FOV 240×180 mm², NEX = 1, voxel size = 1×1×1 mm³, 50 slices and scan time = 5:43 min; 2) PD-weighted and T2-weighted images: TE1/TE2 = 19/85 ms, TR = 3500 ms, FOV 240×180 mm², NEX = 1, voxel size = 1×1×3 mm³, 50 slices and scan time = 4:01 min. DTI was also performed in the axial-oblique plane, with 32 distributed diffusion encoding directions ($b = 0$ and $b = 1000$ s/mm²) and the following parameters: TE = 92 ms, TR = 9714 ms, FOV 248×248 mm², NEX = 1, voxel size = 2×2×2 mm³, 70 slices and scan time = 6:46 min.

7.8.4. MRI imaging processing

The analyses in this section were based on the whole brain structural connectivity network reconstructed for the thirty-three MS patients in **chapter 6**, and the steps including DWI and structural imaging pre-processing, the generation of the probabilistic tractogram, and the whole brain connectivity connectome

reconstruction kept same as the description in **section A**. FSL v5.0.9 (<https://fsl.fmrib.ox.ac.uk/fsl>), Jim 6.0 (<http://www.xinapse.com/Manual/index.html>), and MRtrix3 v0.3.14 package (<http://www.mrtrix.org>) were used for whole brain connectivity network reconstruction. Matlab R2017b was applied to create connectivity matrix.

7.8.5. Selection of GM regions for the OAB symptoms in MS

Different from the way of selecting GM regions in **section A**, the GM regions selection in this section were directly from the working model of LUT control (see details in **chapter 3**; Griffiths, 2015). The GM regions were selected according to the GIF parcellation (<http://cmictig.cs.ucl.ac.uk/niftyweb>; Cardoso *et al.*, 2015; Prados *et al.*, 2016), including brainstem, thalamus, insula, anterior cingulate cortex, para-hippocampal gyrus, supplementary motor area, lateral prefrontal cortex and medial prefrontal cortex. However, considering various of studies and atlases involved in the working model of LUT control, it was challenging to identify the border of the lateral prefrontal cortex and medial prefrontal cortex. Therefore, slightly broader areas in GM regions from GIF parcellation, without obvious incongruent areas, in frontal lobes were included in this section, so that all GM areas involved in the working model of LUT control were included.

7.8.6. Statistical analysis

SPSS version 24 was used for basic statistical analysis and the group difference analysis between the MS-OAB and MS-no-LUTS group on the streamlines

between each two nodes selected from the previous step. Stata 14 was used to calculate the residuals of the streamlines adjusted for age and EDSS score. The Student's t test and Mann-Whitney U test were applied. A p value < 0.05 was considered statistically significant, and p value < 0.1 was considered a favourable statistical trend.

7.8.7. Structural connectivity network visualization

A LUT working model network was then created starting from the LUT working model nodes and selecting those with streamlines showing statistically significant difference ($p < 0.05$) between the MS-OAB and MS-no-LUTS group. The BrainNet Viewer (<https://www.nitrc.org/projects/bnv/>; Xia, Wang and He, 2013) was applied to draw the generated structural connectivity for a better visualization of the results.

7.9. Results

7.9.1. Participants

The participants are the same cohort with the ones in **Section A**. As discussed, detailed demographic participants characteristics were shown in Table 7.1.

7.9.2. GM regions for the OAB symptoms in MS

Table 7.5 listed the thirty-nine GM regions involved in the OAB symptoms in MS based on working model of LUT control. Though all GM areas involved in the LUT working model were initially included, there are key regions in the functional model indicating not relevant to the OAB symptoms in MS in the structural network. For example, we did not identify any connection between thalamus and other GM regions.

7.9.3. The structural connectivity network for the OAB symptoms in MS based on working model of LUT control

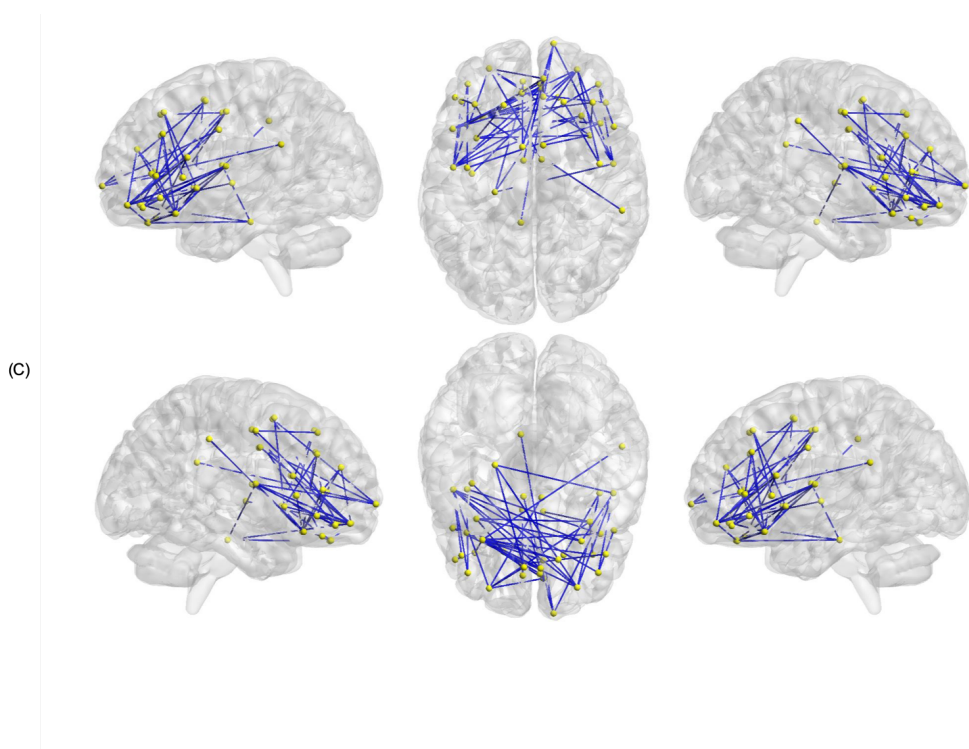
Figure 7.2 presented the LUT working model network drawn by the BrainNet Viewer, with relevant GM regions involved in the working model of LUT control and the streamlines showing statistical significance between the MS-OAB and MS-no-LUTS group. Different from the MS-OAB-network, the LUT working model network had a clear drift to the frontal part of the brain.

Table 7.5. List of the GM regions for LUT working model network.

1	Right anterior cingulate gyrus	21	Left middle frontal gyrus
2	Left anterior cingulate gyrus	22	Right medial orbital gyrus
3	Right anterior insula	23	Right superior frontal gyrus medial segment
4	Left anterior insula	24	Right opercular part of the inferior frontal gyrus
5	Right anterior orbital gyrus	25	Left opercular part of the inferior frontal gyrus
6	Left anterior orbital gyrus	26	Right orbital part of the inferior frontal gyrus
7	Right central operculum	27	Left orbital part of the inferior frontal gyrus
8	Left central operculum	28	Left posterior cingulate gyrus
9	Right frontal operculum	29	Left parahippocampal gyrus
10	Left frontal operculum	30	Left posterior insula
11	Right frontal pole	31	Right posterior orbital gyrus
12	Right gyrus rectus	32	Left posterior orbital gyrus
13	Left gyrus rectus	33	Right precentral gyrus
14	Right lateral orbital gyrus	34	Left precentral gyrus
15	Left lateral orbital gyrus	35	Right superior frontal gyrus
16	Right middle cingulate gyrus	36	Left superior frontal gyrus
17	Left middle cingulate gyrus	37	Right supplementary motor cortex
18	Right medial frontal cortex	38	Left supplementary motor cortex

19	Left medial frontal cortex	39	Right supramarginal gyrus
20	Right middle frontal gyrus		

Figure. 7.2. LUT working model network.



The LUT working model network was created by the BrainNet Viewer. Nodes are in yellow and edges are in blue.

7.10. Discussion

The LUT working model network was reconstructed with selected GM regions involved in working model of LUT control from GIF parcellation and the streamlines showing statistical significance between the MS-OAB and MS-no-LUTS group. It offered another structural connectivity network for OAB symptoms in MS reconstructed with GM regions from previous literatures, rather than from our study data. It provided structural information based on the functional connectivity, and ideally would share some similarities with the proposed pathways in LUT working model and the MS-OAB-network proposed in **section A**. The LUT working model network (Table 7.5 and Figure 7.2) confirmed the connection between insula and frontal lobe in the functional circuit from structural prospects. Considering the working model of LUT control was proposed in general population including health and disease, the LUT working model network proposed in right-handed female MS-OAB cohort furtherly validated the application of the LUT working model and emphasized the importance of structural and functional pathways between insula and frontal lobe for LUTS. In LUT working model network, the lack of findings on connections to thalamus provided additional proof of pathology from MS, bringing into correspondence with the findings from MS-OAB-network (see relevant discussion in **section A**). Besides, as the LUT working model network was created with limited GM regions derived from the working model of LUT control, the structural pathways between insula and temporal lobe, and insula and occipital lobe presented in MS-OAB-network, were not able to be reconstructed.

Considering the Desikan-Killiany-Tourville atlas was used in GIF parcellation (Prados *et al.*, 2016), while the GM regions from the working model of LUT control were concluded from various studies using other atlases including Brodmann areas, MNI coordinates and Talairach coordinates, there were no completely matching regions between GIF parcellation and the working model of LUT control when selecting lateral and medial prefrontal cortex. Moreover, the definition of prefrontal cortex was unclear with imprecise description on anatomy but emphasizing its functions in the literatures: the frontal/anterior part of the frontal lobe, carrying out executive function, received projections from various sensation associations and had strong connections with thalamic nucleus and motor control systems (Fuster, 2001; Barbas, 2009). So, it was more challenging to localize the lateral and medial prefrontal cortex. Therefore, as discussed in **methods**, except for the GM regions definitely belonging to the prefrontal lobe, slightly broader areas were included in this study, so that all key regions proposed in the working model of LUT control were included for structural network analysis. For example, there were six regions involving operculum, which were the regions comprising frontal, temporal and parietal lobe parts and like covers to insula (Chen *et al.*, 1996), within the 120 parcellated GM regions. The parietal operculum was easily removed as it belonged to the parietal lobe, but the central operculum was kept by visually checking as there was no definition found and the parcellated central operculum occupied parts of both frontal lobe and temporal lobe. In case any WM pathway would be mistakenly ignored in future analysis for LUTS, the central operculum was included in this first proposed LUT working model network based on the working model of LUT control. As a result, regions involved in frontal lobe were included. With group difference analysis

between MS-OAB and MS-no-LUTS adjusting for age and EDSS score, ideally the non-relevant regions were removed from the LUT working model network.

7.11. Conclusion

This section successfully created the LUT working model network based on the working model of LUT control and confirmed the connectivity between insula and frontal lobe from structural prospects. Compared with the MS-OAB-network created in **section A**, the LUT working model network shared similar connectivity between key regions involved in the working model of LUT control and provided another proof for the pathological changes in thalamus due to MS. However, the connectivity between insula and temporal lobe, and insula and occipital lobe were not included in the LUT working model network. Considering the working model of LUT control were proposed in wide participants cohorts with various study protocols, the differences between LUT working model network and MS-OAB-network indicated the importance of studying LUTS in neurological conditions. The methods applied in this study could be furtherly extended to other neurological diseases with different aspects of LUTS.

Bibliography

- Altman, N. S. (1992) 'An Introduction to Kernel and Nearest-Neighbor Nonparametric Regression', *The American Statistician*. Taylor & Francis, 46(3), pp. 175–185. doi: 10.1080/00031305.1992.10475879.
- Andersson, J. L. R. and Sotiropoulos, S. N. (2016) 'An integrated approach to correction for off-resonance effects and subject movement in diffusion MR imaging', *NeuroImage*. The Authors, 125, pp. 1063–1078. doi: 10.1016/j.neuroimage.2015.10.019.
- Barbas, H. (2009) 'Prefrontal Cortex: Structure and Anatomy', in Squire, L. R. B. T.-E. of N. (ed.). Oxford: Academic Press, pp. 909–918. doi: <https://doi.org/10.1016/B978-008045046-9.00427-7>.
- Bhushan, C. *et al.* (2012) 'Correcting Susceptibility-Induced Distortion in Diffusion-Weighted MRI using Constrained Nonrigid Registration.', *Signal and Information Processing Association Annual Summit and Conference (APSIPA), ... Asia-Pacific. Asia-Pacific Signal and Information Processing Association Annual Summit and Conference*. United States, 2012.
- Blok, B. F. M., Willemsen, A. T. M. and Holstege, G. (1997) 'A PET study on brain control of micturition in humans', *Brain*, 120(November), pp. 111–121. Available at: [papers2://publication/uuid/6D92BADC-420C-4308-89DE-10BAFD7E4A9F](https://pubmed.ncbi.nlm.nih.gov/9411111/).
- Bodini, B. *et al.* (2009) 'Exploring the Relationship Between White Matter and Gray Matter Damage in Early Primary Progressive Multiple Sclerosis : An In Vivo Study With TBSS and VBM', *Human Brain Mapping*, 2861(November 2008), pp. 2852–2861. doi: 10.1002/hbm.20713.
- Cardoso, M. J. *et al.* (2015) 'Geodesic Information Flows: Spatially-Variant Graphs and Their Application to Segmentation and Fusion', *IEEE Transactions on Medical Imaging*. IEEE, 34(9), pp. 1976–1988. doi: 10.1109/TMI.2015.2418298.
- Chen, C. Y. *et al.* (1996) 'MR of the cerebral operculum: abnormal opercular formation in infants and children.', *AJNR. American journal of neuroradiology*. United States, 17(7), pp. 1303–1311.
- Demšar, J. *et al.* (2013) *Orange: Data Mining Toolbox in Python*, *Journal of Machine Learning Research*.
- Eshaghi, A. *et al.* (2018) 'Progression of regional grey matter atrophy in multiple sclerosis.', *Brain: a journal of neurology*. England, 141(6), pp. 1665–1677. doi: 10.1093/brain/awy088.
- Fuster, J. (2001) 'Prefrontal Cortex', *International encyclopedia of the social & behavioral sciences* /. Amsterdam , pp. 11969–11976. doi: 10.1016/B0-08-043076-7/03465-3.
- Griffiths, D. *et al.* (2009) 'Cerebral control of the lower urinary tract: how age-related changes might predispose to urge incontinence', *NeuroImage*, 47(5), pp. 213–223. doi: 10.1007/978-1-62703-673-3.
- Griffiths, D. (2015) *Functional imaging of structures involved in neural control of the lower urinary tract*. 1st edn, *Handbook of clinical neurology*. 1st edn. Elsevier B.V. doi: 10.1016/B978-0-444-63247-0.00007-9.
- Haab, F. *et al.* (2008) 'Comprehensive Evaluation of Bladder and Urethral Dysfunction Symptoms: Development and Psychometric Validation of the Urinary Symptom Profile (USP) Questionnaire', *Urology*, 71(4), pp. 646–656. doi: 10.1016/j.urology.2007.11.100.

- Ho, T. K. (1998) 'The random subspace method for constructing decision forests', *IEEE Transactions on Pattern Analysis and Machine Intelligence*, 20(8), pp. 832–844. doi: 10.1109/34.709601.
- Kuchel, G. A. *et al.* (2009) 'Localization of Brain White Matter Hyperintensities and Urinary Incontinence in Community-Dwelling Older Adults', *The Journals of Gerontology Series A: Biological Sciences and Medical Sciences*, 64A(8), pp. 902–909. doi: 10.1093/gerona/glp037.
- Kurtzke, J. F. (1983) 'Rating neurologic impairment in multiple sclerosis: An expanded disability status scale (EDSS)', *Neurology*, 33(11), pp. 1444–1444. doi: 10.1212/WNL.33.11.1444.
- Latora, V. and Marchiori, M. (2001) 'Efficient behavior of small-world networks.', *Physical review letters*. United States, 87(19), p. 198701. doi: 10.1103/PhysRevLett.87.198701.
- De Marchis, G. M. *et al.* (2010) 'Mild cognitive impairment in medical inpatients: the Mini-Mental State Examination is a promising screening tool.', *Dementia and geriatric cognitive disorders*. Switzerland, 29(3), pp. 259–264. doi: 10.1159/000288772.
- Polman, C. H. *et al.* (2011) 'Diagnostic criteria for multiple sclerosis: 2010 Revisions to the McDonald criteria', *Annals of Neurology*, 69(2), pp. 292–302. doi: 10.1002/ana.22366.
- Prados, F. *et al.* (2016) 'NiftyWeb : web based platform for image processing on the cloud', *24th Scientific Meeting and Exhibition of the International Society for Magnetic Resonance in Medicine (ISMRM)*, (ISMRM).
- Rubinov, M. and Sporns, O. (2010) 'NeuroImage Complex network measures of brain connectivity : Uses and interpretations', *NeuroImage*. Elsevier Inc., 52(3), pp. 1059–1069. doi: 10.1016/j.neuroimage.2009.10.003.
- Sakakibara, R. *et al.* (2012) 'Vascular incontinence: incontinence in the elderly due to ischemic white matter changes.', *Neurology international*. Italy, 4(2), p. e13. doi: 10.4081/ni.2012.e13.
- Seseke, S. *et al.* (2013) 'Monitoring brain activation changes in the early postoperative period after radical prostatectomy using fMRI', *NeuroImage*. Elsevier Inc., 78, pp. 1–6. doi: 10.1016/j.neuroimage.2013.04.005.
- Smith, R. E. *et al.* (2012) 'Anatomically-constrained tractography: improved diffusion MRI streamlines tractography through effective use of anatomical information.', *NeuroImage*. United States, 62(3), pp. 1924–1938. doi: 10.1016/j.neuroimage.2012.06.005.
- Smith, R. E. *et al.* (2015) 'SIFT2: Enabling dense quantitative assessment of brain white matter connectivity using streamlines tractography.', *NeuroImage*. United States, 119, pp. 338–351. doi: 10.1016/j.neuroimage.2015.06.092.
- Sugiyama, M. *et al.* (2009) *Cerebellar Ataxia and Overactive Bladder after Encephalitis Affecting the*, *Case Reports In Neurology*. doi: 10.1159/000226119.
- Tadic *et al.* (2010) 'Brain Activity During Bladder Filling Is Related To White Matter Structural Changes in Older Women with Urinary Incontinence', *NeuroImage*, 51(4), pp. 1294–1302. doi: 10.1016/j.neuroimage.2010.03.016.BRAIN.
- Tax, C. M. W. *et al.* (2014) 'Recursive calibration of the fiber response function for spherical deconvolution of diffusion MRI data.', *NeuroImage*. United States, 86, pp. 67–80. doi: 10.1016/j.neuroimage.2013.07.067.
- Tournier, J.-D. *et al.* (2004) 'Direct estimation of the fiber orientation density

- function from diffusion-weighted MRI data using spherical deconvolution.', *NeuroImage*. United States, 23(3), pp. 1176–1185. doi: 10.1016/j.neuroimage.2004.07.037.
- Tournier, J.-D., Calamante, F. and Connelly, A. (2007) 'Robust determination of the fibre orientation distribution in diffusion MRI: non-negativity constrained super-resolved spherical deconvolution.', *NeuroImage*. United States, 35(4), pp. 1459–1472. doi: 10.1016/j.neuroimage.2007.02.016.
- Tustison, N. J. *et al.* (2010) 'N4ITK: improved N3 bias correction.', *IEEE transactions on medical imaging*. United States, 29(6), pp. 1310–1320. doi: 10.1109/TMI.2010.2046908.
- Watts, D. J. and Strogatz, S. H. (1998) 'Collective dynamics of "small-world" networks.', *Nature*. England, 393(6684), pp. 440–442. doi: 10.1038/30918.
- Winder, K. *et al.* (2016) 'Neuroanatomic Correlates of Female Sexual Dysfunction in Multiple Sclerosis.', *Annals of neurology*. United States, 80(4), pp. 490–498. doi: 10.1002/ana.24746.
- Xia, M., Wang, J. and He, Y. (2013) 'BrainNet Viewer: a network visualization tool for human brain connectomics.', *PloS one*. United States, 8(7), p. e68910. doi: 10.1371/journal.pone.0068910.

Chapter 8

8. Limitations, conclusion and future directions

8.1. Limitations

There were several limitations to the studies. The main limitation was the small number of subjects (for TBSS study, HC = 14 and MS = 29; for tractography study, HC = 13 and MS = 33), especially when doing analysis between MS-no-LUTS and MS-OAB group (for TBSS study, MS-no-LUTS = 9 and MS-OAB = 17; for tractography study, MS-no-LUTS = 16 and MS-OAB = 17). The small subject number limited the power of the study. It could be a possible reason that there was a trend of significance ($p = 0.072$) when comparing the FA value between MS-no-LUTS and MS-OAB group, and no significant correlation identified from urodynamic and bladder diary parameters.

In the TBSS study (**chapter 5**), it was observed in the group difference analysis, that there was a trend towards a significantly reduced FA ($p = 0.072$) in the MS-OAB group compared with MS-no-LUTS group, after adjusting for age and EDSS. LUTS is common in MS and therefore identifying MS patients without LUTS was challenging ($n = 9$; 33% of MS participants). This was despite intense efforts to

recruit across different MS clinics. As a result, these two groups were not matched for number of subjects and this could have contributed to the lack of significance.

It just be emphasized that the streamlines in the structural network are quantitative figures estimating the course of WM tracts rather than the actual WM tracts, Though several approaches have been applied on the network to minimize the bias on expressing biologically meaningful information, the streamlines could not be considered as the actual WM tracts. However, this is an accepted limitation for the methodology as a whole; the imaging processing procedures have been carefully checked and optimized biologically meaningful information.

This study has focused on structural connectivity between different suprapontine GM regions. However in reality, LUTS may result from spinal cord lesions as well. Therefore, future studies should be explored on the spinal cord lesions.

The EDSS score was used for assessing MS disability. This includes an assessment on the bladder and bowel. This could be a confounder hence it could be a reason that regressing EDSS for LUT studies in MS decreases of significance of findings in LUTS. On the other hand, not correcting for EDSS would make any finding non-specific given that there is a natural correlation between LUTS and increased disability.

This study focused on the LUTS, rather than LUTD, which could be identified from the urodynamic studies. Initially, we were planning to use urodynamic studies, however, there was no correlation between urodynamic findings and LUTS. This is not surprising considering the limited correlation between LUTS and LUTD were reported in the literatures. Patients reported outcome introduced an element of subjectivity as it is challenging to measure. Standardised questionnaires were used to address this. Bladder diaries were used as well but patients were not filling these due to time consuming efforts on the diary. In the future, the urodynamic studies should be introduced for more accurate assessment of OAB.

8.2. Conclusion

The overarching aim of this thesis is to investigate the WM abnormalities subtending the OAB symptoms in MS, using DWI techniques. In **chapter 5**, it was established by the TBSS approach that there were significant differences in FA value suggesting an association between presence of OAB symptoms and WM abnormalities. In chapter 7, a structural network subtending OAB symptoms in MS was created, and the structural network was able to explain the working model of LUT control.

Using TBSS, difference of microstructural WM indices between MS-OAB patients and MS-no-LUT patients, was identified, and a reduced FA value, representing

more severe WM changes, was found in the cohort of patients with MS reporting OAB symptoms. A negative correlation was identified between the OAB score and FA value, suggesting an association between OAB symptoms severity and WM changes. Moreover, a non-dominant hemispheric prevalence was observed for the OAB symptoms related WM abnormalities.

A structural network for OAB symptoms in MS was reconstructed using advanced techniques to provide biologically meaningful information in the network. This is the first structural connectivity network for LUTS in neurological conditions so far. The MS-OAB-network and working model network were created with different GM regions, but sharing similarities in GM regions selection and the connections in the networks. Compared with the established LUT working model network, the MS-OAB-network not only connected regions known to be involved in the working model of LUT control, such as the insula, frontal lobe and cingulate, but also confirmed connectivity between insula and temporal lobe, and insula and occipital lobe. It is likely that these connections could underpin the circuit with functional alterations involving insula and frontal lobe seen in fMRI studies.

The following can be concluded from this work:

1. WM abnormalities subtending the OAB symptoms in MS are established with advanced DWI techniques;
2. The structural network subtending OAB symptoms in MS not only includes the key areas in the working model of LUT control, such as the insula and the GM regions in frontal lobes, but also include other posterior regions

including parietal lobes, occipital lobes, temporal lobes and cerebellum. The MS-OAB-network raise the possibility that the indirect ways between insula and frontal lobes (connectome between frontal lobes and occipital lobes, and frontal lobes and parietal lobes) could underpin the functional connectivity in the working model of LUT control;

3. The GM regions appearing in the MS-OAB-network, not included in the working model of LUT control, such as GM regions in occipital lobes (the lingual gyrus), parietal lobes (the precuneus) and cerebellum, could contribute to the OAB symptoms in MS;
4. The structural findings in this study compensate the current understanding of cerebral control of LUTS from WMH and brain functional imaging studies.

8.3. Future directions

From a methodology prospect, the methods and approaches used in this thesis were validated and could be extended to other neurological conditions. The brain networks for different aspects of LUTS in various neurological conditions may help to confirm the critical LUTS related regions and present the differences in the WM abnormalities caused by neurological pathology.

For the TBSS study, only FA was used presenting the diffusivity. However, it was reported that there were differences between HC and MS in other diffusion

indices (MD, AD and RD) in previous studies, indicating potentially correlation between other indices and OAB symptoms and differences between MS-no-LUTS and MS-OAB group. With all diffusion indices analysed, a clearer understanding on the WM abnormalities subtending OAB symptoms could be observed. Besides, with significant difference between the FA value in MS-no-LUTS and MS-OAB group, some OAB symptoms related WM tracts, such as ACC, ACR and SLF, could be selected for a further step analysis, for example, exploring the correlation between FA value and USP-OAB score in a specific tract.

Considering MS is a demyelinating and neurodegenerative disease affecting the CNS, including brain and the spinal cord, and the OAB symptoms could be caused by lesions from brain and upper spinal cord (infrapontine to suprasacral) level, research on the WM changes at infrapontine to suprasacral level and their association with OAB symptoms in MS needs to be explored. Besides, voiding difficulties, with and without OAB symptoms (in this thesis, there were two MS patients reporting predominant voiding problems and one reporting mixed bladder symptoms), were observed in MS patients, it would give us an intact understanding of bladder symptoms in MS if different aspects of bladder symptoms and the whole spinal cord can be involved in the further research. Furthermore, WM studies regarding bladder symptoms in other neurological conditions could be explored to compare the differences from various pathological changes and potentially provide clearer underlying mechanism of bladder dysfunctions resulted from neurological diseases.

The current understanding of LUTS from fMRI are concluded from various cohort, and few WM analysis were combined with the fMRI findings in the same cohort, especially in a neurological condition. Therefore, fMRI analysis could be potentially combined with the findings from the current work and help with identifying the LUTS related GM regions. As this work presented only one part of the full study protocol, and the fMRI protocol was applied in the same cohort, one further plan is to explore the analysis using fMRI data from current protocol. The functional activities observed from fMRI combined with the structural network would provide an intact understanding of the OAB symptoms in MS.

The aim of further research is to recognise different WM and GM imaging biomarkers of OAB symptoms in neurological disease, that could serve as reliable tools for evaluating the central effects of successful treatments for OAB symptoms in MS, such as pelvic floor muscle training, botulinum toxin A and percutaneous tibial nerve stimulation (PTNS), and also for providing objective neurological measures of success.

In inclusion criteria, MS patients should fulfil McDonald criteria 2010. However, as the protocol was designed in 2013, but the studies continued till now, there could be a change in MS diagnosis after applying the McDonald criteria 2017. To keep the research up with the times, it would be good to check whether all MS patients recruited in the studies fulfil the new criteria.

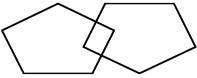
Appendices

Appendix 1. Mini-Mental State Examination (MMSE)

Mini-Mental State Examination (MMSE)

Patient's Name: _____ Date: _____

Instructions: Score one point for each correct response within each question or activity.

Maximum Score	Patient's Score	Questions
5		"What is the year? Season? Date? Day? Month?"
5		"Where are we now? State? County? Town/city? Hospital? Floor?"
3		The examiner names three unrelated objects clearly and slowly, then the instructor asks the patient to name all three of them. The patient's response is used for scoring. The examiner repeats them until patient learns all of them, if possible.
5		"I would like you to count backward from 100 by sevens." (93, 86, 79, 72, 65, ...) Alternative: "Spell WORLD backwards." (D-L-R-O-W)
3		"Earlier I told you the names of three things. Can you tell me what those were?"
2		Show the patient two simple objects, such as a wristwatch and a pencil, and ask the patient to name them.
1		"Repeat the phrase: 'No ifs, ands, or buts.'"
3		"Take the paper in your right hand, fold it in half, and put it on the floor." (The examiner gives the patient a piece of blank paper.)
1		"Please read this and do what it says." (Written instruction is "Close your eyes.")
1		"Make up and write a sentence about anything." (This sentence must contain a noun and a verb.)
1		"Please copy this picture." (The examiner gives the patient a blank piece of paper and asks him/her to draw the symbol below. All 10 angles must be present and two must intersect.) 
30		TOTAL

Appendix 2. Detailed inclusion and exclusion criteria

1. Inclusion Criteria

In order to be eligible to enter the study, all participants will meet the following criteria:

- At least 18 years old
- Able to understand the patient information sheet (PIS)
- Written informed consent to take part and follow the requirements of the protocol

For patients with MS:

- Diagnosis according to the McDonald criteria
- Having a score on the Kurtzke Expanded Disability Status Scale (EDSS; Kurtzke, 1983) ≤ 6.5
- Free of relapses in the previous 3 months

For patients with MSA:

- Diagnosed with “probable MSA” according to the Gilman criteria (Gilman *et al.*, 1998): autonomic failure/urinary dysfunction plus poorly levodopa responsive parkinsonism or cerebellar dysfunction
- Abnormal anal sphincter electromyogram (EMG) showing evidence for reinnervation

For patients with idiopathic LUTS:

- Routine clinical assessments excluding a neurological cause for symptoms

For patients with predominant storage symptoms:

- Urinary urgency (≥ 2 episodes per week), urinary frequency ($>8/24$ h) and/or incontinence
- Post void residual volume <150 ml

For patients with predominant voiding symptoms:

- Hesitancy, slow or intermittent stream, straining to void, or relying on catheterisation for bladder emptying
- Post void residual volume >150 ml

For healthy subjects:

- Good mental and physical health
- Normal functioning of the LUT
- No episodes of urinary urgency or incontinence; urinary frequency $<8/24$ h
- No malignancy or previous surgery of the LUT or genitalia
- No previous spine or pelvic surgery

2. Exclusion Criteria

- Pregnant, breast feeding, or planning to become pregnant during the study duration
- Any contraindications to having MRI (e.g. ferromagnetic implants), as assessed by the NMR unit's MRI safety checklist
- Craniocerebral injuries or surgeries
- Known neurological disease other than that being used for the investigation
- Cognitive impairment, as assessed by a Mini-mental State Examination (MMSE) score < 23
- Presence of additional active urological disease that might explain LUT symptoms
- Surgery of the LUT or genitalia within the last year or that is related to the LUT symptoms, as per the discretion of the investigator
- Any anatomical anomaly of LUT/genitalia
- Active LUT malignancy or metabolic disease, as per the discretion of the investigator
- For the functional brain imaging part additional exclusion criteria apply:
 - Receiving concomitant treatment for LUTS
 - Received tibial nerve stimulation or intravesical Botulinum A toxin injections within the previous six months
 - If on an antimuscarinic medication, unwilling to discontinue for at least 5 days prior to having MRI assessment

The presence of hematuria and urinary tract infection (UTI) are not principle exclusion criteria, but need to be appropriately evaluated and managed prior to inclusion. Before each MRI investigation, urine will be checked for infection. In case of UTI, the patient will receive a course of antibiotic therapy reflecting standard clinical care, and will be re-scheduled for the functional scans of the MRI investigation, when UTI and possible related symptoms are absent for at least 3 days.

Bibliography

Gilman, S. *et al.* (1998) 'Consensus statement on the diagnosis of multiple system atrophy.', *Journal of the autonomic nervous system*. Netherlands, 74(2-3), pp. 189-192.

Kurtzke, J. F. (1983) 'Rating neurologic impairment in multiple sclerosis: An expanded disability status scale (EDSS)', *Neurology*, 33(11), pp. 1444-1444. doi: 10.1212/WNL.33.11.1444.

Appendix 3. Urinary Symptom Profile (USP)

LUTfMRI01_ _ _ _ _

Urinary Symptom Profile - USP[©]

➤ Before starting the questionnaire, please fill in today's date:

/ _ / _ / / _ / _ / / _ / _ /
Day Month Year

The following questions concern the intensity and frequency of urinary symptoms that you have had over the past 4 weeks.

To answer the following questions, please tick the box which best applies to you. There are no "right" or "wrong" answers. If you are not quite sure how to answer, choose the answer which best applies to you.

Please answer this questionnaire somewhere quiet and preferably on your own. Take as long as you need to fill it in.

Once you have finished, put the questionnaire into the envelope provided and hand it to your doctor.

Thank you for your cooperation.

You may sometimes experience urine leaks during physical effort. This effort could be strenuous (such as doing sport or having a violent coughing fit), moderate (climbing or coming down the stairs) or even light (walking or changing position).

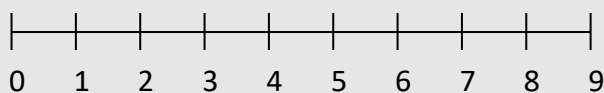
1. **Over the past 4 weeks**, please specify the number of times a week you have had leaks during physical effort:

Please tick one box for each of the lines 1a, 1b and 1c.

	No urine leaks	Less than one urine leak a week	Several urine leaks a week	Several urine leaks a day
1a. During strenuous physical effort	<input type="checkbox"/> ₀	<input type="checkbox"/> ₁	<input type="checkbox"/> ₂	<input type="checkbox"/> ₃
1b. During moderate physical effort	<input type="checkbox"/> ₀	<input type="checkbox"/> ₁	<input type="checkbox"/> ₂	<input type="checkbox"/> ₃
1c. During light physical effort	<input type="checkbox"/> ₀	<input type="checkbox"/> ₁	<input type="checkbox"/> ₂	<input type="checkbox"/> ₃

For the doctor only: note the sum of items 1a + 1b + 1c on the scale below

“STRESS URINARY INCONTINENCE” SCORE



Over the past 4 weeks and under everyday conditions of social, professional or family life:

2. How many times a week have you had to rush to the toilet to urinate because you urgently needed to go?

- | | | | |
|---------------------------------------|---------------------------------------|---------------------------------------|---------------------------------------|
| <input type="checkbox"/> ₀ | <input type="checkbox"/> ₁ | <input type="checkbox"/> ₂ | <input type="checkbox"/> ₃ |
| Never | Less than once a week | Several times a week | Several times a day |

3. When you have had an urgent need to urinate, for how many minutes on average have you been able to hold on?

- | | | | |
|---------------------------------------|---------------------------------------|---------------------------------------|---------------------------------------|
| <input type="checkbox"/> ₀ | <input type="checkbox"/> ₁ | <input type="checkbox"/> ₂ | <input type="checkbox"/> ₃ |
| More than 15 minutes | From 6 to 15 minutes | From 1 to 5 minutes | Less than 1 minute |

4. How many times a week have you experienced a urine leak preceded by an urgent need to urinate that you were unable to control?

- | | | | |
|---------------------------------------|---------------------------------------|---------------------------------------|---------------------------------------|
| <input type="checkbox"/> ₀ | <input type="checkbox"/> ₁ | <input type="checkbox"/> ₂ | <input type="checkbox"/> ₃ |
| Never | Less than once a week | Several times a week | Several times a day |

4 a. In the above case, what kind of leaks did you have?

- | | | | |
|---------------------------------------|---------------------------------------|---------------------------------------|---------------------------------------|
| <input type="checkbox"/> ₀ | <input type="checkbox"/> ₁ | <input type="checkbox"/> ₂ | <input type="checkbox"/> ₃ |
| No leaks in this case | A few drops | Light leaks | Heavy leaks |

Over the past 4 weeks and under everyday conditions of social, professional or family life:



5. During the day, in general, how long elapsed between urinating?

- | | | | |
|---------------------------------------|---------------------------------------|---------------------------------------|---------------------------------------|
| <input type="checkbox"/> ₀ | <input type="checkbox"/> ₁ | <input type="checkbox"/> ₂ | <input type="checkbox"/> ₃ |
| 2 hours or more | Between 1 and 2 hours | Between 30 minutes and 1 hour | Less than 30 minutes |



6. How many times on average have you been woken up during the night by a need to urinate?

- | | | | |
|---------------------------------------|---------------------------------------|---------------------------------------|---------------------------------------|
| <input type="checkbox"/> ₀ | <input type="checkbox"/> ₁ | <input type="checkbox"/> ₂ | <input type="checkbox"/> ₃ |
| Never or Once | Twice | 3 or 4 times | More than 4 times |

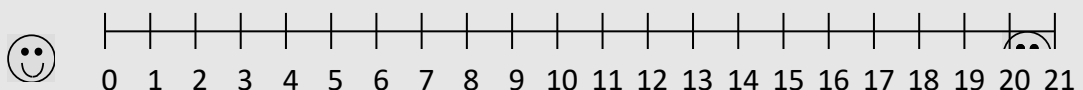


7. How many times a week have you had a urine leak while asleep or have you woken up wet?

- | | | | |
|---------------------------------------|---------------------------------------|---------------------------------------|---------------------------------------|
| <input type="checkbox"/> ₀ | <input type="checkbox"/> ₁ | <input type="checkbox"/> ₂ | <input type="checkbox"/> ₃ |
| Never | Less than once a week | Several times a week | Several times a day |

For the doctor only: note the sum of items 2 + 3 + 4 + 4a + 5 + 6 + 7 on the scale below

“OVERACTIVE BLADDER” SCORE



Over the past 4 weeks and under everyday conditions of social, professional or family life:

8. How would you describe your usual urination over these past 4 weeks?

- | | | | |
|---------------------------------------|---|--|---------------------------------------|
| <input type="checkbox"/> ₀ | <input type="checkbox"/> ₁ | <input type="checkbox"/> ₂ | <input type="checkbox"/> ₃ |
| Normal | Needed to push with abdominal (stomach) muscles or lean forward (or required a change of position) to urinate | Needed to press on the lower stomach with my hands | Used a catheter |

9. In general, how would you describe your urine flow?

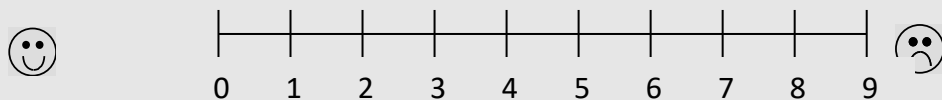
- | | | | |
|---------------------------------------|---------------------------------------|---------------------------------------|---------------------------------------|
| <input type="checkbox"/> ₀ | <input type="checkbox"/> ₁ | <input type="checkbox"/> ₂ | <input type="checkbox"/> ₃ |
| Normal | Weak | Drop by drop | Used a catheter |

10. In general, how has your urination been?

- | | | | | |
|---------------------------------------|---------------------------------------|---------------------------------------|---------------------------------------|---------------------------------------|
| <input type="checkbox"/> ₀ | <input type="checkbox"/> ₁ | <input type="checkbox"/> ₁ | <input type="checkbox"/> ₂ | <input type="checkbox"/> ₃ |
| Normal and quick | Difficult to start, then normal | Easy at first but slow to finish | Very slow from start to finish | Used a catheter |

For the doctor only: note the sum of items 8 + 9 + 10 on the scale below

“LOW STREAM” SCORE



Please check that you have answered all the questions.

Thank you for your cooperation

Appendix 4. ICIQ-OAB questionnaire

<input type="text"/>	<input type="text"/>	<input type="text"/>	<input type="text"/>	<input type="text"/>	<input type="text"/>
----------------------	----------------------	----------------------	----------------------	----------------------	----------------------

Initial number

ICIQ-OAB (UK English) 11/05

CONFIDENTIAL

<input type="text"/>	<input type="text"/>	<input type="text"/>	<input type="text"/>	<input type="text"/>	<input type="text"/>
----------------------	----------------------	----------------------	----------------------	----------------------	----------------------

DAY

MONTH

YEAR

Today's date

Overactive bladder

Many people experience urinary symptoms some of the time. We are trying to find out how many people experience urinary symptoms, and how much they bother them. We would be grateful if you could answer the following questions, thinking about how you have been, on average, over the PAST FOUR WEEKS.

1. Please write in your date of birth:

<input type="text"/>	<input type="text"/>	<input type="text"/>	<input type="text"/>	<input type="text"/>	<input type="text"/>
----------------------	----------------------	----------------------	----------------------	----------------------	----------------------

DAY

MONTH

YEAR

2. Are you (tick one):

Female

Male

3a. How often do you pass urine during the day?

1 to 6 times 0

7 to 8 times 1

9 to 10 times 2

11 to 12 times 3

13 or more times 4

3b. How much does this bother you?

Please ring a number between 0 (not at all) and 10 (a great deal)

0 1 2 3 4 5 6 7 8 9 10
not at all a great deal

4a. During the night, how many times do you have to get up to urinate, on average?

none 0

one 1

two 2

three 3

four or more 4

4b. How much does this bother you?

Please ring a number between 0 (not at all) and 10 (a great deal)

0 1 2 3 4 5 6 7 8 9 10
not at all a great deal

5a. Do you have to rush to the toilet to urinate?

never 0
occasionally 1
sometimes 2
most of the time 3
all of the time 4

5b. How much does this bother you?
Please ring a number between 0 (not at all) and 10 (a great deal)

0 1 2 3 4 5 6 7 8 9 10
not at all a great deal

6a. Does urine leak before you can get to the toilet?

never 0
occasionally 1
sometimes 2
most of the time 3
all of the time 4

6b. How much does this bother you?
Please ring a number between 0 (not at all) and 10 (a great deal)

0 1 2 3 4 5 6 7 8 9 10
not at all a great deal

© ICSmale/BFLUTS

Thank you very much for answering these questions.

Appendix 5. ICIQ-FLUTS questionnaire

Initial number

ICIQ-FLUTS 08/04

CONFIDENTIAL

DAY

MONTH

YEAR

Today's date

Urinary symptoms

Many people experience urinary symptoms some of the time. We are trying to find out how many people experience urinary symptoms, and how much they bother them. We would be grateful if you could answer the following questions, thinking about how you have been, on average, over the PAST FOUR WEEKS.

1. Please write in your date of birth:

DAY

MONTH

YEAR

2a. During the night, how many times do you have to get up to urinate, on average?

none 0

one 1

two 2

three 3

four or more 4

2b. How much does this bother you?

Please ring a number between 0 (not at all) and 10 (a great deal)

0 1 2 3 4 5 6 7 8 9 10
not at all a great deal

3a. Do you have a sudden need to rush to the toilet to urinate?

never 0

occasionally 1

sometimes 2

most of the time 3

all of the time 4

3b. How much does this bother you?

Please ring a number between 0 (not at all) and 10 (a great deal)

0 1 2 3 4 5 6 7 8 9 10
not at all a great deal

4a. Do you have pain in your bladder?

never 0

occasionally 1

sometimes 2

most of the time 3

all of the time 4

4b. How much does this bother you?

Please ring a number between 0 (not at all) and 10 (a great deal)

0 1 2 3 4 5 6 7 8 9 10
not at all a great deal

5a. How often do you pass urine during the day?

1 to 6 times 0
 7 to 8 times 1
 9 to 10 times 2
 11 to 12 times 3
 13 or more times 4

5b. How much does this bother you?
Please ring a number between 0 (not at all) and 10 (a great deal)

0 1 2 3 4 5 6 7 8 9 10
 not at all a great deal

F score: sum scores 2a-5a

6a. Is there a delay before you can start to urinate?

never 0
 occasionally 1
 sometimes 2
 most of the time 3
 all of the time 4

6b. How much does this bother you?
Please ring a number between 0 (not at all) and 10 (a great deal)

0 1 2 3 4 5 6 7 8 9 10
 not at all a great deal

7a. Do you have to strain to urinate?

never 0
 occasionally 1
 sometimes 2
 most of the time 3
 all of the time 4

7b. How much does this bother you?
Please ring a number between 0 (not at all) and 10 (a great deal)

0 1 2 3 4 5 6 7 8 9 10
 not at all a great deal

8a. Do you stop and start more than once while you urinate?

never 0
 occasionally 1
 sometimes 2
 most of the time 3
 all of the time 4

8b. How much does this bother you?
Please ring a number between 0 (not at all) and 10 (a great deal)

0 1 2 3 4 5 6 7 8 9 10
 not at all a great deal

V score: sum scores 6a+7a+8a

9a. Does urine leak before you can get to the toilet?

never 0
 occasionally 1
 sometimes 2
 most of the time 3
 all of the time 4

9b. How much does this bother you?
Please ring a number between 0 (not at all) and 10 (a great deal)

0 1 2 3 4 5 6 7 8 9 10
 not at all a great deal

10a. How often do you leak urine?

never 0
 once or less per week 1
 two to three times per week 2
 once per day 3
 several times per day 4

10b. How much does this bother you?
Please ring a number between 0 (not at all) and 10 (a great deal)

0 1 2 3 4 5 6 7 8 9 10
 not at all a great deal

11a. Does urine leak when you are physically active, exert yourself, cough or sneeze?

never 0
 occasionally 1
 sometimes 2
 most of the time 3
 all of the time 4

11b. How much does this bother you?
Please ring a number between 0 (not at all) and 10 (a great deal)

0 1 2 3 4 5 6 7 8 9 10
 not at all a great deal

12a. Do you ever leak urine for no obvious reason and without feeling that you want to go?

never 0
 occasionally 1
 sometimes 2
 most of the time 3
 all of the time 4

12b. How much does this bother you?
Please ring a number between 0 (not at all) and 10 (a great deal)

0 1 2 3 4 5 6 7 8 9 10
 not at all a great deal

13a. Do you leak urine when you are asleep?

never 0
 occasionally 1
 sometimes 2
 most of the time 3
 all of the time 4

13b. How much does this bother you?
Please ring a number between 0 (not at all) and 10 (a great deal)

0 1 2 3 4 5 6 7 8 9 10
 not at all a great deal

I score: sum scores9a-13a

© BFLUTS-SF

Thank you very much for answering these questions.

Appendix 6. ICIQ-LUTSqol questionnaire

Initial number

ICIQ-LUTSqol 08/04

CONFIDENTIAL

DAY

MONTH

YEAR

Today's date

Quality of life

Below are some daily activities that can be affected by urinary problems. How much does your urinary problem affect you? We would like you to answer every question. Simply tick the box that applies to you.

We would be grateful if you could answer the following questions, thinking about how you have been, on average, over the PAST FOUR WEEKS.

1. Please write in your date of birth:

DAY

MONTH

YEAR

2. Are you (tick one):

Female Male

3a. To what extent does your urinary problem affect your household tasks (e.g. cleaning, shopping, etc.)

not at all 1

slightly 2

moderately 3

a lot 4

3b. How much does this bother you?

Please ring a number between 0 (not at all) and 10 (a great deal)

0 1 2 3 4 5 6 7 8 9 10
not at all a great deal

4a. Does your urinary problem affect your job, or your normal daily activities outside the home?

not at all 1

slightly 2

moderately 3

a lot 4

4b. How much does this bother you?

Please ring a number between 0 (not at all) and 10 (a great deal)

0 1 2 3 4 5 6 7 8 9 10
not at all a great deal

5a. Does your urinary problem affect your physical activities (e.g. going for a walk, run, sport, gym, etc.)?

not at all 1
 slightly 2
 moderately 3
 a lot 4

5b. How much does this bother you?
Please ring a number between 0 (not at all) and 10 (a great deal)

0 1 2 3 4 5 6 7 8 9 10
 not at all a great deal

6a. Does your urinary problem affect your ability to travel?

not at all 1
 slightly 2
 moderately 3
 a lot 4

6b. How much does this bother you?
Please ring a number between 0 (not at all) and 10 (a great deal)

0 1 2 3 4 5 6 7 8 9 10
 not at all a great deal

7a. Does your urinary problem limit your social life?

not at all 1
 slightly 2
 moderately 3
 a lot 4

7b. How much does this bother you?
Please ring a number between 0 (not at all) and 10 (a great deal)

0 1 2 3 4 5 6 7 8 9 10
 not at all a great deal

8a. Does your urinary problem limit your ability to see/visit friends?

not at all 1
 slightly 2
 moderately 3
 a lot 4

8b. How much does this bother you?
Please ring a number between 0 (not at all) and 10 (a great deal)

0 1 2 3 4 5 6 7 8 9 10
 not at all a great deal

9a. Does your urinary problem affect your relationship with your partner?

not applicable 8
 not at all 1
 slightly 2
 moderately 3
 a lot 4

9b. How much does this bother you?
Please ring a number between 0 (not at all) and 10 (a great deal)

0 1 2 3 4 5 6 7 8 9 10
 not at all a great deal

10a. Does your urinary problem affect your sex life?

not applicable 8
 not at all 1
 slightly 2
 moderately 3
 a lot 4

10b. How much does this bother you?
Please ring a number between 0 (not at all) and 10 (a great deal)

0 1 2 3 4 5 6 7 8 9 10
 not at all a great deal

11a. Does your urinary problem affect your family life?

not applicable 8
 not at all 1
 slightly 2
 moderately 3
 a lot 4

11b. How much does this bother you?
Please ring a number between 0 (not at all) and 10 (a great deal)

0 1 2 3 4 5 6 7 8 9 10
 not at all a great deal

12a. Does your urinary problem make you feel depressed?

not at all 1
 slightly 2
 moderately 3
 very much 4

12b. How much does this bother you?
Please ring a number between 0 (not at all) and 10 (a great deal)

0 1 2 3 4 5 6 7 8 9 10
 not at all a great deal

13a. Does your urinary problem make you feel anxious or nervous?

not at all 1
slightly 2
moderately 3
very much 4

13b. How much does this bother you?
Please ring a number between 0 (not at all) and 10 (a great deal)

0 1 2 3 4 5 6 7 8 9 **10**
not at all a great deal

14a. Does your urinary problem make you feel bad about yourself?

not at all 1
slightly 2
moderately 3
very much 4

14b. How much does this bother you?
Please ring a number between 0 (not at all) and 10 (a great deal)

0 1 2 3 4 5 6 7 8 9 **10**
not at all a great deal

15a. Does your urinary problem affect your sleep?

never 1
sometimes 2
often 3
all the time 4

15b. How much does this bother you?
Please ring a number between 0 (not at all) and 10 (a great deal)

0 1 2 3 4 5 6 7 8 9 **10**
not at all a great deal

16a. Do you feel worn out/tired?

never 1
sometimes 2
often 3
all the time 4

16b. How much does this bother you?
Please ring a number between 0 (not at all) and 10 (a great deal)

0 1 2 3 4 5 6 7 8 9 **10**
not at all a great deal

Do you do any of the following? If so, how much?

17a. Wear pads to keep dry?

never 1
 sometimes 2
 often 3
 all the time 4

17b. How much does this bother you?
Please ring a number between 0 (not at all) and 10 (a great deal)

0 1 2 3 4 5 6 7 8 9 10
 not at all a great deal

18a. Be careful how much fluid you drink?

never 1
 sometimes 2
 often 3
 all the time 4

18b. How much does this bother you?
Please ring a number between 0 (not at all) and 10 (a great deal)

0 1 2 3 4 5 6 7 8 9 10
 not at all a great deal

19a. Change your underclothes when they get wet?

never 1
 sometimes 2
 often 3
 all the time 4

19b. How much does this bother you?
Please ring a number between 0 (not at all) and 10 (a great deal)

0 1 2 3 4 5 6 7 8 9 10
 not at all a great deal

20a. Worry in case you smell?

never 1
 sometimes 2
 often 3
 all the time 4

20b. How much does this bother you?
Please ring a number between 0 (not at all) and 10 (a great deal)

0 1 2 3 4 5 6 7 8 9 10
 not at all a great deal

21a. Get embarrassed because of your urinary problem?

never	<input type="checkbox"/>	1
sometimes	<input type="checkbox"/>	2
often	<input type="checkbox"/>	3
all the time	<input type="checkbox"/>	4

21b. How much does this bother you?
Please ring a number between 0 (not at all) and 10 (a great deal)

0	1	2	3	4	5	6	7	8	9	10
not at all										a great deal

22. Overall, how much do urinary symptoms interfere with your everyday life?
Please ring a number between 0 (not at all) and 10 (a great deal)

0	1	2	3	4	5	6	7	8	9	10
not at all										a great deal

© KHQ

Thank you very much for answering these questions.

Appendix 7. IPSS questionnaire

IPSS (INTERNATIONAL PROSTATE SYMPTOM SCORE QUESTIONNAIRE)

Name: _____ ID: _____

Date: _____

International-Prostate Symptom Score (I-PSS2) (S)						
All question concern the past 4 weeks	Never	About 1 time in 5	About 1 time in 3	About 1 time in 2	About 2 times in 3	Almost always
1. Over the past month, how often have you had a sensation of not emptying your bladder completely after you finished urinating?	0	1	2	3	4	5
2. Over the past month, how often have you had to urinate again less than two hours after you finished urinating?	0	1	2	3	4	5
3. Over the past month, how often have you found you stopped and started again several times when you urinated?	0	1	2	3	4	5
4. Over the past month, how often have you found it difficult to hold back urinating after you have felt the need?	0	1	2	3	4	5
5. Over the past month, how often have you noticed a reduction in the strength and force of your urinary stream?	0	1	2	3	4	5
6. Over the past month, how often have you had to push or strain to begin urination?	0	1	2	3	4	5
7. Over the past month, how many times did you most typically get up to urinate from the time you went to bed at night until the time you got up in the morning?	None (0)	1 time (1)	2 times (2)	3 times (3)	4 times (4)	5 times or more (5)
Total IPS score S = _____						

Quality of life due to urinary symptoms (L)							
If you were to spend the rest of your life with your urinary condition the way it is now, how would you feel about that?	Delighted	Pleased	Mostly Satisfied	Mixed – about equally satisfied and dissatisfied	Mostly dis-satisfied	Unhappy	Terrible
	(0)	(1)	(2)	(3)	(4)	(5)	(6)
Quality of life assessment index L = _____							

*The American Urological Association Symptom Index for Benign Prostatic Hyperplasia
Barry MJ et al. J Urol 1992;148:1549–57.*

Appendix 8. SF-Qualiveen Questionnaire

Center N°

Visit N°

Patient N°

Patient's initials

SF-QUALIVEEN®

How to answer the questionnaire:

The following questions are about the bladder problems you may have and how you deal and live with them.

Please fill in this questionnaire in a quiet place and preferably on your own. Take the time you need. There are no right or wrong answers. If you are not sure how to answer a question, choose the answer which best applies to you. Please note that your answers will remain strictly anonymous and confidential.

When answering the questions, think about how you pass urine at present.

Thank you for your participation.

➤ Before filling in this questionnaire, please write today's date :

Day Month Year

THE INFORMATION CONTAINED IN THIS QUESTIONNAIRE IS STRICTLY ANONYMOUS AND CONFIDENTIAL

YOUR BLADDER PROBLEMS AND HOW YOU PASS URINE AT PRESENT:

Please answer all the questions by ticking the appropriate box.

	NOT AT ALL	Slightly	Moderately	Quite a bit	Extremely
1. In general, do your bladder problems complicate your life?	<input type="checkbox"/> ₀	<input type="checkbox"/> ₁	<input type="checkbox"/> ₂	<input type="checkbox"/> ₃	<input type="checkbox"/> ₄
2. Are you bothered by the time spent passing urine or realizing catheterization	<input type="checkbox"/> ₀	<input type="checkbox"/> ₁	<input type="checkbox"/> ₂	<input type="checkbox"/> ₃	<input type="checkbox"/> ₄
3. Do you worry about your bladder problems worsening	<input type="checkbox"/> ₀	<input type="checkbox"/> ₁	<input type="checkbox"/> ₂	<input type="checkbox"/> ₃	<input type="checkbox"/> ₄
4. Do you worry about smelling of urine	<input type="checkbox"/> ₀	<input type="checkbox"/> ₁	<input type="checkbox"/> ₂	<input type="checkbox"/> ₃	<input type="checkbox"/> ₄
5. Do you feel worried because of your bladder problems	<input type="checkbox"/> ₀	<input type="checkbox"/> ₁	<input type="checkbox"/> ₂	<input type="checkbox"/> ₃	<input type="checkbox"/> ₄
6. Do you feel embarrassed because of your bladder problems	<input type="checkbox"/> ₀	<input type="checkbox"/> ₁	<input type="checkbox"/> ₂	<input type="checkbox"/> ₃	<input type="checkbox"/> ₄
	Never	Rarely	From time to time	Often	Always
7. Is your life regulated by your bladder problems?	<input type="checkbox"/> ₀	<input type="checkbox"/> ₁	<input type="checkbox"/> ₂	<input type="checkbox"/> ₃	<input type="checkbox"/> ₄
8. Can you go out without planning anything in advance?	<input type="checkbox"/> ₄	<input type="checkbox"/> ₃	<input type="checkbox"/> ₂	<input type="checkbox"/> ₁	<input type="checkbox"/> ₀

Thank you for valuable help

Appendix 9. The three-day bladder diary



Bladder Diary

Name:

Study ID:

Hospital Number:

Date of Birth:

Instructions

Please complete this bladder diary for three consecutive days as accurately as possible. This will enable us to exactly assess the function of your bladder and to find the optimal treatment if needed. Please fill the diary columns each time you drink and pass water providing the time and details. Please use a separate page for each day.

Date - Start the diary with the first time you pass water after you usually get out of the bed in the morning. Continue to record the volume and sensation each time you get up at night to pass water.

Time - You can mention the time using am/pm or the hours (0000 - 2400)

Voided Volume – You can use any measuring container to record the volume in milliliters (mL).

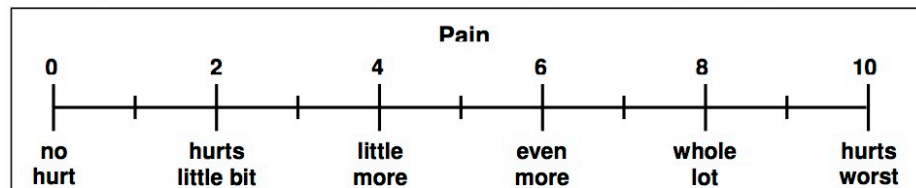
Catheterized Volume - is measured if you self-catheterize, and is the volume that is drained using a catheter after you have voided when you had a desire to pass water.



Sensation - What is the reason you went to urinate (pass water)? This can be graded as:

Grade	Sensation of bladder fullness
0	Convenience (no urge)
1	Mild urge (can hold more than 1 hour)
2	Moderate urge (can hold for 10 to 60 minutes)
3	Severe urge (can hold less than 10 minutes)
4	Desperate urge (must go immediately)

Pain – can be graded from 0 to 10 according to the following visual analogue rating scale:



After completing, please return a copy of the completed bladder diary to:

Uroneurology-research@ucl.ac.uk

or by letter to:

LUTfMRI study 13/0523
 Department of Uro-neurology
 Internal Mail Box 71
 National Hospital for Neurology
 & Neurosurgery
 Queen Square London WC1N 3BG
 Tel – 02034484713, Fax - 02034484748

LUT_MRI_BladderDiary_v3_20160329

Day 2; date: _____
 Time out of bed: _____

Time to bed: _____

Time	Fluid intake in mL	Voided volume * in mL	Catheterized volume in mL	Urinary leakage (none, slight, moderate, heavy)	Bladder sensation (0 to 4) **	Pain (0 to 10)	Pad replaced (x)	Wetness of pad (dry, moist, soaked)
Total:								

*** Examples for volumes:**
 Small cup = 100 mL
 Large cup = 200 mL
 Normal glass = 200 mL
 Medium glass = 300-400 mL
 Large glass = 500 mL

Grade	** Sensation of bladder fullness
0	Convenience (no urge)
1	Mild urge (can hold more than 1 hour)
2	Moderate urge (can hold for 10 to 60 minutes)
3	Severe urge (can hold less than 10 minutes)
4	Desperate urge (must go immediately)

LUT_MRI_BladderDiary_v3_20160329

Day 3; date: _____

Time out of bed: _____

Time to bed: _____

Time	Fluid intake in mL	Voided volume * in mL	Catheterized volume in mL	Urinary leakage (none, slight, moderate, heavy)	Bladder sensation (0 to 4) **	Pain (0 to 10)	Pad replaced (x)	Wetness of pad (dry, moist, soaked)
Total:								

*** Examples for volumes:**
 Small cup = 100 mL
 Large cup = 200 mL
 Normal glass = 200 mL
 Medium glass = 300-400 mL
 Large glass = 500 mL

Grade	** Sensation of bladder fullness
0	Convenience (no urge)
1	Mild urge (can hold more than 1 hour)
2	Moderate urge (can hold for 10 to 60 minutes)
3	Severe urge (can hold less than 10 minutes)
4	Desperate urge (must go immediately)

Appendix 10. Unified MSA Rating Scale (UMSARS)

Part I: Historical Review

Rate the average functional situation for the past 2 weeks (unless specified) according to the patient and caregiver interview. Indicate the score that best fits with the patient status. Rate the function independently from the nature of the signs.

1. Speech		
0	Not affected.	_____
1	Mildly affected. No difficulties being understood.	
2	Moderately affected. Sometimes (less than half of the time) asked to repeat statements.	
3	Severely affected. Frequently (more than half of the time) asked to repeat statements.	
4	Unintelligible most of the time.	
2. Swallowing		_____
0	Normal.	
1	Mild impairment. Choking less than once a week.	
2	Moderate impairment. Occasional food aspiration with choking more than once a week.	
3	Marked impairment. Frequent food aspiration.	
4	Nasogastric tube or gastrostomy feeding.	
3. Handwriting		_____
0	Normal	
1	Mildly impaired, all words are legible.	
2	Moderately impaired, up to half of the words are not legible.	
3	Markedly impaired, the majority of words are not legible.	
4	Unable to write.	
4. Cutting food and handling utensils		_____
0	Normal.	
1	Somewhat slow and/or clumsy, but no help needed.	
2	Can cut most foods, although clumsy and slow; some help needed.	
3	Food must be cut by someone, but can still feed slowly.	
4	Needs to be fed.	
5. Dressing		_____
0	Normal.	
1	Somewhat slow and/or clumsy, but no help needed.	
2	Occasional assistance with buttoning, getting arms in sleeves.	
3	Considerable help required, but can do some things alone.	
4	Completely helpless.	
6. Hygiene		_____
0	Normal.	
1	Somewhat slow and/or clumsy, but no help needed.	
2	Needs help to shower or bathe; or very slow in hygienic care.	
3	Requires assistance for washing, brushing teeth, combing hair, using the toilet.	
4	Completely helpless.	

(Part I, continued)

7. Walking			_____
0	Normal.		
1	Mildly impaired. No assistance needed. No walking aid required (except for unrelated disorders).		
2	Moderately impaired. Assistance and/or walking aid needed occasionally.		
3	Severely impaired. Assistance and/or walking aid needed frequently.		
4	Cannot walk at all even with assistance.		
8. Falling (rate the past month)			_____
0	None.		
1	Rare falling (less than once a month).		
2	Occasional falling (less than once a week).		
3	Falls more than once a week.		
4	Falls at least once a day (if the patient cannot walk at all, rate 4).		
9. Orthostatic symptoms			_____
0	No orthostatic symptoms.*		
1	Orthostatic symptoms are infrequent and do not restrict activities of daily living.		
2	Frequent orthostatic symptoms developing at least once a week. Some limitation in activities of daily living.		
3	Orthostatic symptoms develop on most occasions. Able to stand > 1 min on most occasions. Limitation in most of activities of daily living.		
4	Symptoms consistently develop on orthostasis. Able to stand < 1 min on most occasions. Syncope/presyncope is common if patient attempts to stand.		
	*Syncope, dizziness, visual disturbances or neck pain, relieved on lying flat.		
10. Urinary function*			_____
0	Normal.		
1	Urgency and/or frequency, no drug treatment required.		
2	Urgency and/or frequency, drug treatment required.		
3	Urge incontinence and/or incomplete bladder emptying needing intermittent catheterization.		
4	Incontinence needing indwelling catheter.		
	*Urinary symptoms should not be due to other causes.		
11. Sexual function			_____
0	No problems.		
1	Minor impairment compared to healthy days.		
2	Moderate impairment compared to healthy days.		
3	Severe impairment compared to healthy days.		
4	No sexual activity possible.		
12. Bowel function			_____
0	No change in pattern of bowel function from previous pattern.		
1	Occasional constipation but no medication needed.		
2	Frequent constipation requiring use of laxatives.		
3	Chronic constipation requiring use of laxatives and enemas.		
4	Cannot have a spontaneous bowel movement.		
Total score Part I:			_____

Part II: Motor Examination Scale

Always rate the worst affected limb.

1. Facial expression			_____
0	Normal.		
1	Minimal hypomimia, could be normal ("Poker face").		
2	Slight but definitely abnormal diminution of facial expression.		
3	Moderate hypomimia; lips parted some of the time.		
4	Masked or fixed facies with severe or complete loss of facial expression, lips parted 0.25 inch or more.		
2. Speech			_____
	The patient is asked to repeat several times a standard sentence.		
0	Normal.		
1	Mildly slow, slurred, and/or dysphonic. No need to repeat statements.		
2	Moderately slow, slurred, and/or dysphonic. Sometimes asked to repeat statements.		
3	Severely slow, slurred, and/or dysphonic. Frequently asked to repeat statements.		
4	Unintelligible.		

-
3. Ocular motor dysfunction
Eye movements are examined by asking the subject to follow slow horizontal finger movements of the examiner, to look laterally at the finger at different positions, and to perform saccades between two fingers, each held at an eccentric position of approximately 30°. The examiner assesses the following abnormal signs: (1) broken-up smooth pursuit, (2) gaze-evoked nystagmus at an eye position of more than 45 degrees, (3) gaze-evoked nystagmus at an eye position of less than 45 degrees, (4) saccadic hypermetria. Sign 3 suggests that there are at least two abnormal ocular motor signs, because Sign 2 is also present.
- 0 None.
 - 1 One abnormal ocular motor sign.
 - 2 Two abnormal ocular motor signs.
 - 3 Three abnormal ocular motor signs.
 - 4 Four abnormal ocular motor signs.
4. Tremor at rest (rate the most affected limb)
- 0 Absent.
 - 1 Slight and infrequently present.
 - 2 Mild in amplitude and persistent. Or moderate in amplitude, but only intermittently present.
 - 3 Moderate in amplitude and present most of the time,
 - 4 Marked in amplitude and present most of the time,
5. Action tremor
Assess postural tremor of outstretched arms (A) and action tremor on finger pointing (B). Rate maximal tremor severity in Task A and/or B (whichever is worse), and rate the most affected limb.
- 0 Absent.
 - 1 Slight tremor of small amplitude (A). No interference with finger pointing (B).
 - 2 Moderate amplitude (A). Some interference with finger pointing (B).
 - 3 Marked amplitude (A). Marked interference with finger pointing (B).
 - 4 Severe amplitude (A). Finger pointing impossible (B).
6. Increased tone (rate the most affected limb)
Judged on passive movement of major joints with patient relaxed in sitting position; ignore cogwheeling.
- 0 Absent.
 - 1 Slight or detectable only when activated by mirror or other movements.
 - 2 Mild to moderate.
 - 3 Marked, but full range of motion easily achieved.
 - 4 Severe, range of motion achieved with difficulty.
7. Rapid alternating movements of hands
Pro-supination movements of hands, vertically or horizontally, with as large an amplitude as possible, each hand separately, rate the worst affected limb. Note that impaired performance on this task can be caused by bradykinesia and/or cerebellar incoordination. Rate functional performance regardless of underlying motor disorder.
- 0 Normal.
 - 1 Mildly impaired.
 - 2 Moderately impaired.
 - 3 Severely impaired.
 - 4 Can barely perform the task.
8. Finger taps
Patient taps thumb with index finger in rapid succession with widest amplitude possible, each hand at least 15 to 20 seconds. Rate the worst affected limb. Note that impaired performance on this task can be caused by bradykinesia and/or cerebellar incoordination. Rate functional performance regardless of underlying motor disorder.
- 0 Normal.
 - 1 Mildly impaired.
 - 2 Moderately impaired.
 - 3 Severely impaired.
 - 4 Can barely perform the task.
9. Leg agility
Patient is sitting and taps heel on ground in rapid succession, picking up entire leg. Amplitude should be approximately 10 cm, rate the worst affected leg. Note that impaired performance on this task can be caused by bradykinesia and/or cerebellar incoordination. Rate functional performance, regardless of underlying motor disorder.
- 0 Normal.
 - 1 Mildly impaired.
 - 2 Moderately impaired.
 - 3 Severely impaired.
 - 4 Can barely perform the task.
10. Heel-knee-shin test
The patient is requested to raise one leg and place the heel on the knee, and then slide the heel down the anterior tibial surface of the resting leg toward the ankle. On reaching the ankle joint, the leg is again raised in the air to a height of approximately 40 cm and the action is repeated. At least three movements of each limb must be performed for proper assessment. Rate the worst affected limb.
- 0 Normal.
 - 1 Mildly dysmetric and ataxic.
 - 2 Moderately dysmetric and ataxic.
 - 3 Severely dysmetric and ataxic.
 - 4 Can barely perform the task.
-

11. Arising from chair	_____
Patient attempts to arise from a straight-back wood or metal chair with arms folded across chest.	
0	Normal.
1	Clumsy, or may need more than one attempt.
2	Pushes self up from arms of seat.
3	Tends to fall back and may have to try more than once but can get up without help.
4	Unable to arise without help.
12. Posture	_____
0	Normal.
1	Not quite erect, slightly stooped posture; could be normal for older person.
2	Moderately stooped posture, definitely abnormal; can be slightly leaning to one side.
3	Severely stooped posture with kyphosis; can be moderately leaning to one side.
4	Marked flexion with extreme abnormality of posture.
13. Body sway	_____
Rate spontaneous body sway and response to sudden, strong posterior displacement produced by pull on shoulder while patient erect with eyes open and feet slightly apart. Patient has to be warned.	
0	Normal.
1	Slight body sway and/or retropulsion with unaided recovery.
2	Moderate body sway and/or deficient postural response; might fall if not caught by examiner.
3	Severe body sway. Very unstable. Tends to lose balance spontaneously.
4	Unable to stand without assistance.
14. Gait	_____
0	Normal.
1	Mildly impaired.
2	Moderately impaired. Walks with difficulty, but requires little or no assistance.
3	Severely impaired. Requires assistance.
4	Cannot walk at all, even with assistance.
Total score Part II:	_____

Part III: Autonomic Examination

Supine blood pressure and heart rate are measured after 2 minutes of rest and again after 2 minutes of standing. Orthostatic symptoms may include lightheadedness, dizziness, blurred vision, weakness, fatigue, cognitive impairment, nausea, palpitations, tremulousness, headache, neck and "coat-hanger" ache.

Systolic blood pressure	Supine	_____
	Standing (2 minutes)	_____
	Unable to record	_____
Diastolic blood pressure	Supine	_____
	Standing (2 minutes)	_____
	Unable to record	_____
Heart rate	Supine	_____
	Standing (2 minutes)	_____
	Unable to record	_____
Orthostatic symptoms	Yes	_____
	No	_____

Part IV: Global Disability Scale

-
1. Completely independent. Able to do all chores with minimal difficulty or impairment. Essentially normal. Unaware of any difficulty.
 2. Not completely independent. Needs help with some chores.
 3. More dependent. Help with half of chores. Spends a large part of the day with chores.
 4. Very dependent. Now and then does a few chores alone or begins alone. Much help needed.
 5. Totally dependent and helpless. Bedridden.
-

Appendix 11. Other work beyond this thesis during my PhD

The studies involved in this thesis were parts of a whole project and I was involved in other work beyond my studies stated in this thesis. Here, I would like to list briefly the other main work I have done during my PhD:

1. I helped with recruitment for MSA patients, including attending MSA clinics, spreading patient information leaflet (PIL), calling potential participants and arranging their transport;
2. I did screening tests and clinical assessments for the MSA patients, including history taking to make sure the patients fulfilled the inclusion criteria (obtaining their MMSE, medication history and bladder diary, etc.), neurological examination, testing their autonomic functions, urological tests (test for UTI and PVR), and SSEP test;
3. I was involved in all procedures during MRI data acquisition for MSA patients, including clinical scans, diffusion MRI, functional MRI resting states and task (preparing study instruments, recording parameters and manually doing infusion task with syringes during the functional MRI task);
4. I manually identified the WM lesions on PDT2 images for all MSA participants;
5. I collected and analyzed data from urodynamic, three-day BD and six questionnaires evaluating bladder symptoms and the impact on QoL, for all participants in the whole project, including both MS and MSA patients. Though there were no significant results related to most of the measures, the work I have done was helpful to identify the best clinical parameter (USP-OAB score) indicating the severity of OAB symptoms. This could be a preparatory work to establish the design for future studies.